NASA CONTRACTOR REPORT

NASA CR-2615

NASA CR-2615

PHYSICAL AND DYNAMICAL STUDIES OF METEORS

Meteor-Fragmentation and Stream-Distribution Studies

Zdenek Sekanina and Richard B. Southworth

Prepared by
SMITHSONIAN INSTITUTION
Cambridge, Mass. 02138
for Langley Research Center

NATIONAL AERONAUTICS AND SPACE ADMINISTRATION • WASHINGTON, D. C. • NOVEMBER 1975

1. Report No. NASA CR-2615	2. Government Accession No.	3. Recipient's Catalog No.
4. Title and Subtitle PHYSICAL AND DYNAMICAL STUDIES OF METEORS Meteor-Fragmentation and Stream-Distribution Studies		5. Report Date November 1975
		6. Performing Organization Code
7. Author(s) Zdenek Sekanina and Richard B. Southworth		8. Performing Organization Report No.
		10. Work Unit No. 188-45-52-03
9. Performing Organization Name and Address Smithsonian Institution, Astrophysical Observatory Cambridge, Mass. 02138		11. Contract or Grant No. NAS1-11204
		13. Type of Report and Period Covered Contractor Report
12. Sponsoring Agency Name and Address National Aeronautics and Space Administration Washington, DC 20546		14. Sponsoring Agency Code 188-45-52-03

15. Supplementary Notes

This is a final report.

16. Abstract

Population parameters of 275 streams including 20 additional streams in the synoptic-year sample have been found by a computer technique. Some 16 percent of the sample is in these streams. Four meteor streams that have close orbital resemblance to Adonis cannot be positively identified as meteors ejected by Adonis within the last 12000 years. Ceplecha's discrete levels of meteor height are not evident in our radar meteors.

The spread of meteoroid fragments along their common trajectory has been computed for most of the observed radar meteors. There is an unexpected relationship between spread and velocity that perhaps conceals relationships between fragmentation and orbits; a theoretical treatment will be necessary to resolve these relationships.

Revised unbiased statistics of synoptic-year orbits are presented, together with parallel (new) statistics for the 1961-65 radar meteor orbits.

17. Key Words (Suggested by Author(s)) meteor; radar observation; distributions, selection effects; space density; fragmentation; meteor streams; luminosity, recombination; diffusion; meteor masses; orbital parameters		18. Distribution Statement Subject Category 88	
19. Security Classif. (of this report) Unclassified	20. Security Classif. (of this page) Unclassified	21. No. of Pages 98	22. Price* $4.75

*For sale by the National Technical Information Service, Springfield, Virginia 22161

TABLE OF CONTENTS

TABLE OF CONTENTS (Cont.)

SUMMARY

Population parameters of 275 streams (including 20 additional streams) in the synoptic-year sample have been found by a computer technique. Some 16% of the sample is in these streams.

Four meteor streams that have close orbital resemblance to Adonis cannot be positively identified as meteors ejected by Adonis within the last 12000 years.

Ceplecha's discrete levels of meteor height are not evident in our radar meteors.

The spread of meteoroid fragments along their common trajectory has been computed for most of our observed meteors. There is an unexpected relationship between spread and velocity that perhaps conceals relationships between fragmentation and orbits; a theoretical treatment is necessary.

Revised unbiased statistics of synoptic-year orbits are presented, together with parallel (new) statistics for 1961–65 orbits.

PHYSICAL AND DYNAMICAL STUDIES OF METEORS

Meteor-Fragmentation and Stream-Distribution Studies

Zdenek Sekanina and Richard B. Southworth

Center for Astrophysics
Harvard College Observatory and Smithsonian Astrophysical Observatory
Cambridge, Massachusetts 02138

1. DISTRIBUTION OF METEORS IN THE STREAMS DETECTED IN THE SYNOPTIC-YEAR SAMPLE

1.1 Introduction

We reported previously (Southworth and Sekanina, 1973) that our two-phase computerized stream search among 19,698 radio-meteor orbits of the synoptic-year sample resulted in the detection of 256 streams.

The distribution of radio-meteor orbits in these 256 streams has now been studied in terms of the D-test, which measures the similarity of any two orbits by the differences in their Keplerian elements (Southworth and Hawkins, 1963). The D-test was utilized by Sekanina (1970a) in the formulation of his statistical model of meteor streams. The model describes the D-distribution function of meteors in a stream by two parameters: the population coefficient Λ, which measures the stream's strength relative to the level of the ambient sporadic background; and the dispersion coefficient σ, which determines the degree of scatter in the distribution of meteor orbits within the stream.

1.2 New Method of Determining the Distribution-Function Parameters Λ and σ

In our previous studies of radio-meteor streams (Sekanina, 1970b, 1973), the two parameters of the D-distribution function were derived graphically from the log-log plots of the cumulative number of meteors versus the D-test (Sekanina, 1970a). To avoid the laborious plotting of hundreds of distribution curves, we have now developed a new, fully computerized method.

The theoretical cumulative D-distribution of the statistical model of meteor streams has the form

$$\mathcal{N}(D) = C \cdot f\left(\frac{D}{\sigma\sqrt{2}}\right) \quad , \tag{1-1}$$

where $\mathcal{N}(D)$ is the number of meteors of the studied sample whose values from the D-test are less than or equal to D, relative to the mean orbit of the stream in question; C is the normalizing constant; and

$$f(x) = x^{3.8} + 2.64\,\Lambda\left(\int_0^x e^{-t^2}\,dt - xe^{-x^2}\right) \quad . \tag{1-2}$$

Since the parameters Λ and σ cannot be determined explicitly, an iterative least-squares procedure has been proposed as follows.

We start from an arbitrary pair of values for the two parameters, Λ_0 and σ_0, and calculate $\mathcal{N}_0(D)$ from equation (1-1) with the proper C_0. Then for each point on the D-distribution curve, we calculate $\mathcal{N}/\mathcal{N}_0$ and thus establish a number of conditional equations of the type

$$\Delta \log \mathcal{N} \equiv \log \frac{\mathcal{N}}{\mathcal{N}_0} = \frac{\partial \log \mathcal{N}}{\partial \log \Lambda}\,\Delta \log \Lambda + \frac{\partial \log \mathcal{N}}{\partial \log \sigma}\,\Delta \log \sigma + \frac{\partial \log \mathcal{N}}{\partial \log C}\,\Delta \log C \quad , \tag{1-3}$$

where $\Delta \log \Lambda = \log \Lambda_1 - \log \Lambda_0$, ... are the corrections to be applied to the parameters to obtain their improved values Λ_1, ... Substituting Λ_1 for Λ_0 and calculating new $\mathcal{N}_0(D)$ values from equation (1-1), the procedure can be iterated until it converges. The normal equations for the corrections to the parameters, implied by the conditional equations, are

$$\begin{pmatrix} \Sigma\Delta \log \eta \\ \Sigma A_\sigma \Delta \log \eta \\ \Sigma A_\Lambda \Delta \log \eta \end{pmatrix} = \begin{pmatrix} n & \Sigma A_\sigma & \Sigma A_\Lambda \\ \Sigma A_\sigma & \Sigma A_\sigma^2 & \Sigma A_\sigma A_\Lambda \\ \Sigma A_\Lambda & \Sigma A_\sigma A_\Lambda & \Sigma A_\Lambda^2 \end{pmatrix} \cdot \begin{pmatrix} \Delta \log C \\ \Delta \log \sigma \\ \Delta \log \Lambda \end{pmatrix}, \tag{1-4}$$

where n is the number of points on the cumulative D-distribution curve,

$$A_\sigma = -\frac{3.8\ E^{3.8}}{f(E)} \left(1 + 1.389\ \Lambda E^{-0.8}\ e^{-E^2} \right), \tag{1-5}$$

$$A_\Lambda = 1 - \frac{E^{3.8}}{f(E)}, \tag{1-6}$$

and

$$E = \frac{D}{\sigma\sqrt{2}} \ . \tag{1-7}$$

1.3 The D-Distributions of the Detected Streams

Since the cumulative D-distribution of meteors in a stream is a by-product of the stream-search program, the above differential-correction procedure can work directly with the punched list of meteors from the search program.

The differential-correction procedure was first tested on several streams of the 1961–65 sample, for which Λ and σ had been previously determined graphically (Sekanina, 1970b, 1973). A few examples, listed in Table 1-1, indicate that the agreement between the least-squares solution and the graphical method is reasonably good.

Practical calculations have shown that the selection of the initial values for Λ and σ has no effect on the convergence of the differential-correction procedure. We chose $\Lambda = 40$ and $\sigma = 0.050$ as standard initial values and found that the procedure converged successfully for all but six of the 256 streams of the synoptic-year sample. The maximum number of required iterations was 70, but in most cases less than 10 were necessary. In four cases (May Arietids, α Draconids, L Cepheids, and ϵ Umids) the

Table 1-1. Parameters of the D-distribution from the least-squares and graphical methods.

Stream 1961–65	Least-squares		Graphical	
	Λ	σ	Λ	σ
Quadrantids	85 ± 19	0.038 ± 0.002	50	0.037
Lyrids	154 ± 40	0.039 ± 0.003	200	0.043
October Draconids	4.4 ± 0.6	0.064 ± 0.006	5	0.066
Geminids	189 ± 35	0.037 ± 0.001	200	0.038

procedure failed to converge, and in two (April Ursids and ϵ Ursids) it failed to yield any solution, because the slope of the D-distribution curve at $D \lesssim 0.1$ was steeper than allowed by the model. In one other case (α Aurigids), the solution indicated that this "stream" does not satisfactorily discriminate from the sporadic background. The population and dispersion coefficients of the six streams for which the differential-correction procedure failed have been determined graphically.

1.4 Numerical Results

The results for the 255 streams (omitting α Aurigids) are listed in Table 1-2. The individual columns give the following information (calculated, in many instances, from the referenced formulas of Sekanina, 1970a):

Column 1. Designation of the stream.

Column 2. Population coefficient Λ.

Column 3. Dispersion coefficient σ.

Column 4. Calculated cumulative number of meteors with $D \leq 0.20$, $\int_0^{0.20} N(D)\, dD$ according to Sekanina (1970a).

Columns 5 and 6. Inner (or differential) D_I and outer (or integral) D_{II} limits of the stream [formulas (38)]. They correspond, respectively, to D-values of equal density and equal population between the stream and the background.

Column 7. Relative sporadic contamination (%) between $D = 0$ and 0.20 [formula (33)].

Column 8. Stream-to-background concentration ratio at $D = 0.20$ [formula (32)].

Columns 9–11. Calculated numbers of definite members of the stream within, respectively, $D = 0.20$, $D = D_I$, and $D = D_{II}$ [formula (34)].

Column 12. Calculated total number of definite members of the stream [formula (35)].

Columns 13 and 14. ρ- and C-tests, respectively, of the existence of the stream [formulas (43) and (48)].

Column 15. Cosmic weight of the stream, as defined by Whipple (1954).

Columns 16 and 17. The date (CST) of the middle of the period of activity and its duration (days).

Columns 18–20. Observed cumulative numbers of meteors with $D \leq 0.20$, $D \leq 0.25$, and $D \leq 0.30$, respectively. The degree of consistency between columns 18 and 4 is a measure of the differential-correction fit of the distribution curve.

Table 1-2. A list of D-distribution parameters of 255 streams of the synoptic-year sample.

1	2	3	4	5	6	7	8	9	10	11	12	13	14	15	16	17	18	19	20
BETA TRIANGULIDS	4.3	.066	15.9	.118	.167	65	3.3E-02	5.6	3.7	5.2	5.7	.13	3.3	2.2	JAN 07.5	72.9	16	32	56
ZETA AURIGIDS	22	.051	11.3	.125	.203	48	6.2E-03	5.8	5.2	5.8	5.8	.13	7.4	9.5	DEC 30.9	33.7	11	22	31
JANUARY BOOTIDS	34	.074	11.9	.192	.331	14	7.3E-01	10.3	10.1	11.0	11.0	.65	12.6	.5	JAN 14.9	1.1	12	15	19
THETA CORONA BOREALIDS	26	.047	11.2	.118	.196	52	1.7E-03	5.4	4.9	5.4	5.4	.56	7.8	3.5	JAN 14.9	1.1	15	20	26
LAMBDA BOOTIDS	560	.018	12.8	.062	.168	66	2.3E-25	4.4	4.3	4.4	4.4	.39	32.4	1.9	JAN 14.4	2.2	15	23	33
CORONA BOREALIDS	21	.058	17.3	.141	.228	38	3.7E-02	10.8	9.6	10.9	10.9	.34	9.9	2.7	JAN 14.7	3.5	20	32	36
CANIDS	270	.031	8.0	.101	.239	34	1.0E-07	5.3	5.2	5.3	5.3	.52	24.8	1.2	JAN 20.5	15.1	8	11	16
QUADRANTIDS	16	.055	8.0	.128	.202	49	1.4E-02	4.1	3.5	4.1	4.1	.13	5.3	2.8	JAN 15.5	2.0	7	14	21
JANUARY SAGITTARIIDS	420	.025	7.9	.084	.217	42	1.6E-12	4.5	4.5	4.5	4.5	.38	28.5	2.6	JAN 15.5	2.1	9	14	17
JANUARY DRACONIDS	77	.032	17.6	.092	.178	61	1.1E-07	6.8	6.5	6.8	6.8	.51	15.0	1.3	JAN 15.5	4.7	23	32	41
DELTA CANCRIDS	5.2	.072	21.6	.135	.193	53	8.9E-02	10.2	7.3	10.0	10.7	.39	4.9	.9	JAN 14.1	62.0	24	37	64
JANUARY CANCRIDS	5.5	.084	16.0	.159	.229	39	3.0E-01	9.7	7.7	10.5	11.1	.23	5.1	3.0	JAN 20.6	15.1	14	25	38
PSI LEONIDS	11	.067	24.5	.146	.222	41	9.8E-02	14.6	12.1	14.8	15.0	.49	8.4	1.5	JAN 29.1	32.0	27	38	52
XI SAGITTARIIDS	4.8	.106	16.6	.195	.277	28	8.9E-01	12.0	11.6	16.0	17.4	.30	6.0	.7	JAN 23.0	15.0	15	25	36
JANUARY AQUARIDS	53	.038	9.0	.104	.191	54	2.5E-05	4.1	3.9	4.1	4.1	.50	9.7	7.5	JAN 23.6	16.1	10	14	24
CAPRICORNIDS-SAGITTARIIDS	11	.075	19.4	.164	.249	32	2.6E-01	13.2	11.5	14.0	14.2	.40	8.2	4.1	JAN 29.5	30.0	19	29	40
H DRACONIDS	96	.029	14.1	.085	.170	65	1.8E-09	5.0	4.8	5.0	5.0	.34	14.3	10.3	JAN 29.6	4.8	15	24	39
IOTA DRACONIDS	28	.053	10.9	.134	.225	39	1.4E-02	6.7	6.0	6.7	6.7	.59	8.9	5.8	JAN 30.1	3.4	13	17	21
PSI CYGNIDS	260	.031	8.3	.100	.237	34	9.8E-08	5.4	5.3	5.4	5.4	.65	24.6	8.7	JAN 30.6	2.2	8	10	17
ALPHA LEONIDS	4.9	.088	17.4	.162	.232	39	3.5E-01	10.7	8.5	11.8	12.7	.28	5.2	1.9	JAN 28.7	31.0	17	29	42
LAMBDA CAPRICORNIDS	37	.060	11.7	.157	.274	23	1.0E-01	8.9	8.3	9.0	9.0	.78	12.0	1.4	JAN 30.1	26.9	14	16	21
DELTA LEONIDS	5.2	.137	23.7	.257	.367	17	2.4E00	19.7	29.5	40.4	43.3	.39	9.8	5.2	FEB 03.1	42.0	24	37	55
EPSILON AQUARIDS	6.4	.109	17.1	.214	.311	21	1.3E00	13.5	14.7	19.5	20.3	.44	7.5	6.5	JAN 29.5	28.1	17	25	36

Table 1-2 (Cont.)

1	2	3	4	5	6	7	8	9	10	11	12	13	14	15	16	17	18	19	20
FEBRUARY DRACONIDS	4.1	.101	34.4	.178	.252	34	6.1E-01	22.8	19.5	28.0	31.2	.34	7.4	3.0	FEB 12.1	31.6	35	56	83
XI CYGNIDS	99	.037	13.0	.109	.219	41	2.1E-05	7.6	7.3	7.6	7.6	.48	17.9	.5	FEB 14.2	57.1	14	20	24
KAPPA GEMINIDS	110	.023	12.0	.068	.140	79	1.4E-15	2.5	2.4	2.5	2.5	.60	10.8	.3	FEB 17.7	71.2	17	22	24
RHO LEONIDS	12	.047	17.2	.104	.159	70	8.1E-04	5.1	4.2	5.1	5.1	.28	5.1	.4	FEB 26.1	26.1	17	29	44
MU LEONIDS	28	.040	13.8	.101	.170	65	5.3E-05	4.8	4.4	4.8	4.8	.39	7.6	5.8	MAR 04.1	70.0	15	23	37
PI VIRGINIDS	13	.058	36.6	.130	.201	49	2.3E-02	18.5	15.4	18.5	18.6	.27	10.2	1.4	MAR 12.1	53.9	35	60	92
NORTHERN ETA VIRGINIDS	14	.064	16.8	.146	.226	39	7.8E-02	10.3	8.8	10.4	10.5	.37	7.9	7.7	MAR 05.2	18.0	16	25	35
LEONIDS-URSIDS	110	.031	7.1	.092	.189	55	4.2E-08	3.2	3.1	3.2	3.2	.30	12.2	8.6	MAR 10.6	1.1	6	10	18
SOUTHERN ETA VIRGINIDS	37	.051	11.6	.134	.233	36	1.0E-02	7.4	6.9	7.4	7.4	.56	10.9	1.9	MAR 11.1	.2	12	16	22
MARCH HERCULIDS	440	.026	9.4	.088	.228	38	2.2E-11	5.9	5.8	5.9	5.9	.75	33.2	.6	MAR 11.8	1.1	12	14	17
CHI HERCULIDS	980	.018	8.6	.065	.195	52	4.1E-25	4.1	4.1	4.1	4.1	.63	41.4	7.1	MAR 11.3	2.0	11	14	22
SOUTHERN VIRGINIDS	2.2	.079	32.8	.116	.159	66	7.8E-02	11.1	5.6	9.1	12.2	.11	3.4	3.6	MAR 29.1	38.0	31	63	96
MARCH VIRGINIDS	8.2	.060	9.7	.124	.183	58	2.2E-02	4.1	3.2	4.0	4.2	.26	3.8	2.3	MAR 21.1	69.7	11	19	34
MARCH LYRIDS	55	.044	11.7	.121	.223	40	9.8E-04	7.0	6.6	7.0	7.0	.69	12.9	1.5	MAR 25.4	2.0	14	17	21
HERCULIDS-LYRIDS	200	.023	9.2	.073	.164	68	2.5E-15	2.9	2.9	2.9	2.9	.53	15.8	0.0	MAR 25.3	2.1	11	15	18
TAU DRACONIDS	990	.012	19.6	.043	.130	84	9.2E-59	3.2	3.2	3.2	3.2	.39	36.9	3.1	MAR 27.6	30.5	26	40	58
PI DRACONIDS	17	.050	9.5	.117	.186	57	3.4E-03	4.1	3.5	4.1	4.1	.39	5.5	6.0	APR 03.1	45.3	13	20	29
NORTHERN VIRGINIDS	6.0	.060	31.3	.116	.168	65	1.6E-02	10.9	7.8	10.5	11.0	.06	5.3	2.6	MAR 31.2	42.0	29	63	92
LIBRIDS	86	.025	20.5	.073	.143	78	3.8E-13	4.5	4.3	4.5	4.5	.17	12.8	3.1	MAR 31.2	41.9	20	38	63
LAMBDA AURIGIDS	12	.063	20.4	.140	.214	44	5.7E-02	11.4	9.6	11.5	11.6	.45	7.7	.6	APR 02.5	46.9	24	35	48
APRIL VIRGINIDS	49	.045	8.1	.122	.222	40	1.4E-03	4.9	4.6	4.9	4.9	.56	10.1	9.4	APR 07.6	1.1	9	12	21
NU HERCULIDS	120	.035	11.6	.105	.218	42	4.4E-06	6.7	6.5	6.7	6.7	.42	18.6	3.7	APR 08.3	2.1	12	18	21
ALPHA VIRGINIDS	23	.038	30.7	.093	.153	73	1.1E-05	8.2	7.3	8.2	8.2	.25	9.0	1.1	APR 07.5	56.9	35	61	92

Table 1-2 (Cont.)

1	2	3	4	5	6	7	8	9	10	11	12	13	14	15	16	17	18	19	20
EPSILON LYRIDS	79	.047	6.9	.135	.262	26	5.3E-03	5.1	4.9	5.1	5.1	.65	13.1	.6	APR 02.4	14.0	8	10	14
APRIL CYGNIDS	15	.086	20.6	.198	.310	18	9.4E-01	16.9	16.7	19.6	19.7	.24	11.2	5.3	APR 08.9	1.0	17	30	34
MARCH ANDROMEDIDS	6.1	.084	17.8	.163	.236	37	3.3E-01	11.2	9.2	12.3	12.9	.39	5.8	10.1	MAR 29.2	38.0	17	26	45
Q DRACONIDS	34	.053	10.7	.138	.237	34	1.7E-02	7.0	6.4	7.0	7.0	.42	10.1	1.5	APR 09.5	4.9	10	15	23
GAMMA VIRGINIDS	190	.029	6.6	.091	.204	48	3.5E-09	3.4	3.4	3.4	3.4	.48	16.7	.6	APR 14.1	14.0	7	10	14
THETA LIBRIDS	230	.021	10.9	.067	.155	72	1.4E-18	3.0	3.0	3.0	3.0	.21	17.3	.9	APR 07.7	54.9	11	20	31
APRIL URSIDS	10	.083	16.1	.178	.268	27	5.0E-01	11.8	10.7	13.2	13.4	.75	7.6	1.1	APR 13.5	50.9	18	21	33
G DRACONIDS	44	.029	12.2	.078	.139	80	8.1E-10	2.4	2.3	2.4	2.4	.16	6.8	2.6	APR 22.9	31.5	13	25	33
ETA TAURIDS	52	.037	14.2	.101	.185	57	1.1E-05	6.1	5.7	6.1	6.1	.13	11.6	.7	MAY 09.2	29.0	14	28	41
R DRACONIDS	20	.057	10.0	.137	.222	40	2.8E-02	6.0	5.3	6.0	6.0	.49	7.2	4.4	MAY 07.5	25.8	12	17	24
GAMMA PEGASIDS	3300	.013	9.9	.051	.194	53	2.7E-49	4.6	4.6	4.6	4.6	.34	81.0	13.0	MAY 07.9	1.1	10	16	20
MAY PISCIDS	130	.038	12.3	.115	.242	33	6.1E-05	8.3	8.0	8.3	8.3	.42	21.4	10.1	MAY 08.0	1.2	12	18	21
EPSILON ARIETIDS	19	.059	16.6	.141	.226	39	4.2E-02	10.2	9.0	10.3	10.3	.51	9.1	2.5	MAY 08.1	27.1	18	25	39
OMICRON CETIDS	430	.026	7.9	.088	.227	38	2.2E-11	4.9	4.8	4.9	4.9	.52	30.0	10.0	MAY 14.4	14.1	8	11	16
MAY ARIETIDS	20	.154	36.0	.371	.599	4	1.3E•01	34.6	84.3	95.8	96.0	.41	28.7	2.2	MAY 22.0	29.1	37	56	74
SOUTHERN MAY OPHIUCHIDS	73	.030	11.1	.085	.164	68	6.6E-09	3.6	3.4	3.6	3.6	.20	10.6	1.8	MAY 12.6	43.0	12	22	31
NORTHERN MAY OPHIUCHIDS	3.7	.082	16.6	.141	.198	51	1.7E-01	8.2	5.5	8.1	9.2	.24	3.8	6.8	MAY 12.7	68.8	17	30	45
EPSILON AQUILIDS	53	.053	13.2	.145	.266	25	2.7E-02	9.9	9.4	9.9	9.9	.59	15.0	12.5	MAY 20.2	2.1	13	17	25
MAY URSIDS	9.9	.072	18.8	.154	.232	37	1.7E-01	11.8	9.9	12.3	12.5	.35	7.3	3.5	MAY 21.1	31.8	22	35	46
MAY LYRIDS	49	.048	11.3	.131	.236	35	4.9E-03	7.4	7.0	7.4	7.4	.45	12.5	4.8	MAY 20.8	2.3	11	16	21
MAY DRACONIDS	71	.031	14.7	.088	.168	66	2.7E-08	5.0	4.8	5.0	5.0	.28	12.3	2.0	MAY 21.1	31.8	17	29	42
MAY CASSIOPEIDS	9.6	.052	16.7	.111	.166	67	3.7E-03	5.6	4.4	5.5	5.6	.18	4.8	13.8	MAY 30.3	43.4	16	30	49
CHI SCORPIIDS	6.2	.080	19.5	.156	.226	40	2.4E-01	11.7	9.3	12.4	13.0	.34	5.9	3.7	JUN 03.6	57.0	20	32	38

Table 1-2 (Cont.)

1	2	3	4	5	6	7	8	9	10	11	12	13	14	15	16	17	18	19	20
JUNE CAMELOPARDALIDS	180	.026	14.4	.081	.180	60	9.1E-12	5.8	5.7	5.8	5.8	.32	21.1	14.1	JUN 04.9	3.8	14	23	34
ARIETIDS	12	.065	30.8	.144	.221	41	7.9E-02	18.1	15.2	18.4	18.5	.49	9.8	7.8	JUN 11.4	41.8	34	48	64
PSI AURIGIDS	61	.033	14.6	.092	.172	64	2.6E-07	5.3	5.0	5.3	5.3	.22	11.7	10.3	JUN 18.3	32.5	15	27	41
JUNE AURIGIDS	13	.045	17.4	.101	.156	72	3.7E-04	4.9	4.1	4.9	4.9	.13	5.2	2.4	JUN 13.3	71.3	17	34	62
ZETA PERSEIDS	8.8	.155	35.8	.324	.483	9	5.7E+00	32.7	71.4	90.1	92.0	.34	18.6	4.3	JUN 12.6	44.0	35	56	81
M DRACONIDS	46	.045	8.7	.121	.218	42	1.3E-03	5.1	4.7	5.1	5.1	.60	10.0	1.1	JUN 16.8	1.2	10	13	19
OPHIUCHIDS	32	.035	14.3	.090	.154	73	1.2E-06	3.9	3.5	3.9	3.9	.19	7.3	.2	JUN 10.1	44.1	15	28	44
JUNE LYRIDS	60	.041	6.6	.114	.213	44	2.1E-04	3.7	3.5	3.7	3.7	.36	9.7	8.8	JUN 17.1	1.9	7	11	17
JUNE CYGNIDS	33	.057	15.9	.147	.253	29	4.7E-02	11.2	10.4	11.3	11.3	.49	12.6	.7	JUN 18.5	4.5	17	24	26
JUNE AQUILIDS	48	.036	17.6	.098	.176	62	4.4E-06	6.7	6.3	6.7	6.7	.05	11.8	11.3	JUN 17.2	30.0	16	35	47
SCORPIIDS-SAGITTARIIDS	14	.072	22.5	.164	.255	29	2.4E-01	15.9	14.1	16.6	16.7	.49	10.0	1.5	JUN 23.6	42.9	22	31	46
ALPHA DRACONIDS	2.0	.093	28.4	.133	.181	57	2.0E-01	12.3	6.7	11.0	15.3	.26	3.6	4.4	JUN 25.5	46.6	31	54	80
SIGMA CAPRICORNIDS	6.1	.062	23.9	.120	.174	62	2.4E-02	9.1	6.5	8.8	9.2	.14	4.9	5.8	JUN 30.6	56.9	23	45	71
JUNE SCUTIDS	11	.060	17.9	.131	.199	50	3.0E-02	8.8	7.2	8.8	8.9	.18	6.5	13.3	JUN 30.6	57.0	17	32	48
THETA AURIGIDS	22	.045	21.3	.110	.179	60	6.3E-04	8.5	7.5	8.5	8.5	.10	8.9	4.8	JUL 02.6	56.0	19	39	64
TAURIDS-ARIETIDS	22	.053	17.5	.129	.211	45	1.1E-02	9.7	8.6	9.7	9.7	.29	9.6	3.6	JUL 02.0	29.1	16	27	40
MU SAGITTARIIDS	24	.042	16.5	.104	.171	64	1.5E-04	5.9	5.3	5.9	5.9	.42	7.8	1.5	JUL 07.6	43.0	20	30	41
AQUARIDS-AQUILIDS	190	.020	19.9	.063	.141	79	1.1E-20	4.1	4.1	4.1	4.1	.36	18.3	13.1	JUN 30.7	29.0	24	38	57
CHI SAGITTARIIDS	8600	.010	8.1	.041	.193	53	2.0E-84	3.8	3.8	3.8	3.8	.68	119	2.5	JUL 01.6	1.0	9	11	17
P DRACONIDS	90	.035	11.5	.102	.202	49	3.3E-06	5.9	5.7	5.9	5.9	.36	15.0	5.0	JUL 02.0	4.0	12	19	31
BOOTIDS-DRACONIDS	6800	.009	7.8	.037	.162	69	6.1-105	2.4	2.4	2.4	2.4	.27	84.3	1.6	JUL 02.4	2.9	7	12	19
J DRACONIDS	23	.053	12.0	.130	.214	44	1.2E-02	6.8	6.0	6.8	6.8	.33	8.2	1.5	JUL 01.9	1.6	13	21	30
EPSILON CEPHEIDS	46	.047	9.4	.127	.228	38	3.1E-03	5.8	5.4	5.8	5.8	.63	10.7	.2	JUL 01.8	1.0	11	14	23
BETA ANDROMEDIDS	640	.019	7.8	.066	.184	58	1.6E-22	3.3	3.3	3.3	3.3	.33	30.1	8.5	JUL 01.8	1.1	8	13	18

Table 1-2 (Cont.)

1	2	3	4	5	6	7	8	9	10	11	12	13	14	15	16	17	18	19	20
LACERTIDS	22	.064	14.4	.156	.255	29	1.2E-01	10.2	9.2	10.4	10.4	.58	9.9	.4	JUL 03.1	3.6	16	21	27
OMEGA DRACONIDS	5.8	.147	30.4	.282	.407	14	3.3E+00	26.2	46.4	62.6	66.1	.34	12.8	1.5	JUL 01.4	30.4	30	48	65
CYGNIDS-DRACONIDS	18	.067	16.6	.206	.329	15	1.2E+00	14.1	14.4	16.6	16.6	.56	11.3	5.2	JUL 02.8	3.5	18	24	28
KAPPA PERSEIDS	250	.025	9.9	.081	.189	55	1.1E-12	4.4	4.4	4.4	4.4	.32	21.8	13.4	JUL 01.9	1.1	11	18	23
KAPPA AURIGIDS	20	.042	11.3	.101	.163	68	1.3E-04	3.6	3.1	3.6	3.6	.08	5.5	2.6	JUL 09.6	14.1	10	21	35
BETA TAURIDS	28	.037	19.9	.094	.157	71	6.0E-06	5.7	5.2	5.7	5.7	.10	8.3	.2	JUN 26.1	43.0	20	41	66
TAU CAPRICORNIDS	15	.077	28.2	.177	.277	24	4.4E-01	21.5	19.8	23.2	23.4	.52	12.2	2.6	JUL 07.7	42.8	29	40	54
UPSILON DRACONIDS	120	.032	12.5	.096	.199	50	1.7E-07	6.2	6.0	6.2	6.2	.36	17.9	2.7	JUL 16.6	4.9	12	19	33
SIGMA CASSIOPEIDS	17	.059	14.1	.139	.220	41	3.8E-02	8.3	7.2	8.3	8.3	.52	7.8	2.4	JUL 16.0	3.5	16	22	38
JULY CEPHEIDS	75	.033	17.0	.094	.182	59	3.4E-07	7.0	6.7	7.0	7.0	.32	14.9	.7	JUL 16.6	4.6	19	31	42
JULY CASSIOPEIDS	52	.034	17.3	.093	.170	65	7.1E-07	6.1	5.7	6.1	6.1	.38	11.6	.9	JUL 16.4	4.5	22	34	48
RHO DRACONIDS	51	.042	12.4	.115	.209	46	3.2E-04	6.7	6.4	6.7	6.7	.25	12.1	2.0	JUL 15.9	3.4	12	21	29
KAPPA CASSIOPEIDS	35	.044	13.8	.115	.198	51	6.2E-04	6.8	6.3	6.8	6.8	.16	10.1	6.6	JUL 16.5	4.6	13	25	36
CASSIOPEIDS	13	.066	28.3	.146	.229	38	1.0E-01	17.5	15.0	17.9	18.0	.28	10.0	3.2	JUL 16.5	4.5	27	46	60
J CEPHEIDS	420	.022	7.2	.074	.191	54	1.5E-16	3.3	3.2	3.3	3.3	.85	24.2	3.8	JUL 16.4	2.5	11	12	17
JULY DRACONIDS	29	.062	13.6	.158	.266	26	1.1E-01	10.1	9.3	10.3	10.3	.42	11.3	8.0	JUL 16.6	5.0	12	18	26
ZETA URSIDS	9.7	.061	25.4	.130	.195	52	3.2E-02	12.2	9.8	12.1	12.3	.35	7.2	1.5	JUL 11.9	70.2	27	43	60
PSI CASSIOPEIDS	23	.059	16.4	.145	.238	34	5.1E-02	10.8	9.7	10.9	10.9	.44	10.4	6.2	JUL 16.5	4.6	17	25	34
CANES VENATICIDS	7.3	.091	19.4	.183	.269	28	6.4E-01	14.0	12.7	16.6	17.2	.36	7.3	5.1	JUL 18.4	56.8	19	30	40
OMICRON DRACONIDS	57	.037	8.1	.102	.190	55	1.2E-05	3.6	3.4	3.6	3.6	.25	9.4	2.9	JUL 21.1	14.0	8	14	20
PI AQUARIDS	9.3	.093	22.3	.197	.294	22	9.1E-01	17.3	17.1	21.3	21.7	.44	9.3	8.9	JUL 31.7	35.0	21	31	43
SOUTHERN DELTA AQUARIDS	81	.041	49.2	.118	.230	37	2.8E-04	31.1	29.8	31.1	31.1	.73	32.8	7.8	JUL 31.7	35.0	59	70	80
A CEPHEIDS	18	.071	24.6	.168	.268	25	2.7E-01	18.3	16.7	19.2	19.2	.54	12.2	.5	JUL 30.4	4.6	25	34	46
CEPHEIDS-DRACONIDS	32	.054	15.5	.139	.238	34	2.2E-02	10.2	9.4	10.2	10.2	.27	11.8	1.7	JUL 30.4	4.9	14	24	36

Table 1-2 (Cont.)

1	2	3	4	5	6	7	8	9	10	11	12	13	14	15	16	17	18	19	20
OMICRON CEPHEIDS	24	.044	19.1	.109	.180	60	4.3E-04	7.6	6.8	7.6	7.6	.29	8.9	1.2	JUL 30.4	4.9	25	42	53
IOTA CEPHEIDS	23	.034	12.6	.086	.145	78	3.8E-07	2.8	2.6	2.8	2.8	.19	5.8	.5	JUL 30.5	4.8	21	39	42
B CASSIOPEIDS	51	.040	13.7	.109	.199	50	9.6E-05	6.8	6.4	6.8	6.8	.44	12.2	4.4	JUL 30.5	4.4	15	22	37
GAMMA CEPHEIDS	5.3	.067	21.9	.126	.181	59	4.7E-02	9.1	6.4	8.8	9.3	.30	4.6	5.4	JUL 30.6	4.6	24	40	64
B CEPHEIDS	110	.027	17.3	.080	.165	68	4.9E-11	5.6	5.4	5.6	5.6	.28	16.2	6.8	JUL 30.6	4.6	20	34	55
IOTA CASSIOPEIDS	13	.061	16.0	.137	.211	45	4.3E-02	8.8	7.4	8.9	8.9	.33	7.1	7.2	JUL 30.6	4.6	16	26	39
MU CANCRIDS	140	.024	22.6	.073	.156	72	3.9E-14	6.3	6.2	6.3	6.3	.35	19.5	1.5	JUL 24.1	42.9	27	43	68
D CAMELOPARDALIDS	930	.014	16.2	.050	.150	75	9.8E-43	4.0	4.0	4.0	4.0	.45	40.0	15.4	JUL 30.5	5.0	22	32	48
E DRACONIDS	18	.059	19.2	.140	.223	40	4.0E-02	11.5	10.1	11.6	11.6	.48	9.5	14.3	JUL 30.5	5.0	21	30	42
L DRACONIDS	110	.036	9.7	.107	.219	41	1.0E-05	5.7	5.5	5.7	5.7	.34	16.4	10.4	JUL 30.5	5.0	10	16	21
AUGUST LYNCIDS	11	.059	18.6	.129	.196	52	2.4E-02	8.9	7.3	8.9	9.0	.53	6.5	10.4	JUL 30.5	30.4	22	30	51
AQUARIDS-CAPRICORNIDS	16	.076	30.5	.177	.279	23	4.2E-01	23.4	21.6	25.2	25.3	.30	13.2	.8	AUG 06.6	23.1	27	45	54
ALPHA CAPRICORNIDS	3.5	.100	26.5	.169	.237	38	5.0E-01	16.4	13.0	19.3	22.2	.32	5.8	5.5	AUG 17.1	46.0	27	44	67
SOUTHERN IOTA AQUARIDS	50	.030	34.7	.082	.149	76	4.5E-09	8.5	8.0	8.5	8.5	.33	13.5	2.8	AUG 09.7	78.8	40	65	103
BETA CEPHEIDS	97	.032	13.6	.094	.189	55	1.4E-07	6.0	5.8	6.0	6.0	.23	15.8	0.0	AUG 12.3	2.6	14	25	37
C DRACONIDS	8.9	.092	23.3	.193	.288	23	8.3E-01	17.9	17.2	21.7	22.1	.60	9.2	.8	AUG 12.9	3.9	27	35	46
AUGUST CASSIOPEIDS	21	.053	21.3	.129	.209	46	1.1E-02	11.5	10.2	11.6	11.6	.60	10.2	1.0	AUG 14.7	7.1	30	39	52
GAMMA CYGNIDS	98	.032	6.4	.094	.189	55	1.4E-07	3.7	3.6	3.7	3.7	.38	12.5	14.0	AUG 14.6	7.0	11	17	25
PERSEIDS	470	.026	5.3	.088	.232	36	2.4E-11	3.4	3.4	3.4	3.4	.34	26.1	1.4	AUG 12.2	2.3	5	8	9
GAMMA CASSIOPEIDS	2400	.013	9.9	.050	.178	61	2.0E-49	3.9	3.9	3.9	3.9	.53	63.3	1.5	AUG 13.5	4.4	11	15	24
L CEPHEIDS	2.0	.144	26.2	.205	.280	33	1.1E+00	17.7	18.5	30.5	42.8	.14	6.1	2.7	AUG 13.4	30.4	25	49	72
AUGUST CEPHEIDS	13	.072	19.1	.162	.250	31	2.2E-01	13.2	11.6	13.8	13.9	.25	8.8	1.4	AUG 14.7	6.9	20	35	39
AUGUST DRACONIDS	7.3	.085	40.0	.171	.251	32	4.2E-01	27.2	23.5	30.5	31.5	.36	9.9	1.2	AUG 14.6	7.3	38	60	87

Table 1-2 (Cont.)

1	2	3	4	5	6	7	8	9	10	11	12	13	14	15	16	17	18	19	20
AUGUST CANCRIDS	11	.053	22.7	.116	.176	62	5.6E-03	8.7	7.0	8.6	8.7	.17	6.4	1.9	AUG 07.2	43.0	21	40	69
PHI DRACONIDS	8.6	.073	32.9	.152	.226	39	1.7E-01	19.9	16.3	20.7	21.1	.38	8.8	1.3	AUG 14.6	7.2	35	54	79
AUGUST UMIDS	20	.050	26.4	.120	.194	53	4.1E-03	12.5	11.0	12.5	12.5	.29	10.3	10.1	AUG 14.6	7.0	28	47	67
E CAMELOPARDALIDS	9.7	.078	20.2	.166	.250	32	3.1E-01	13.8	12.0	14.9	15.2	.38	7.9	12.2	AUG 15.0	6.1	20	31	46
AUGUST URSIDS	100	.024	16.1	.071	.143	78	2.8E-14	3.5	3.4	3.5	3.5	.13	12.2	13.9	AUG 14.0	4.0	17	34	49
NORTHERN DELTA AQUARIDS	9.1	.057	23.5	.120	.179	60	1.3E-02	9.4	7.4	9.3	9.5	.11	6.1	8.2	AUG 19.1	44.0	22	45	75
AUGUST CAMELOPARDALIDS	9.2	.064	21.6	.135	.202	49	5.1E-02	11.0	8.8	11.0	11.2	.31	6.6	7.1	AUG 14.6	7.1	20	33	58
EPSILON URSIDS	10	.074	29.2	.159	.239	35	2.1E-01	19.0	16.2	20.0	20.3	.54	9.3	3.0	AUG 21.1	73.4	31	42	67
MU DRACONIDS	2.3	.122	21.8	.182	.250	37	7.4E-01	13.8	11.7	18.8	24.7	.35	4.9	0.0	AUG 30.0	38.0	27	43	58
BETA URSIDS	8.0	.088	13.7	.181	.267	28	5.7E-01	9.8	8.9	11.4	11.7	.58	6.3	2.5	AUG 20.8	45.7	16	21	30
GAMMA LEONIDS	3.1	.098	26.6	.161	.223	42	4.0E-01	15.3	11.3	17.0	20.3	.24	5.2	5.4	AUG 28.1	29.1	26	46	73
NORTHERN IOTA AQUARIDS	4.1	.125	32.3	.221	.312	24	1.4E+00	24.6	28.9	41.4	46.0	.22	9.0	3.2	AUG 26.1	30.1	30	54	78
CASSIOPEIDS-CEPHEIDS	54	.041	8.6	.113	.207	47	1.9E-04	4.6	4.3	4.6	4.6	.65	10.3	0.0	AUG 27.6	2.6	12	15	21
A CASSIOPEIDS	8.6	.082	16.1	.171	.254	31	3.9E-01	11.1	9.7	12.3	12.5	.27	6.8	1.7	AUG 27.1	3.6	14	24	32
XI LEONIDS	31	.054	17.7	.138	.236	35	2.1E-02	11.5	10.5	11.5	11.5	.58	12.4	1.4	AUG 28.0	1.1	19	25	33
OMEGA CASSIOPEIDS	63	.033	19.4	.092	.174	63	2.9E-07	7.2	6.8	7.2	7.2	.42	13.9	.5	AUG 28.0	5.5	24	36	55
E URSIDS	180	.027	8.5	.084	.187	56	8.1E-11	3.7	3.7	3.7	3.7	.50	17.0	10.9	AUG 28.5	4.8	10	14	25
F CAMELOPARDALIDS	18	.061	16.3	.145	.231	37	5.9E-02	10.3	9.1	10.4	10.4	.26	9.0	9.5	AUG 28.4	4.9	15	26	37
XI DRACONIDS	2.2	.092	27.8	.135	.185	55	2.0E-01	12.4	7.1	11.5	15.4	.39	3.8	0.0	SEP 10.9	31.8	32	49	82
SEPTEMBER LYRIDS	2.3	.112	21.4	.167	.229	41	5.4E-01	12.5	9.3	14.9	19.6	.36	4.4	3.3	SEP 01.6	71.1	28	44	53
ALPHA TRIANGULIDS	62	.047	9.7	.131	.246	31	4.2E-03	6.7	6.4	6.7	6.7	.60	13.3	12.3	SEP 08.3	2.2	10	13	20
TAU LEONIDS	15	.073	20.6	.168	.263	27	2.9E-01	15.0	13.5	15.8	15.9	.48	10.1	.8	SEP 11.1	29.0	21	30	37
D CEPHEIDS	9.3	.068	18.8	.144	.215	43	9.5E-02	10.6	8.6	10.8	11.0	.24	6.6	0.0	SEP 09.9	5.9	17	30	49

Table 1-2 (Cont.)

1	2	3	4	5	6	7	8	9	10	11	12	13	14	15	16	17	18	19	20
C CASSIOPEIDS	24	.055	10.2	.136	.224	39	2.1E-02	6.2	5.6	6.2	6.2	.45	8.0	2.0	SEP 09.9	5.5	11	16	28
RHO CEPHEIDS	210	.020	16.6	.063	.144	78	1.2E-20	3.7	3.7	3.7	3.7	.34	18.3	3.8	SEP 09.9	5.5	20	32	52
CASSIOPEIDS-CAMELOPARDALIDS	55	.035	17.8	.097	.178	61	2.0E-06	6.9	6.6	6.9	6.9	.15	12.8	3.5	SEP 10.4	2.7	16	31	50
CEPHEIDS	32	.049	27.8	.126	.216	43	4.6E-03	15.9	14.5	15.9	15.9	.49	14.8	.5	SEP 10.1	5.6	34	48	62
BETA UMIDS	180	.025	12.9	.078	.173	63	7.9E-13	4.7	4.6	4.7	4.7	.39	19.1	6.6	SEP 09.9	5.9	15	23	38
C CAMELOPARDALIDS	110	.026	21.1	.077	.158	71	5.6E-12	6.2	6.0	6.2	6.2	.26	17.0	1.7	SEP 10.1	5.6	23	40	66
RHO URSIDS	35	.041	13.5	.107	.185	57	1.2E-04	5.7	5.3	5.7	5.7	.39	9.3	9.3	SEP 11.2	3.6	15	23	40
B CAMELOPARDALIDS	14	.047	25.2	.107	.166	67	9.4E-04	8.4	7.0	8.3	8.4	.22	7.1	2.0	SEP 11.0	3.7	26	47	68
H CAMELOPARDALIDS	18	.060	14.5	.142	.227	38	4.9E-02	8.9	7.8	9.0	9.0	.54	8.3	2.3	SEP 11.1	3.4	17	23	35
ALPHA CAMELOPARDALIDS	8.6	.058	20.4	.121	.180	60	1.5E-02	8.2	6.4	8.1	8.3	.31	5.5	3.1	SEP 10.1	5.6	23	38	54
SEPTEMBER URSIDS	90	.048	51.4	.140	.277	22	8.9E-03	39.9	38.4	39.9	39.9	.76	39.2	9.0	SEP 09.9	24.2	56	65	77
DRACONIDS-UMIDS	13	.057	24.4	.128	.198	51	1.9E-02	11.9	10.0	11.9	12.0	.21	8.2	8.3	SEP 12.3	28.9	27	49	61
ETA DRACONIDS	15	.055	15.5	.127	.198	51	1.3E-02	7.6	6.5	7.6	7.7	.42	7.0	4.1	SEP 11.0	3.9	22	33	40
EPSILON UMIDS	5.0	.083	14.9	.154	.220	42	2.5E-01	8.6	6.6	9.1	9.8	.30	4.6	1.7	SEP 11.1	3.8	15	25	38
SEPTEMBER DRACONIDS	6.6	.053	25.1	.105	.152	73	3.4E-03	6.8	5.0	6.5	6.8	.16	4.4	0.0	SEP 11.2	29.3	28	54	76
PISCIDS	4.7	.075	52.6	.137	.195	52	1.1E-01	25.2	17.8	24.9	27.0	.15	7.4	2.2	SEP 09.2	56.0	48	93	139
SEPTEMBER CEPHEIDS	2.0	.132	21.5	.188	.256	36	8.3E-01	13.7	12.2	20.0	28.1	.27	4.9	7.0	SEP 16.1	14.1	24	41	54
ARIETIDS-PISCIDS	14	.060	28.0	.136	.212	44	3.8E-02	15.5	13.2	15.6	15.7	.32	9.7	1.3	SEP 16.2	58.0	28	46	71
GAMMA PISCIDS	44	.032	17.3	.086	.153	73	6.1E-08	4.6	4.3	4.6	4.6	.10	9.3	7.3	SEP 23.6	57.0	17	35	47
GAMMA ARIETIDS	140	.032	9.3	.096	.208	46	2.0E-07	5.0	4.9	5.0	5.0	.38	17.3	7.1	SEP 20.7	5.0	11	17	23
ETA PERSEIDS	86	.037	10.5	.107	.211	45	1.8E-05	5.8	5.6	5.8	5.8	.38	14.6	11.8	SEP 23.3	2.2	11	17	26
XI CEPHEIDS	45	.034	16.2	.091	.164	68	6.1E-07	5.2	4.8	5.2	5.2	.13	10.0	8.9	SEP 22.4	8.7	16	32	57
RHO PISCIDS	170	.027	13.0	.084	.184	58	7.6E-11	5.5	5.4	5.5	5.5	.36	20.1	7.2	SEP 20.7	5.0	14	22	37

Table 1-2 (Cont.)

1	2	3	4	5	6	7	8	9	10	11	12	13	14	15	16	17	18	19	20
KAPPA CEPHEIDS	40	.040	24.2	.106	.187	56	7.5E-05	10.6	9.8	10.6	10.6	.30	13.4	4.1	SEP 22.4	8.8	27	45	62
F CEPHEIDS	57	.036	12.3	.100	.184	58	5.3E-06	5.2	4.9	5.2	5.2	.20	11.3	12.1	SEP 20.7	5.3	12	22	37
SEPTEMBER CASSIOPEIDS	20	.052	19.9	.125	.202	49	7.7E-03	10.1	8.9	10.1	10.2	.15	9.3	5.4	SEP 24.0	3.6	18	35	49
D CASSIOPEIDS	580	.022	8.1	.076	.208	46	2.1E-16	4.3	4.3	4.3	4.3	.27	32.8	5.8	SEP 24.5	4.4	7	12	22
H CEPHEIDS	12	.067	12.2	.148	.227	39	1.1E-01	7.5	6.3	7.7	7.7	.51	6.3	2.3	SEP 24.4	4.6	13	18	28
GAMMA UMIDS	120	.029	9.8	.087	.181	59	2.2E-09	4.0	3.9	4.0	4.0	.22	14.3	5.9	SEP 24.4	4.7	10	18	26
D URSIDS	20	.046	12.8	.111	.179	60	8.9E-04	5.0	4.4	5.0	5.0	.24	6.6	8.6	SEP 24.4	4.8	13	23	37
SEPTEMBER CAMELOPARDALIDS	32	.040	28.6	.103	.176	62	6.0E-05	10.9	10.0	10.9	10.9	.17	12.2	.5	SEP 24.5	4.5	30	57	73
CAMELOPARDALIDS	7.1	.068	34.1	.136	.200	50	7.3E-02	17.0	13.0	17.0	17.6	.13	7.3	.5	SEP 24.9	3.8	33	66	86
SEPTEMBER UMIDS	13	.059	16.8	.133	.205	48	2.9E-02	8.8	7.4	8.8	8.9	.35	7.0	3.4	SEP 24.4	4.8	17	27	47
A CAMELOPARDALIDS	660	.013	33.3	.045	.127	85	5.5E-50	5.0	5.0	5.0	5.0	.50	37.7	2.6	SEP 24.4	4.7	37	52	73
D DRACONIDS	10	.116	24.0	.249	.375	13	2.7E+00	20.9	27.5	34.0	34.5	.38	12.2	4.6	SEP 24.4	4.8	22	34	48
DELTA PISCIDS	2.5	.106	27.5	.163	.224	43	4.6E-01	15.8	11.5	18.0	23.0	.34	5.0	.6	OCT 07.1	30.0	28	45	75
OCTOBER ANDROMEDIDS	32	.043	14.2	.111	.189	55	3.4E-04	6.4	5.8	6.4	6.4	.30	9.3	11.7	OCT 07.6	3.0	15	25	32
OCTOBER CEPHEIDS	8.1	.065	19.9	.134	.198	51	5.3E-02	9.8	7.6	9.7	10.0	.26	5.9	4.9	OCT 08.0	4.0	19	33	57
G CEPHEIDS	380	.020	12.3	.067	.169	65	2.1E-20	4.2	4.2	4.2	4.2	.50	26.2	7.7	OCT 08.0	4.0	15	21	31
OCTOBER DRACONIDS	21	.055	28.8	.133	.217	43	1.8E-02	16.5	14.6	16.6	16.6	.48	12.2	1.4	OCT 08.0	4.0	31	44	67
K CAMELOPARDALIDS	56	.045	10.9	.124	.230	37	1.6E-03	6.8	6.5	6.8	6.8	.45	12.8	7.2	OCT 08.0	3.5	11	16	21
THETA DRACONIDS	3.1	.116	19.6	.190	.264	33	8.3E-01	13.2	12.1	18.3	21.8	.42	5.4	7.0	OCT 08.4	32.6	22	33	48
SEXTANTIDS	240	.037	7.2	.119	.277	23	5.2E-05	5.6	5.5	5.6	5.6	.61	24.0	12.0	OCT 08.4	2.1	7	9	11
L CAMELOPARDALIDS	38	.041	19.1	.108	.189	55	1.3E-04	8.5	7.9	8.5	8.5	.34	11.8	1.9	OCT 08.0	3.8	20	32	50
DELTA URSIDS	90	.047	9.7	.137	.272	24	6.1E-03	7.4	7.2	7.4	7.4	.56	16.9	6.4	OCT 08.4	2.7	9	12	19
J CAMELOPARDALIDS	460	.023	9.6	.078	.204	48	5.7E-15	5.0	4.9	5.0	5.0	.56	31.3	4.9	OCT 09.0	3.4	12	16	24

Table 1-2 (Cont.)

1	2	3	4	5	6	7	8	9	10	11	12	13	14	15	16	17	18	19	20
LAMBDA DRACONIDS	10	.094	20.6	.202	.303	20	1.0E+00	16.4	16.6	20.5	20.8	.38	9.4	2.7	OCT 08.4	4.6	20	31	39
A URSIDS	8.3	.118	21.2	.244	.362	15	2.4E+00	18.1	23.6	30.0	30.7	.51	10.4	5.6	OCT 09.0	3.3	23	32	43
N DRACONIDS	57	.031	11.2	.086	.159	71	2.2E-08	3.3	3.1	3.3	3.3	.44	9.0	6.9	OCT 08.8	3.7	15	22	26
G CAMELOPARDALIDS	19	.045	11.4	.108	.173	64	5.4E-04	4.1	3.6	4.1	4.1	.37	5.8	2.7	OCT 10.7	9.0	16	25	39
DRACONIDS-CAMELOPARDALIDS	7.8	.075	34.4	.153	.226	40	1.9E-01	20.8	16.9	21.7	22.3	.58	8.6	1.1	OCT 09.0	3.3	44	58	69
C URSIDS	20	.055	15.3	.132	.214	44	1.8E-02	8.6	7.6	8.6	8.7	.26	8.6	3.1	OCT 08.3	4.7	15	26	39
SOUTHERN ARIETIDS	8.5	.128	57.6	.266	.395	13	3.2E+00	50.4	75.5	95.7	98.0	.47	18.9	1.8	SEP 29.7	45.0	58	83	127
PSI VIRGINIDS	11	.077	13.8	.168	.255	30	3.2E-01	9.7	8.6	10.4	10.6	.13	7.1	2.1	OCT 10.1	27.0	11	22	27
ORIONIDS	76	.044	12.2	.126	.243	32	1.4E-03	8.3	7.9	8.3	8.3	.49	16.4	.8	OCT 20.8	1.0	12	17	18
M CEPHEIDS	44	.041	10.5	.110	.196	52	1.5E-04	5.1	4.7	5.1	5.1	.17	9.8	12.2	OCT 22.5	4.7	10	19	24
E CEPHEIDS	330	.019	11.6	.063	.155	73	8.0E-23	3.2	3.1	3.2	3.2	.13	21.2	10.1	OCT 22.1	3.8	11	22	24
BETA CAMELOPARDALIDS	190	.028	6.9	.088	.197	51	6.0E-10	4.3	4.2	4.3	4.3	.46	18.7	10.0	OCT 22.0	3.4	9	13	20
B URSIDS	51	.036	16.7	.098	.179	60	4.7E-06	6.6	6.2	6.6	6.6	.38	12.0	3.9	OCT 23.0	3.9	20	31	52
TAU URSIDS	27	.050	12.7	.126	.210	45	5.5E-03	7.0	6.3	7.0	7.0	.36	9.0	.5	OCT 23.1	3.5	12	19	30
OCTOBER URSIDS	8.5	.064	21.7	.133	.198	51	4.7E-02	10.6	8.3	10.6	10.8	.55	6.3	.8	OCT 23.2	3.6	26	35	50
PSI DRACONIDS	64	.032	21.5	.090	.169	65	8.9E-08	7.4	7.1	7.4	7.4	.15	14.3	0.0	OCT 22.6	4.8	22	43	59
B DRACONIDS	15	.051	18.5	.117	.184	58	4.2E-03	7.8	6.6	7.8	7.8	.32	7.1	2.6	OCT 23.0	4.0	22	36	59
OCTOBER UMIDS	9.4	.045	17.9	.095	.143	78	2.7E-04	4.0	3.1	3.9	4.0	.17	4.0	4.5	OCT 22.5	32.7	20	38	66
ALPHA URSIDS	35	.043	18.0	.112	.194	53	3.8E-04	8.4	7.8	8.4	8.4	.40	11.3	2.7	OCT 23.0	3.9	21	32	41
A DRACONIDS	20	.057	23.6	.137	.222	40	2.8E-02	14.0	12.4	14.1	14.1	.31	11.0	.4	OCT 23.2	3.6	23	38	49
OCTOBER HERCULIDS	21	.049	18.5	.119	.193	53	3.0E-03	8.6	7.6	8.6	8.7	.36	8.8	6.2	OCT 23.0	31.6	21	33	57
TAURIDS	8.0	.084	54.7	.173	.255	31	4.3E-01	37.9	33.2	42.3	43.5	.40	12.2	0.0	NOV 08.1	47.8	53	81	117
TRIANGULIDS	11	.052	13.5	.113	.172	64	4.2E-03	4.9	4.0	4.9	4.9	.30	4.8	13.6	NOV 03.6	25.0	15	25	41

Table 1-2 (Cont.)

1	2	3	4	5	6	7	8	9	10	11	12	13	14	15	16	17	18	19	20
C CEPHEIDS	7.2	.054	15.9	.109	.159	70	4.9E-03	4.8	3.6	4.7	4.8	.21	3.9	13.5	OCT 29.1	17.8	17	31	52
GAMMA TAURIDS	32	.044	19.5	.113	.194	53	5.7E-04	9.2	8.4	9.2	9.2	.40	11.2	6.2	NOV 02.7	27.0	21	32	49
KAPPA DRACONIDS	4.3	.074	17.9	.132	.187	55	9.2E-02	8.0	5.4	7.7	8.5	.38	4.0	.4	OCT 29.9	17.9	22	34	52
EPSILON DRACONIDS	20	.096	15.7	.231	.373	11	2.3E+00	14.0	15.9	18.1	18.2	.71	12.5	6.8	NOV 04.5	3.1	15	18	26
NOVEMBER ORIONIDS	250	.041	6.1	.132	.310	16	8.8E-04	5.1	5.0	5.1	5.1	.75	23.4	10.1	NOV 04.7	3.0	6	7	8
PHI TAURIDS	19	.084	25.0	.201	.322	16	1.0E+00	21.1	21.2	24.2	24.2	.56	14.0	6.9	NOV 05.6	5.1	24	32	43
IOTA AURIGIDS	66	.033	14.5	.093	.176	62	3.0E-07	5.5	5.2	5.5	5.5	.23	12.5	9.4	NOV 05.7	5.0	14	25	35
K CEPHEIDS	890	.018	6.7	.064	.190	55	3.7E-25	3.0	3.0	3.0	3.0	.61	33.9	6.2	NOV 04.3	2.4	7	9	13
DRACONIDS-URSIDS	5.6	.079	31.1	.150	.216	43	2.0E-01	17.6	13.4	18.3	19.4	.29	6.8	3.4	NOV 05.5	5.0	31	52	74
NOVEMBER DRACONIDS	14	.069	19.5	.157	.244	33	1.6E-01	13.1	11.5	13.6	13.6	.42	9.0	.6	NOV 05.4	4.9	22	33	41
IOTA VIRGINIDS	9300	.010	5.4	.041	.196	52	2.1E-84	2.6	2.6	2.6	2.6	.56	102	5.1	NOV 06.0	1.1	6	8	9
F DRACONIDS	76	.035	16.7	.100	.193	53	2.8E-06	7.8	7.5	7.8	7.8	.52	16.0	.4	NOV 06.0	3.7	21	29	38
NOVEMBER CAMELOPARDALIDS	22	.055	16.7	.134	.219	41	1.9E-02	9.8	8.7	9.8	9.8	.48	9.6	4.9	NOV 05.9	3.9	19	27	41
SIGMA TAURIDS	160	.029	9.7	.090	.195	52	2.9E-09	4.6	4.5	4.6	4.6	.53	17.8	.1	DEC 02.6	1.1	11	15	22
MONOCERIDS	110	.038	21.2	.113	.232	36	5.2E-05	13.4	13.0	13.4	13.4	.58	25.2	6.3	NOV 30.2	28.0	22	29	32
K DRACONIDS	56	.039	11.7	.108	.199	50	5.4E-05	5.8	5.5	5.8	5.8	.30	11.8	.8	DEC 04.5	5.0	12	20	28
DECEMBER DRACONIDS	22	.048	22.1	.117	.191	54	2.2E-03	10.1	9.0	10.1	10.1	.55	9.8	1.0	DEC 04.5	5.0	26	35	46
MU GEMINIDS	4.1	.128	28.3	.226	.319	23	1.6E+00	21.8	26.6	38.1	42.4	.35	8.6	.6	NOV 24.7	43.0	27	43	65
CHI ORIONIDS	9.6	.080	32.3	.170	.255	30	3.7E-01	22.6	19.8	24.6	25.1	.40	10.2	.2	DEC 01.1	30.1	31	47	70
GAMMA CAMELOPARDALIDS	5.8	.100	22.1	.192	.277	27	8.3E-01	16.1	15.3	20.7	21.8	.23	7.4	12.8	DEC 03.6	34.9	19	34	51
GEMINIDS	160	.040	85.5	.124	.269	24	3.0E-04	64.6	63.2	64.6	64.6	.72	66.5	8.2	DEC 09.2	14.0	99	118	134
DECEMBER LYNCIDS	57	.036	11.3	.100	.184	58	5.3E-06	4.8	4.5	4.8	4.8	.30	10.8	14.4	DEC 16.4	8.7	12	20	27
DELTA DRACONIDS	21	.047	14.2	.114	.185	57	1.4E-03	6.1	5.4	6.1	6.1	.29	7.4	6.9	DEC 16.5	9.0	16	27	40

2. ADDENDUM TO THE STREAM SEARCH AMONG THE RADIO METEORS OF THE SYNOPTIC-YEAR SAMPLE

2.1 High-Inclination and Retrograde Streams

Since the distribution of meteors of the synoptic-year sample showed a sharp drop at high inclinations and an extremely low level of population in retrograde orbits, we have relaxed somewhat, for these types of orbits, the restrictions in the screening procedure we used to delineate the 256 streams.

The relaxed screening resulted in the detection of 20 more high-inclination and retrograde streams, which are listed in Table 2-1. This table is arranged in the same way as Table 9-2 of Southworth and Sekanina (1973). For the sake of convenience, we list here the contents of the individual columns (all angles are referred to the standard equinox 1950.0):

Column 1. Designation of the stream.

Column 2. Argument of perihelion ω and its mean error (degrees).

Column 3. Longitude of the ascending node Ω and its mean error (degrees).

Column 4. Inclination i and its mean error (degrees).

Column 5. Perihelion distance q and its mean error (a.u.).

Column 6. Eccentricity e and its mean error.

Column 7. Semimajor axis a (a.u.) and revolution period P (years).

Column 8. Longitude of perihelion $\pi = \omega + \Omega$ (degrees) and the date of passage through the node (UT and days in 1950).

Column 9. No-atmosphere velocity V_∞ and its mean error (km sec^{-1}).

Column 10. Right ascension α_R of the corrected mean radiant from individual meteor radiants and its mean error (degrees).

Column 11. Declination δ_R of the corrected mean radiant from individual meteor radiants and its mean error (degrees).

Column 12. Right ascension α_R and sun-oriented celestial longitude $\lambda_R - \lambda_\odot$ of the corrected mean radiant from the stream's mean orbit (degrees).

Column 13. Declination δ_R and celestial latitude β_R of the corrected mean radiant from the stream's mean orbit (degrees).

Column 14. Geocentric V_G and heliocentric V_H velocity at the node (km sec^{-1}).

Column 15. The node (A = ascending; D = descending) and the type of stream (C = circumpolar, with the mean radiant permanently above the horizon at Havana, Illinois; D = daytime; M = mixed, with the mean radiant never more than 10° below the horizon; N = nighttime).

Column 16. Height at maximum ionization h_{max} and its mean error (km).

Column 17. Number of meteors in the sample with $D \leq 0.25$ with respect to the mean orbit, with an asterisk to indicate that the stream was detected in the 1961–65 sample.

The additional search increased the number of retrograde streams from the previous two (Perseids and Orionids) to 15. The most abundant of the new retrograde streams, August Triangulids, is about as populous in our sample as the Orionids are. The other ones are more comparable in population to the Perseids, with an average of stream members of only three or four.

2.2 Revisions among the 256 Previously Reported Streams

The considerations involving the distribution of meteors in the streams and their periods of activity resulted in several minor changes in the list of the detected streams. We already commented (Section 1.3) that the analysis of the D-distribution of α Aurigids showed that the stream does not satisfactorily discriminate from the sporadic background.

Table 2-1. A supplementary list of streams detected in the synoptic-year sample.

1	2	3	4	5	6	7	8	9	10	11	12	13	14	15	16	17
ETA TAURIDS	128.2	37.9	.6	.863	.595	2.129	166.1	16.6	59.3	21.9	59.7	22.2	12.5	D	83.3	28
	1.1	1.1	.7	.006	.009	3.11	APR 28.7	.2	.9	1.8	24.2	1.6	36.7	D	1.0	
ALPHA PEGASIDS	.7	86.1	144.5	.700	.185	.860	86.8	54.2	349.3	13.8	349.5	13.9	53.3	D	92.8	6
	4.7	.2	.8	.019	.024	.80	JUN 17.8	.2	.7	.3	269.9	16.9	26.6	N	2.3	
JUNE PEGASIDS	280.1	86.3	143.0	.774	.256	1.041	6.4	56.6	341.6	11.9	341.7	11.9	55.7	D	93.5	6
	4.5	.3	.7	.015	.022	1.06	JUN 18.0	.2	.7	.5	261.6	18.1	29.8	N	2.2	
ALPHA LACERTIDS	9.3	99.9	72.8	.752	.156	.891	109.2	35.3	342.8	49.5	343.4	49.5	33.5	D	90.8	24
	4.6	.1	.6	.012	.015	.84	JUL 2.2	.3	.8	.4	272.1	50.5	27.0	M	.6	
KAPPA AURIGIDS	72.6	101.9	3.7	.455	.744	1.774	174.5	26.3	94.0	27.5	94.4	27.4	24.0	D	87.6	21
	.9	.5	.9	.008	.011	2.36	JUL 4.3	.4	.4	1.0	352.0	4.0	35.2	D	1.0	
JULY TRIANGULIDS	7.8	113.0	86.4	.094	.839	.581	120.8	33.8	28.2	35.0	28.3	35.3	32.0	D	89.7	8
	1.0	.4	1.3	.010	.018	.44	JUL 16.0	.2	1.9	1.2	286.1	22.1	14.6	D	2.1	
THETA CASSIOPEIDS	32.2	113.2	72.5	.430	.456	.791	145.4	34.4	22.5	55.7	22.8	55.9	32.7	D	90.9	20
	1.6	.2	.9	.010	.014	.70	JUL 16.2	.3	1.3	.5	292.5	42.3	24.9	C	.9	
JULY ANDROMEDIDS	43.0	113.4	106.5	.693	.233	.904	156.4	46.7	13.0	43.8	13.5	43.7	45.2	D	93.5	7
	6.8	.2	.3	.009	.017	.86	JUL 16.4	.2	1.3	.6	278.0	34.5	27.2	M	.9	
AUGUST TRIANGULIDS	264.7	139.1	150.0	.886	.166	1.062	43.8	58.3	36.9	30.5	36.8	30.5	57.3	D	92.7	7
	9.0	.2	1.5	.020	.028	1.09	AUG 12.2	.3	.7	.9	265.3	15.1	30.1	N	.8	
ALPHA ARIETIDS	324.6	165.8	148.3	.125	.937	1.989	130.4	54.7	32.6	21.8	32.8	21.8	53.3	D	96.3	6
	1.1	.4	.9	.010	.013	2.81	SEP 8.9	.7	1.6	.8	232.2	8.1	35.8	N	.3	
RHO AURIGIDS	97.5	166.7	143.2	.797	.320	1.172	264.2	58.5	85.5	41.7	86.0	41.7	57.5	D	97.0	8
	3.8	.1	.8	.014	.023	1.27	SEP 9.8	.3	.7	.4	280.2	18.3	31.6	M	.2	
N CAMELOPARDALIDS	197.2	179.3	119.8	.985	.632	2.674	16.5	59.5	81.5	57.2	81.8	57.2	58.5	D	91.0	7
	1.6	.2	.5	.003	.023	4.37	SEP 22.7	.2	.5	.4	265.4	33.9	37.9	C	.4	
BETA AURIGIDS	353.9	180.3	141.5	.799	.116	.904	174.2	55.4	90.3	42.1	90.5	42.1	54.3	D	97.7	6
	6.9	.4	1.4	.014	.017	.86	SEP 23.7	.3	.9	.7	270.1	18.7	27.9	M	2.8	
CAMELOPARDALIDS	10.7	182.2	66.5	.814	.110	.914	192.9	33.6	104.2	77.3	105.2	77.2	31.6	D	97.6	66
	3.2	.2	.4	.008	.009	.87	SEP 25.7	.2	1.8	.2	273.5	54.1	27.9	C	.6	
THETA GEMINIDS	188.3	189.2	162.7	.995	.183	1.217	17.5	62.1	100.3	31.9	100.5	32.1	61.4	D	97.4	10
	4.7	2.2	1.2	.004	.018	1.34	OCT 2.8	.2	2.3	.7	269.8	9.0	32.4	N	.8	
TAU TAURIDS	311.8	193.5	163.1	.231	.858	1.632	145.3	57.4	70.3	20.8	70.7	28.1	56.5	D	94.9	6
	1.5	.2	1.1	.014	.012	2.08	OCT 7.2	.3	.8	.5	239.5	5.8	35.0	N	.9	

Table 2-1 (Cont.)

1	2	3	4	5	6	7	8	9	10	11	12	13	14	15	16	17
OCTOBER LYNCIDS	140.3	194.0	115.9	.945	.290	1.330	334.3	54.5	120.7	54.9	121.3	54.8	53.5	D	90.2	8
	4.3	.1	.8	.010	.016	1.53	OCT 7.7	.3	.7	.5	277.1	33.6	33.3	C	1.3	
M CAMELOPARDALIDS	176.6	195.2	74.4	.997	.786	4.657	11.8	44.2	168.5	81.0	168.9	81.1	42.9	D	96.6	15
	1.3	.3	.8	.001	.015	10.05	OCT 8.9	.4	3.8	.5	274.7	63.4	39.8	C	1.8	
CEPHEIDS-CAMELOPARDALIDS	212.7	195.2	78.3	.937	.627	2.513	47.9	44.5	77.0	79.9	78.0	80.1	43.1	D	94.7	10
	1.2	.3	.8	.004	.013	3.98	OCT 8.9	.3	3.5	.5	251.1	56.8	37.7	C	1.5	
PSI VIRGINIDS	258.1	21.6	2.6	.525	.653	1.513	279.7	23.6	192.8	-9.2	193.0	-9.3	21.1	A	89.0	22
	1.6	1.6	.7	.007	.017	1.86	OCT 15.3	.4	1.1	.9	354.0	-3.4	34.4	D	1.0	
NU AURIGIDS	311.0	207.3	134.3	.267	.794	1.298	158.3	54.1	86.6	39.5	87.0	39.5	53.1	D	96.6	7
	1.5	.2	.7	.013	.015	1.48	OCT 21.1	.3	1.2	.3	240.3	16.1	33.0	N	1.2	
E CEPHEIDS	263.0	207.4	32.6	.848	.210	1.073	110.4	21.0	343.6	79.8	352.2	80.4	17.8	D	92.4	22
	3.4	.2	.6	.009	.015	1.11	OCT 21.2	.3	8.3	.8	218.6	66.0	30.7	C	1.3	
A LYNCIDS	336.6	207.6	80.1	.318	.553	.711	184.2	36.3	104.1	59.5	104.5	59.5	34.5	D	94.1	7
	2.4	.2	1.1	.009	.014	.60	OCT 21.4	.4	3.1	.4	251.5	36.5	22.8	C	1.3	
S DRACONIDS	186.1	209.0	80.3	.990	.702	3.325	35.1	46.2	157.8	75.8	158.6	75.8	44.9	D	103.2	11
	1.7	.3	1.0	.001	.014	6.06	OCT 22.8	.4	2.2	.8	267.0	58.6	39.0	C	2.8	
DECEMBER LEONIDS	318.4	263.9	153.8	.206	.827	1.193	222.3	55.5	149.5	21.6	149.8	21.5	54.4	D	90.9	5
	1.7	.4	.3	.009	.015	1.30	DEC 16.2	.6	.8	.3	240.5	8.6	32.4	N	1.5	

The periods of activity of five streams required adjustments that also brought about minor changes in the streams' mean orbital elements. The revised data on these streams are also included in Table 2-1, replacing the corresponding figures in Table 9-2 of Southworth and Sekanina (1973).

2.3 The D-Distribution of the Additional and Revised Streams; Total Number of Stream Meteors in the Sample

The data on the distribution of meteors in the five revised streams, as listed in Table 1-2, are based on the corrected figures. The distribution parameters of the 20 additional high-inclination and retrograde streams are given in Table 2-2, which is arranged identically to Table 1-2. For the details, see Section 1.4.

The minor high-inclination and especially retrograde streams have mostly rather low dispersion coefficients, typical for compact streams, and very high population coefficients, indicating practically no interference from the sporadic background in small values of D.

In total, we have delineated 275 streams in the synoptic-year sample (256 originally detected minus α Aurigids plus 20 additional). The total number of definite stream members in the 275 streams is 3142, which is about 16% of the whole sample. The average population of the detected streams is 11 to 12 meteors per stream.

Table 2-2. A list of D-distribution parameters of 20 additional high-inclination and retrograde streams.

1	2	3	4	5	6	7	8	9	10	11	12	13	14	15	16	17	18	19	20
ALPHA PEGASIDS	28000	.010	4.5	.044	.262	26	6.5E-84	3.3	3.3	3.3	3.3	1.00	198	0.0	JUN 17.3	2.0	6	6	8
JUNE PEGASIDS	18000	.011	4.8	.047	.256	28	5.3E-69	3.5	3.5	3.5	3.5	1.00	164	.8	JUN 17.3	2.0	6	6	9
ALPHA LACERTIDS	18	.063	16.0	.149	.238	34	8.5E-02	10.5	9.3	10.6	10.7	.42	9.1	.6	JUL 02.6	2.6	16	24	30
JULY TRIANGULIDS	100	.035	5.4	.103	.208	46	3.7E-06	2.9	2.8	2.9	2.9	.34	11.1	6.8	JUL 15.3	2.1	5	8	8
THETA CASSICPEIDS	21	.073	15.5	.177	.288	21	4.0E-01	12.2	11.4	12.9	13.0	.65	10.8	6.9	JUL 16.1	3.6	16	20	27
JULY ANDROMEDIDS	720	.024	5.0	.084	.240	33	2.0E-13	3.3	3.3	3.3	3.3	.50	32.0	1.6	JUL 15.8	1.1	5	7	10
AUGUST TRIANGULIDS	150	.079	7.3	.243	.522	3	5.3E+00	7.1	7.7	7.9	7.9	1.00	22.5	.4	AUG 12.3	2.1	7	7	10
ALPHA ARIETIDS	1700	.022	4.8	.082	.276	23	6.0E-16	3.7	3.7	3.7	3.7	.71	52.1	3.5	SEP 08.2	2.1	5	6	7
RHO AURIGIDS	180	.031	5.9	.097	.215	43	6.8E-08	3.4	3.3	3.4	3.4	.34	16.1	.9	SEP 09.9	1.0	5	8	10
N CAMELOPARDALIDS	980	.023	4.9	.083	.249	30	1.2E-14	3.4	3.4	3.4	3.4	.75	37.8	.6	SEP 23.2	2.1	6	7	8
BETA AURIGIDS	2100	.018	5.2	.068	.238	34	8.7E-25	3.4	3.4	3.4	3.4	1.00	55.4	.1	SEP 23.3	2.1	6	6	11
THETA GEMINIDS	78	.043	6.8	.123	.239	34	8.4E-04	4.5	4.3	4.5	4.5	.65	12.3	.0	SEP 30.9	15.0	8	10	14
TAU TAURIDS	1100	.016	6.3	.058	.179	60	3.1E-32	2.5	2.5	2.5	2.5	.71	34.2	1.5	OCT 06.7	1.1	5	6	6
OCTOBER LYNCIDS	350	.031	6.2	.103	.256	28	1.3E-07	4.4	4.4	4.4	4.4	.56	25.8	.9	OCT 07.8	1.2	6	8	11
M CAMELOPARDALIDS	23	.061	12.3	.150	.246	31	7.6E-02	8.4	7.6	8.5	8.5	.65	9.2	.4	OCT 08.4	4.6	12	15	27
CEPHEIDS-CAMELOPARDALIDS	580	.025	6.8	.086	.236	35	2.6E-12	4.5	4.4	4.5	4.5	.48	33.3	3.0	OCT 07.9	3.5	7	10	16
NU AURIGIDS	5200	.014	4.7	.056	.235	35	5.5E-42	3.0	3.0	3.0	3.0	.75	82.3	3.8	OCT 20.8	1.0	6	7	8
A LYNCIDS	780	.027	5.6	.095	.275	23	3.5E-10	4.3	4.3	4.3	4.3	1.00	38.0	6.1	OCT 20.8	1.1	7	7	8
S DRACONIDS	39	.066	9.3	.174	.306	17	3.0E-01	7.7	7.3	7.9	7.9	.52	11.5	.5	OCT 22.4	2.7	8	11	16
DECEMBER LEONIDS	2400	.028	4.9	.107	.384	8	7.6E-09	4.6	4.6	4.6	4.6	1.00	68.5	2.3	DEC 15.3	2.0	5	5	6

3. THE POTENTIAL ASSOCIATION OF FOUR METEOR STREAMS WITH THE MINOR PLANET ADONIS

3.1 The Problem

Four streams in the synoptic-year sample have mean orbits that match the orbit of the minor planet Adonis within D = 0.20 (see Table 10-1 of Southworth and Sekanina, 1973): χ Sagittariids, Scorpiids-Sagittariids, ϵ Aquarids, and Capricornids-Sagittariids.

The orbital similarity may, of course, suggest an evolutionary relationship between the stream and the minor planet, which in turn could imply that Adonis might have been an active comet long ago and that the associated meteor streams currently observed represent its debris. In that case, the streams should indeed move in orbits similar to but not identical with that of Adonis. The orbital difference is partly due to the nonzero momentum gained by the meteoroids at ejection and enhanced later by the accumulation of differential perturbations by the major planets, and partly due to the effects of radiation pressure on the meteoroids. The Poynting-Robertson effect can be shown to accumulate, over the spans of time considered here, to no more than 0.1 a.u. in the semimajor axis, which is less than the uncertainty in the semimajor axis of the mean orbits of the streams.

3.2 The Calculations

We have attempted to explore the observed difference between the orbits of Adonis and the orbits of the potentially related streams to learn something about the time and circumstances of ejection.

Since Adonis has its aphelion at 3.3 a.u., close encounters with Jupiter are excluded. Because of this circumstance and the rather low precision of the starting data, we considered only secular perturbations in order to facilitate calculations as much as possible.

Applying the same method that was used to investigate a potential evolutionary relationship between Adonis and a radio-meteor stream from the 1961–65 Smithsonian-Harvard sample (Sekanina, 1971), we started our model calculations by running the orbit of Adonis for 12000 years backward in time, taking the secular perturbations by Jupiter to Neptune into account. Next we varied the following quantities to study the effects on the orbital modification of a meteoroid ejected from Adonis:

A. The time of ejection (on a gross scale).

B. The position of Adonis in orbit at the time of ejection (relative to perihelion).

C. The magnitude of the velocity of ejection.

D. The direction of ejection (relative to the sunward direction in the orbit plane).

We adopted five discrete times of ejection, 4000 to 12000 years ago, 2000 years apart. For each time, the ejections were assumed to take place at 1.2 and 0.7 a.u. from the sun before perihelion, at perihelion, and also at 0.7 and 1.2 a.u. after perihelion. Furthermore, five different directions of ejection were considered: toward the sun and deviating, both ahead of and behind the solar direction, by 30° and 60°. Finally, the magnitude of the ejection velocity was estimated from Probstein's (1968) fluid-dynamics model. Assuming that at the time of ejection the nuclear radius of Adonis was between 1 and 20 km and that the surface was covered by water snow (contaminated by meteoric matter), and accepting that at 1 a.u. from the sun the vaporization rate was between 1×10^{17} and 7×10^{17} molecules cm^{-2} sec^{-1} (owing to uncertainties in the emissivity of the surface), we can establish from Probstein's model that the ejection velocity of meteoroids of individual masses of about 10^{-4} g and densities of 1 g cm^{-3} should vary between 17 and 200 r^{-1} (m sec^{-1}), where r is the heliocentric distance in a.u. Calculations were carried out for the two extreme values as well as for 60 r^{-1} (m sec^{-1}), which has been thought to be a reasonable mean value.

3.3 Corrections to the Initial Elements of Ejected Meteoroids

The magnitude of the impulse on a meteoroid separating from the parent body shows up in the differences between the orbital elements of the two bodies at the time of ejection. If the known position of ejection in the orbit is given by the true anomaly v and the known velocity of ejection is defined by its radial component $\dot{\xi}$ (counted positive away from the sun) and transverse component $\dot{\eta}$ (positive in the direction of motion) in the orbit plane, we need to apply the following corrections to the orbital elements of the parent body:

$$\Delta\omega = \frac{B}{e}\left(-\dot{\xi}\cos v + \dot{\eta}\,\frac{2 + e\cos v}{1 + e\cos v}\sin v\right) \quad ,$$

$$\Delta\Omega = \Delta i = 0 \quad ,$$

$$\Delta q = \frac{Bq}{1 + e}\left(-\dot{\xi}\sin v + \dot{\eta}\,\frac{1 - \cos v + e\sin^2 v}{1 + e\cos v}\right) \quad , \tag{3-1}$$

$$\Delta e = B\left[\dot{\xi}\sin v + \dot{\eta}\,\frac{2\cos v + e(1 + \cos^2 v)}{1 + e\cos v}\right] \quad ,$$

where

$$B = \frac{[q(1 + e)]^{1/2}}{U} \tag{3-2}$$

and $U = 2.978 \times 10^4$, if $\dot{\xi}$ and $\dot{\eta}$ are expressed in meters per second.

Furthermore, additional corrections have to be applied because of the effect of radiation pressure. If $\Delta k^2/k^2 < 0$ is the relative reduction in the gravitational constant due to radiation pressure, the corrections are

$$\Delta\omega_{rp} = -\frac{\sin v}{e}\,\frac{\Delta k^2}{k^2} \quad ,$$

$$\Delta\Omega_{rp} = \Delta i_{rp} = 0 \quad ,$$

$$\Delta q_{rp} = -q\,\frac{1 - \cos v}{1 + e}\,\frac{\Delta k^2}{k^2} \quad , \tag{3-3}$$

$$\Delta e_{rp} = -(e + \cos v)\,\frac{\Delta k^2}{k^2} \quad .$$

Here v is the true anomaly at ejection and

$$\frac{\Delta k^2}{k^2} = -\frac{6 \times 10^{-5}}{\rho_s a_s} Q_{rp} \quad , \tag{3-4}$$

where ρ_s and a_s are the density and radius of the meteoroid, and $Q_{rp} \doteq 1$ is its scattering efficiency for radiation pressure. For meteoroid masses of the order of 10^{-4} g, we find $\rho_s a_s \simeq 0.03$ g cm^{-2} and, therefore, $\Delta k^2/k^2 \simeq -0.002$.

3.4 The Results

With five ejection times considered, each with $5 \times 5 \times 3 = 75$ options in regard to the circumstances at ejection, we have a total of 375 individual model orbits per stream. For each of them, the initial orbital elements (at ejection) were computed from the orbital elements of Adonis at the time of ejection by adding the specified corrections for the effects of ejection velocity [eq. (3-1)] and radiation pressure [eq. (3-3)]. The secular perturbations by Jupiter to Neptune were then applied to calculate the present orbits of the 375 model ejections. These orbits have been compared with those of the four meteor streams potentially related to Adonis.

The results are summarized in Tables 3-1 to 3-4 for Scorpiids-Sagittariids, χ Sagittariids, Capricornids-Sagittariids, and ϵ Aquarids, respectively. The tables list the values of the D-test (in units of 0.001) between the model orbits and the mean orbit of the stream. Values exceeding D = 0.25 (i.e., >250 in the tables) have not been printed. The time of ejection and the magnitude of the velocity of ejection are the two basic parameters. The location in orbit at ejection is printed as a subparameter for each time of ejection, and the following abbreviations are used: 1 = before perihelion, heliocentric distance 1.2 a.u.; 2 = before perihelion, 0.7 a.u.; 3 = perihelion; 4 = after perihelion, 0.7 a.u.; 5 = after perihelion, 1.2 a.u. The direction of ejection is expressed in terms of the ejection angle, which is printed as a subparameter to the velocity of ejection. The ejection angle is counted from the sunward direction and in the orbit plane. Its negative values indicate the ejections "ahead of" Adonis, i.e., in the general direction of the orbital motion of the parent body; the positive values represent the ejections "behind," i.e., opposite, the motion of Adonis. If we choose to associate the angle of ejection with the spin orientation of the parent body, in analogy to Whipple's (1950) interpretation of the nongravitational effects on cometary nuclei, the positive ejection angles would imply direct rotation, and the negative angles, retrograde rotation.

Inspection of Tables 3-1 to 3-4 suggests that the results do not allow us to make any clear-cut conclusions as to the existence of any genetic relationship between the minor planet and the four streams. The minima in the D-test distribution, which pick up the best models, are very shallow and in many instances barely show any improvement over the value of the D-test between the orbit of the stream and that of Adonis. Furthermore, the amplitude of the D-variations systematically increases with the velocity of ejection. Thus, we could formally improve the fit by increasing the ejection velocity to completely unrealistic values. Consequently, the ejection velocity cannot be determined from the variations in the D-test, but must be postulated. Therefore, in the tables we have marked the minimum values of the D-test separately for each of the adopted velocities of ejection. Even then, however, the age of the streams and the location of ejections in orbit are rather indeterminate, and only the direction of ejection comes out consistent for each stream. Scorpiids-Sagittariids, χ Sagittariids, and Capricornids-Sagittariids show a preference for positive ejection angles, and ϵ Aquarids, for negative.

Table 3-1. D-test comparison of model ejections from Adonis with the Scorpiid-Sagittariid stream. D(Adonis) = 0.135. (D's in units of 0.001.)

VELOCITY OF EJECTION (M/SEC)	ANGLE OF EJECTION (DEG)	TIME OF EJECTION (YEARS AGO)																								
		12000					10000					8000					6000					4000				
		LOCATION IN ORBIT					LOCATION IN ORBIT					LOCATION IN ORBIT					LOCATION IN ORBIT					LOCATION IN ORBIT				
		1	2	3	4	5	1	2	3	4	5	1	2	3	4	5	1	2	3	4	5	1	2	3	4	5
	-60	140	149	164	150	142	137	143	155	147	140	137	143	153	146	141	136	140	147	145	140	136	137	143	142	139
	-30	140	146	159	147	141	137	140	152	143	139	140	141	150	145	141	136	138	146	142	139	136	136	142	141	138
17/R	0	141	145	151	144	141	137	141	147	141	138	139	140	147	143	140	137	139	144	141	139	136	137	140	140	138
	+30	138	143	147	140	141	136	140	142	137	139	137	141	143	140	139	135	138	141	138	139	$\boxed{134}$	137	139	137	137
	+60	137	142	143	140	137	135	138	140	137	137	137	140	140	138	138	136	138	139	137	137	$\boxed{134}$	136	137	136	136
	-60	143	161	200	161	146	139	150	185	155	142	140	149	176	153	144	137	144	163	150	143	136	139	152	146	142
	-30	143	157	180	146	142	138	150	170	142	140	140	147	163	144	141	137	143	156	142	140	135	139	148	141	139
60/R	0	141	154	155	138	138	137	148	149	137	135	138	147	149	138	138	137	143	146	138	137	135	139	143	138	137
	+30	143	145	137	134	134	138	140	136	132	132	139	142	138	134	135	138	139	137	134	134	136	137	137	134	134
	+60	141	138	149	148	134	139	136	147	147	132	139	138	149	$\boxed{131}$	134	138	137	149	$\boxed{131}$	134	137	136	134	132	134
	-60	151	218		192	154	144	196		180	151	142	181		176	152	138	162		168	150	135	148	209	160	149
	-30	156	215		153	141	147	195	245	149	139	145	181	226	151	142	140	163	201	150	141	135	149	177	147	141
200/R	0	157	186	163	151	150	149	173	158	151	148	147	165	158	151	150	143	156	155	151	132	138	145	149	154	134
	+30	149	154	153	149	145	145	149	153	147	144	144	150	153	144	144	143	145	153	144	146	140	142	155	147	128
	+60	143	152	165	148	141	140	152	160	144	141	142	154	153	141	142	141	138	150	142	$\boxed{124}$	140	140	153	144	125

Table 3-2. D-test comparison of model ejections from Adonis with the χ Sagittariid stream. D(Adonis) = 0.089. (D's in units of 0.001.)

VELOCITY OF EJECTION (M/SEC)	ANGLE OF EJECTION (DEG)	TIME OF EJECTION (YEARS AGO) 12000 LOCATION IN ORBIT 1	2	3	4	5	10000 LOCATION IN ORBIT 1	2	3	4	5	8000 LOCATION IN ORBIT 1	2	3	4	5	6000 LOCATION IN ORBIT 1	2	3	4	5	4000 LOCATION IN ORBIT 1	2	3	4	5
	-60	92	97	111	99	93	90	93	103	96	92	89	93	101	96	93	89	90	96	95	92	89	89	94	93	92
	-30	91	96	107	96	92	89	91	100	93	91	91	91	98	95	93	89	90	96	93	92	89	89	93	92	91
17/R	0	92	95	100	95	93	89	92	96	92	91	91	91	97	94	92	90	90	94	92	92	89	90	91	92	91
	+30	90	93	96	92	92	89	91	93	90	91	90	91	93	92	91	$\boxed{88}$	90	92	90	91	$\boxed{88}$	90	91	91	90
	+60	89	92	94	92	90	$\boxed{88}$	90	91	90	90	90	91	92	91	91	89	90	91	90	90	$\boxed{88}$	89	90	90	89
	-60	93	107	146	107	96	90	98	131	103	94	91	96	122	102	95	88	93	110	99	94	89	90	100	96	93
	-30	92	105	126	96	93	89	98	116	93	92	90	95	110	95	93	89	93	103	93	92	88	91	97	93	91
60/R	0	92	102	102	91	91	89	97	98	91	89	90	96	98	91	91	89	93	96	91	90	88	91	94	91	90
	+30	94	95	91	90	89	90	92	90	88	88	90	93	91	89	89	90	91	91	89	88	89	90	91	89	88
	+60	92	91	90	87	88	91	90	89	$\boxed{87}$	$\boxed{87}$	91	91	89	$\boxed{87}$	88	91	90	89	$\boxed{87}$	88	90	90	89	87	88
	-60	98	164		136	102	93	142		125	100	91	126	247	121	102	88	107	201	114	100	87	96	155	107	98
	-30	103	162	217	101	94	95	141	191	100	93	93	127	171	101	95	89	109	147	100	94	87	98	124	97	93
200/R	0	104	133	110	141	90	97	119	105	141	89	96	112	107	92	89	93	104	104	90	88	90	95	99	91	89
	+30	99	103	155	157	87	95	98	154	151	87	94	99	146	140	85	94	96	140	88	85	92	94	94	88	86
	+60	94	91	189	161	85	93	92	178	153	84	94	94	162	144	$\boxed{83}$	94	93	151	139	$\boxed{83}$	93	94	147	87	84

Table 3-3. D-test comparison of model ejections from Adonis with the Capricornid-Sagittariid stream. D(Adonis) = 0.199. (D's in units of 0.001.)

VELOCITY OF EJECTION (M/SEC)	ANGLE OF EJECTION (DEG)	TIME OF EJECTION (YEARS AGO)																								
		12000					10000					8000					6000					4000				
		LOCATION IN ORBIT					LOCATION IN ORBIT					LOCATION IN ORBIT					LOCATION IN ORBIT					LOCATION IN ORBIT				
		1	2	3	4	5	1	2	3	4	5	1	2	3	4	5	1	2	3	4	5	1	2	3	4	5
	-60	207	218	237	219	207	203	212	228	215	205	203	211	225	214	206	201	207	217	211	205	201	203	212	208	204
	-30	207	215	231	215	206	203	209	223	210	204	205	209	220	211	206	201	206	216	207	204	200	203	211	206	203
17/R	0	208	214	222	212	206	203	209	216	208	203	205	208	217	209	205	203	206	212	206	204	200	203	207	205	203
	+30	204	211	215	206	206	201	207	210	202	204	203	207	210	205	204	200	204	208	203	204	$\boxed{199}$	203	205	203	202
	+60	203	209	210	206	202	200	205	206	202	201	203	207	207	204	203	201	204	205	202	201	$\boxed{199}$	201	203	202	200
	-60	210	234		230	211	206	223		224	207	206	220		222	209	202	214	238	218	208	200	208	225	213	206
	-30	210	230		212	206	205	222	244	208	204	206	218	237	210	205	203	212	227	208	204	200	208	218	206	203
60/R	0	209	226	225	201	201	204	219	219	200	198	205	217	218	201	201	203	212	214	201	200	200	207	210	201	200
	+30	210	214	200	196	196	205	209	199	193	196	205	210	201	197	199	204	207	201	196	198	201	204	201	196	198
	+60	206	204	$\boxed{164}$	190	198	205	201	$\boxed{184}$	188	195	205	204	190	193	198	204	203	192	193	198	203	201	195	194	198
	-60	222				218	214				214	211			245	216	205	238		237	214	200	222		229	212
	-30	228			217	202	219			213	199	215			214	203	208	239		214	202	202	224		211	203
200/R	0	229		234	181	186	221	250	227	182	187	218	241	227	188	191	212	230	223	190	192	206	218	218	194	194
	+30	221	226	168	158	179	215	220	172	163	180	214	220	180	169	184	212	215	187	173	186	208	212	192	180	188
	+60	211	194	$\boxed{146}$	150	177	208	195	150	154	178	209	200	158	161	183	209	202	164	166	185	207	204	175	173	186

Table 3-4. D-test comparison of model ejections from Adonis with the ϵ Aquarid stream. D(Adonis) = 0.193. (D's in units of 0.001.)

VELOCITY OF EJECTION (M/SEC)	ANGLE OF EJECTION (DEG)	TIME OF EJECTION (YEARS AGO)																								
		12000					10000					8000					6000					4000				
		LOCATION IN ORBIT					LOCATION IN ORBIT					LOCATION IN ORBIT					LOCATION IN ORBIT					LOCATION IN ORBIT				
		1	2	3	4	5	1	2	3	4	5	1	2	3	4	5	1	2	3	4	5	1	2	3	4	5
	-60	189	184	$\boxed{181}$	183	167	191	188	183	185	189	190	186	182	185	188	191	189	186	186	188	192	191	188	188	190
	-30	189	186	$\boxed{181}$	184	188	191	189	183	187	190	189	188	184	186	188	191	190	186	187	189	192	192	188	189	191
17/R	0	188	186	184	187	188	191	189	186	189	190	189	189	185	187	188	191	190	187	188	189	192	192	190	190	191
	+30	191	187	186	189	188	192	189	188	191	190	191	188	188	190	190	192	190	189	190	190	193	192	190	191	191
	+60	191	187	188	189	191	192	191	189	191	191	191	189	189	190	190	192	190	190	191	192	193	192	191	192	192
	-60	186	182	182	$\boxed{178}$	186	190	186	181	181	187	188	185	180	181	187	190	187	182	183	187	191	190	185	185	188
	-30	187	183	179	185	187	190	185	180	187	189	188	185	180	186	188	190	188	182	188	189	192	191	185	189	190
60/R	0	188	183	182	190	191	191	185	185	191	193	190	185	185	190	190	191	187	186	191	191	192	190	187	191	191
	+30	188	187	191	194	194	190	189	193	196	196	190	188	191	194	193	190	190	192	193	194	192	192	191	193	194
	+60	188	190	202	198	194	190	192	203	199	195	189	190	198	196	193	190	192	197	196	193	191	192	194	195	194
	-60	163			$\boxed{172}$	180	187			173	181	187	185		$\boxed{172}$	181	189	184		176	182	192	188		178	183
	-30	163			180	189	186	186		183	190	186	184	185	182	188	188	183	179	183	188	192	188	181	185	189
200/R	0	183	183	178	204	199	185	183	180	203	200	185	182	180	198	196	188	184	181	196	195	191	189	184	193	194
	+30	186	184	219	228	206	187	185	216	223	206	188	185	208	214	202	189	187	200	209	200	190	189	194	203	199
	+60	169	196		238	208	169	196		232	208	188	193	234	222	204	189	193	220	215	202	191	191	206	208	201

4. HEIGHT–VELOCITY DIAGRAM

4.1 The Problem of Meteor Heights

We reported previously (Southworth and Sekanina, 1973) that we had failed to detect in the synoptic-year sample the discrete levels of meteor height that had originally been reported by Ceplecha (1967, 1968) for photographic meteors. However, more recent inspection of the utilized height data indicated that the punched output of the main reduction program (height–density cards), which served as the source, contained heights from diffusion for some meteors and geometric heights for others (plus radiant heights for a minor part of the sample). The three types of heights differ from each other sometimes by as much as 10 km or more, and the geometric heights, which are generally considered less reliable than the diffusion heights, constituted a significant part of the sample. To rectify this situation, we have now consulted the much more extensive printed (rather than punched) output of the main reduction program; we eliminated both the geometric and the radiant heights and have finally ended up with 14502 meteors with diffusion heights.

4.2 The Height–Velocity Plots

Figure 4-1 shows one of the computer-generated plots of meteor height at maximum ionization h_{max} versus the no-atmosphere velocity V_∞. We have also secured similar plots for beginning height; they look much the same, but have slightly larger scatter.

Although the degree of precision of the present data is definitely greater than that of our previous study (cf. Figures 11-1 to 11-7 of Southworth and Sekanina, 1973), it is still too low to disclose the discrete levels that showed up in the photographic sample. The resolution power has not been enhanced either by applying more restrictive criteria (e.g., by accepting only well-observed, fully reduced meteors and/or those at small enough zenith distances), or by dividing the sample into physically more homogeneous groups (e.g., by separating "bright" meteors from "faint" ones, etc.).

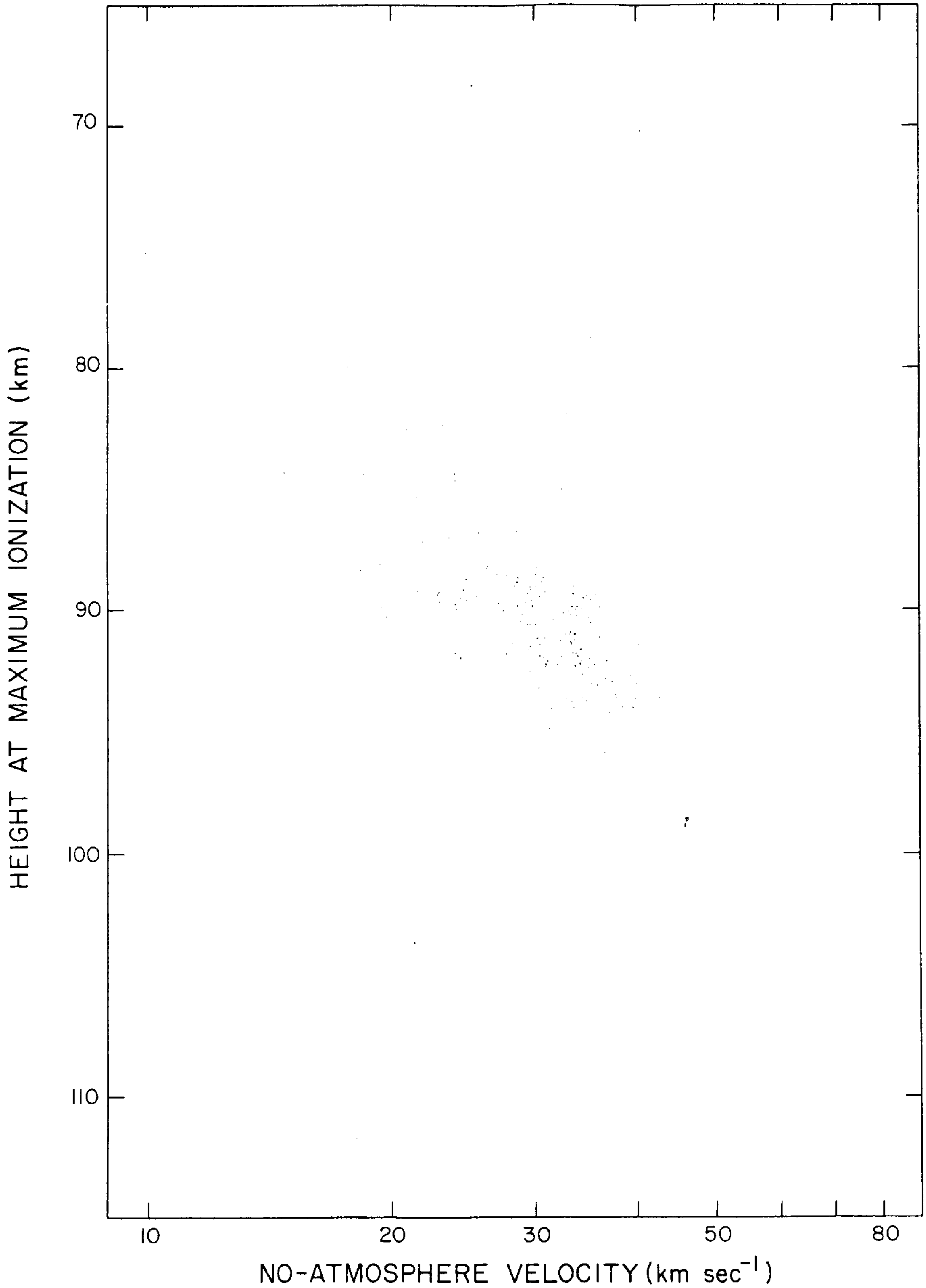

Figure 4-1. Height–velocity diagram of 7639 meteors of the synoptic-year sample for which geometric heights have been found. The plot shows diffusion heights.

The only four features that we can detect on the height–velocity diagrams are those reported by us previously (Southworth and Sekanina, 1973): the separation between the major cluster of meteors at low V_∞ and the minor cluster at high V_∞, the considerably larger scatter in the major cluster, the minor cluster more pronounced among the brighter meteors, and the absence of the high-velocity cluster for small-perihelion meteors.

4.3 Results from Least-Squares Solutions

The negative results from the height–velocity plots led us to attack the problem numerically. We divided the whole sample into a number of groups and forced, for each group, a fit of the form

$$h = h_{30} + A \log \left(\frac{V_\infty}{30}\right) , \qquad (4\text{-}1)$$

where h_{30} is the height at $V_\infty = 30$ km sec^{-1}. In addition, we also made runs with the retained quadratic term $[\log (V_\infty/30)]^2$ and found that it was never important.

The results of the linear solutions are included in Table 4-1. For each group, the table gives the number of meteors N, the height at V = 30 km sec^{-1} (h_{30}) and its mean error, the height slope A and its mean error, and the standard deviation of the individual meteor heights from the solution.

Most of the data in the table refer to the diffusion height at maximum ionization, but five groups give solutions for the beginning height: Groups 2, 4, 8, 10, and 12. These runs are marked by an asterisk in the table. The individual groups include:

Groups 1 and 2. All meteors.

Groups 3 and 4. Meteors for which geometric heights were found. Being more fully reduced, these meteors are considered to give better precision.

Group 5. Meteors for which geometric heights were not found. The data for these meteors are considered, on an average, to be of lower precision. These meteors are not used in any of the groups after 6.

Table 4-1. Results of the least-squares solutions of the height–velocity diagrams.

Group number	N	h_{30}	A	m.e.
1	14502	89.87 ± 0.03	19.1 ± 0.2	±3.6
2*	14502	93.76 ± 0.03	18.6 ± 0.2	±3.7
3	7639	89.77 ± 0.04	19.7 ± 0.3	±3.3
4*	7639	93.68 ± 0.04	19.2 ± 0.3	±3.5
5	6863	90.01 ± 0.05	18.4 ± 0.3	±3.8
6	7299	89.61 ± 0.04	18.0 ± 0.3	±3.6
7	3944	89.59 ± 0.05	19.0 ± 0.4	±3.4
8*	3944	93.92 ± 0.06	17.7 ± 0.4	±3.5
9	4410	90.21 ± 0.05	19.5 ± 0.3	±3.2
10*	3226	93.59 ± 0.06	19.1 ± 0.4	±3.4
11	2468	90.08 ± 0.06	19.1 ± 0.4	±3.3
12*	1900	93.66 ± 0.08	18.1 ± 0.5	±3.5
13	2451	90.46 ± 0.07	15.6 ± 0.5	±3.2
14	1959	90.38 ± 0.07	24.3 ± 0.5	±3.1
15	746	89.90 ± 0.14	20.1 ± 1.3	±3.1
16	817	90.31 ± 0.11	17.9 ± 0.9	±3.1
17	844	90.35 ± 0.11	20.0 ± 0.8	±3.2
18	2003	90.23 ± 0.07	19.9 ± 0.4	±3.3
19	1876	90.36 ± 0.07	15.7 ± 0.5	±3.1
20	1030	90.35 ± 0.10	21.0 ± 0.7	±3.2
21	1504	90.10 ± 0.08	22.2 ± 0.5	±3.2
22	952	90.14 ± 0.11	22.4 ± 0.6	±3.2
23	596	90.15 ± 0.14	22.5 ± 0.8	±3.3

*This run refers to the beginning height.

Group 6. All meteors at zenith distances less than 45°.

Groups 7 and 8. Well-reduced meteors at zenith distances less than 45°.

Groups 9 and 10. Well-reduced meteors with reliable ionization curves.

Groups 11 and 12. Well-reduced meteors with reliable ionization curves and at zenith distances less than 45°.

The following groups are subdivisions of group 9:

Group 13. Meteors with intrinsic magnitudes at maximum ionization $M \leq 11.5$.

Group 14. Meteors with $M > 11.5$.

Group 15. Meteors with perihelion distances $q \leq 0.25$ a.u.

Group 16. Meteors with $0.25 < q \leq 0.50$ a.u.

Group 17. Meteors with $0.50 < q \leq 0.75$ a.u.

Group 18. Meteors with $q > 0.75$ a.u.

Group 19. Meteors with aphelion distances $q' \geq 2.5$ a.u.

Group 20. Meteors with $1.5 \leq q' < 2.5$ a.u.

Group 21. Meteors with $q' < 1.5$ a.u.

Group 22. Meteors with $q' < 1.5$ a.u. and $q > 0.5$ a.u.

Group 23. Meteors with $q' < 1.5$ a.u. and $q > 0.75$ a.u.

We make the following conclusions from the results in Table 4-1:

A. The beginning heights are about 3.5 to 4 km above the heights at maximum ionization. (This difference is relatively smaller for meteors with reliable ionization curves only because of the reduction procedure, described in Section 6.1.)

B. The meteors for which the geometric heights could be found appear to be of better quality, as expected.

C. The meteors with reliable ionization curves appear to be only slightly better than those whose curves are less reliable.

D. The zenith distance does not have any improving effect on the solution. We note, however, that it is difficult to reconcile numerically the effects of zenith-distance selection in Table 4-1 with the results in Tables 5-3 and 6-1; and we tentatively conclude that the selection process for meteors in Table 4-1 was somehow anomalous with respect to zenith distance.

E. A sharp difference occurs between the height slope A of the bright meteors and that of the faint ones. This effect is apparently due to the fact, already mentioned, that the high-velocity cluster of meteors is more pronounced among the brighter meteors. However, we have not yet taken the selection effects of diffusion and recombination into account in this part of the analysis.

F. The height slope A is on an average 20 ± 5 and corresponds to the density-velocity dependence $\rho \sim V_\infty^{-n}$, with $n = 1.5 \pm 0.4$. This is considerably less than Ceplecha's (1968) $n = 2.5$. However, qualitative allowance for the selection effects of recombination and diffusion would result in closer agreement with Ceplecha.

G. The meteors with $q \leq 0.25$ a.u. appear to have somewhat smaller heights, but the difference from the other groups is only about 0.4 km.

H. The aphelion distance, like the perihelion distance, appears to have only a small effect on the heights. In both cases, however, the effects are formally significant in a statistical sense, so that further study might well be repaid.

5. FRAGMENTATION

5.1 Introduction

The research described here constitutes a continuation of our previous studies of fragmentation, and certainly does not reach the end of the problem. The limitation of time unfortunately prohibited use of the measured amplitudes of individual Fresnel extrema, which are the best available data for fragmentation studies. Instead, we used the measured number of Fresnel extrema and have obtained the first set of values of the spread of meteoroid fragments along the trajectory, but mathematical peculiarities prevent our computing the complete distribution of values of the spread.

5.2 Inferring Fragment Spread from the Observed Number of Extrema

This section describes computations of the number of Fresnel-pattern extrema that a human measurer or the pattern-measuring computer program would measure, taking into account diffusion and fragmentation in the ion trail and noise and limited dynamic range in the radar equipment. A Fortran program was written for the computations, which were then to be used to infer the spread of the fragments along the meteor trajectory.

McKinley (1961, p. 191) showed that when a meteor has passed the specular reflection point by a distance x, the signal amplitude (the power or the voltage squared) returned to the radar receiver is

$$A_u^2 = \frac{q^2 F^2 (C^2 + S^2)}{2} \quad , \tag{5-1}$$

where

$$F = \left(\frac{\lambda R}{2}\right)^{1/2} \tag{5-2}$$

is the effective length of the principal Fresnel zone, λ is the radar wavelength, R is the range from the radar to the electron column, q is the number of electrons per unit length in the column, and C and S are Fresnel integrals. Here we have assumed that the electrons are uniformly distributed along the electron column within the interval of interest (a few times F). The unit of A_u^2 is the response to a single electron at distance R. The subscript u denotes that diffusion and fragmentation have been neglected. Without loss of generality for this purpose, we shall assume

$$q = 1 \tag{5-3}$$

since only relative values of A enter into determining the number of extrema. McKinley introduced the Cauchy approximations for the Fresnel integrals

$$C = 1 + \frac{1}{\pi y} \sin\left(\frac{\pi y^2}{2}\right) \quad , \tag{5-4}$$

$$S = 1 - \frac{1}{\pi y} \cos\left(\frac{\pi y^2}{2}\right) \quad , \tag{5-5}$$

where

$$y = \frac{\sqrt{2}}{F} x \quad . \tag{5-6}$$

The successive maxima i = 1, 2, ... of A_u^2 are found at approximately

$$y^2 = 4\,i - \frac{5}{2} \quad . \tag{5-7}$$

Equations (5-4) and (5-5) are sufficiently accurate for the present purpose when $y > 1$, i.e., at and after the first Fresnel maximum.

Study of Loewenthal's (1956) diagrams shows that an alternative representation of A can be found in the vector sum of two components, D_u ("deferent") indicating the response of the principal Fresnel zone and E_u ("epicycle") indicating the fluctuating integral response of the later zones; E_u rotates continuously with respect to D_u. Representing the relative phase by ϕ, we have

$$A_u^2 = D_u^2 + E_u^2 + 2 D_u E_u \cos\phi \quad . \tag{5-8}$$

Substituting equations (5-2) through (5-6) into (5-1) and comparing terms with equation (5-8), we find

$$D_u = F \quad , \tag{5-9}$$

$$E_u = \frac{F^2}{2\pi x} \quad , \tag{5-10}$$

and

$$\phi = \pi\left[\left(\frac{x}{F}\right)^2 - \frac{3}{4}\right] \quad . \tag{5-11}$$

Accurate integrations by Southworth (1962a, b), i.e., without use of the Cauchy approximations, showed the validity of the epicycle–deferent representation; it will be equally valid to use the Cauchy approximations here because our applications are limited to observations of 5 to 30 extrema ($3.1 < y < 7.7$), where the approximations are very good.

Ambipolar diffusion of the electrons and ions away from the meteroid trajectory leads to attenuation of the radar return from the electron column. McKinley showed that the return at time t after formation of the column is reduced by a factor

$$a^2(t) = \exp\left(-\frac{32\,\pi^2\,Gt}{\lambda^2}\right) \quad , \tag{5-12}$$

where G is the ambipolar diffusion coefficient. Greenhow and Neufeld's (1955) observational representation of G is

$$\log_{10} G\ (\mathrm{cm}^2\ \mathrm{sec}^{-1}) = 0.068\ h - 1.67 \quad , \tag{5-13}$$

where h is the height above sea level (km). Equation (5-13) is reasonably good for synoptic-year meteors and is exact by definition for the 1961–65 meteors, where h was determined from G and equation (5-13).

We take diffusion into account in this analysis by introducing appropriate attenuation factors in the D- and E-components of the returned signal. The D-component is affected by diffusion during the time $t = x/V$ (where V is the meteoroid velocity) since the meteoroid passed the specular reflection point; accordingly, we can multiply D by the factor

$$a = \exp\left(-\frac{16\,\pi^2 G\,x}{V\lambda^2}\right) \quad . \tag{5-14}$$

Introducing Loewenthal's (1956) parameter

$$C = \frac{8\pi\,G\,F}{\lambda^2 V} \quad , \tag{5-15}$$

we then have

$$a_d = \exp\left(-\frac{2\pi\,C\,x}{F}\right) \quad . \tag{5-16}$$

The E-component is affected by diffusion over a much shorter time, and accurate calculation of the relatively small effect is complicated. For completeness, however, we estimate that the E-component is effectively formed one-quarter revolution earlier; by differentiation of equation (5-11), this corresponds to a distance

$$\Delta x = \frac{F^2}{4x} \tag{5-17}$$

earlier; and by comparison with equation (5-16), we multiply E by the factor

$$c = \exp\left(-\frac{\pi\,C\,F}{x}\right) \quad . \tag{5-18}$$

Fragmentation of the meteoroid and the consequent spread of the fragments along the trajectory by differential deceleration replace the Fresnel pattern of a single meteoroid with the sum of the Fresnel patterns of the separate fragments relatively out of phase. The effect is to reduce the E-component of the returned signal. We model the fragment spread by a Gaussian distribution of fragments about the fragment mean, with a root-mean-square (rms) deviation σ from the mean. Then, the relative number of fragments $s \pm \frac{1}{2}$ ds from the mean is

$$n(s) = \frac{1}{\sigma\sqrt{\pi}} \exp\left[-\left(\frac{s}{\sigma}\right)^2\right] \quad . \tag{5-19}$$

The relative phase of a fragment at $x + s$, with respect to the fragment mean at x, is

$$\phi_s = \frac{\pi}{F^2} \left[(x+s)^2 - x^2\right] \tag{5-20}$$

[cf. eq. (5-11)], which we approximate by

$$\phi_{sa} = \frac{2\pi sx}{F^2} \quad . \tag{5-21}$$

Then the relative amplitude of the E-component is given by

$$b = \frac{\int_{-\infty}^{\infty} n(s) \cos \phi_{sa} \, ds}{\int_{-\infty}^{\infty} n(s) \, ds} = \exp\left[-\left(\frac{\pi\sigma x}{F^2}\right)^2\right] \quad , \tag{5-22}$$

and we can accordingly multiply E by b.

In theoretical Fresnel patterns (with the use of the above assumptions), the oscillating component never vanishes in the direction of increasing x, but there is nonetheless a definite bound to the number of observable extrema. Beyond that bound, the slope of the returned signal, though oscillating, is always negative. Both the human film measurers and the computer program that later measured Fresnel patterns started at the first maximum and proceeded as far as possible. Both stopped when there were no further extrema, as just described, even though an oscillating slope could often still be seen. They also stopped when there were too few pulses per extremum or too much noise in the data to recognize the next extremum, as well as when the returned signal became too small to be recorded. Moreover, the human measurers (1961–65 meteors) stopped at 20 extrema, and the program (synoptic-year meteors), at 30.

To find the theoretical number of extrema, we computed the slope of the Fresnel pattern at points where $\phi = 3\pi/2$ (modulo 2π), i.e., approximately halfway between each minimum and the following maximum. This is the point where the slope has a local maximum in the Fresnel pattern of a meteor unaffected by diffusion and fragmentation and approximately where it has a local maximum when diffusion and fragmentation are brought into account. Denoting these points by m = 1, 2, ..., according to the order in which they follow the m^{th} minimum, we have

$$\phi = \pi\left(2m - \frac{1}{2}\right) \tag{5-23}$$

and

$$x = F\left(2m + \frac{1}{4}\right)^{1/2} \quad . \tag{5-24}$$

Introduction of a [eq. (5-14)], c [eq. (5-18)], and b [eq. (5-22)] transforms equation (5-8) to

$$A^2 = (aD_u)^2 + (bcE_u)^2 + 2\,abcD_uE_u \cos\phi \quad . \tag{5-25}$$

Substitution of equations (5-9), (5-10), and (5-11), differentiation, and substitution of equation (5-24) yield the approximate local maximum slope

$$\frac{d}{dx}(A^2) = 2F^2\left[a\frac{da}{dx} + \frac{(c/2\pi)^2}{2m+1/4}\, b\frac{db}{dx} + \frac{abc}{F} - \frac{(bc/2\pi)^2}{F(2m+1/4)^{3/2}}\right] , \tag{5-26}$$

where dc/dx has been neglected.

The accuracy with which the above slope could be measured was estimated as follows. We are, in fact, concerned with the relative slope $(1/A^2)\,[d(A^2)/dx]$, i.e., the logarithmic derivative of A^2, because all signals were recorded in logarithmic units and the "noise" of recorded signals was more nearly constant in a logarithmic scale than in an absolute scale. The slope in question occurs near a point of inflection of the Fresnel pattern, where the observed pattern is sensibly straight over an interval of roughly one-sixth the local period Δx of the Fresnel oscillations. To the human measurer, the uncertainty e_s in measuring this slope is thus approximately the uncertainty e_d in the difference of the signal at the two ends of this interval, divided by the length of the interval, or

$$e_s = \frac{6\,e_d}{\Delta x} = \frac{6\,e_d}{F\,[(2m + 5/4)^{1/2} - (2m - 3/4)^{1/2}]} \quad , \tag{5-27}$$

where we have used equation (5-24) to evaluate the length of the interval. We estimate e_d to be

$$e_d = \frac{0.05\,N}{(p - 3)^{1/2}} \quad , \tag{5-28}$$

where 0.05 is the relative change in A^2 corresponding to a single step of the digital recording equipment near the middle of the dynamic range of the receivers, N is the noise of a single recorded signal in digital-recording-equipment units, and p is the number of pulses between successive maxima. Our estimate of the effective value of N for the synoptic year is 1, and the equivalent value for 1961–65 (when digital recording was not used) is 2. Nonetheless, N is left as a free parameter in the computations. Since 738 pulses $\sec^{-1}$ were transmitted, we have

$$p = \frac{738\,F\,[(2m + 5/4)^{1/2} - (2m - 3/4)^{1/2}]}{V} \quad . \tag{5-29}$$

Both measuring techniques considered approximately one cycle of the Fresnel oscillation in measuring each extremum, and both were instructed to stop measuring if there were fewer than 3 pulses per cycle. Thus, $p - 3$ is appropriate in equation (5-28); the 1/2 power is used in the expectation that the mean error is inversely proportional to the square root of the number of observations.

The computer program to determine the observable number of extrema evaluated

$$T(m) = \frac{1}{A^2} \frac{d}{dx} (A^2) - e_s \tag{5-30}$$

for successive values of $m = 1, 2, \ldots$. A value $T(m) = 0$ implies that

$$n = 2m + 1 \tag{5-31}$$

extrema could be observed, to wit the m maxima and m minima preceding the point at which $T(m) = 0$ and the following maximum. Strictly speaking, a value $T(m) > 0$ followed by $T(m+1) < 0$ also implies that $n = 2m+1$ extrema are observable. However, the subsequent use of n requires that it be a continuous variable, so that n is determined in that case by inverse linear interpolation as

$$n = 2m + 1 + \frac{2\, T(m)}{T(m) - T(m+1)} \quad . \tag{5-32}$$

An approximate correction for the limited dynamic range of the receivers was introduced. We are concerned only with the lower end of the range, because echoes bounded at the upper end were not reduced. The number of meteors increases rapidly with decreasing mass, so that most of the meteor echoes are near the faint observing limit. We estimated that the average reduced meteor was $L = 10$ db above this limit at its first maximum. It was not possible to test the estimate, as it would entail an elaborate analysis of calibration data, but trial computations showed that computed values of n were not at all sensitive to the estimate. The correction consisted of subtracting from $T(m)$, when $A^2/F^2 < 10^{1/2}$, the quantity

$$T' = 0.1 \log_{10} (A^{-2} F^2 10^{1/2}) \quad , \tag{5-33}$$

which simulates the added difficulty of observing extrema after an echo has decayed by more than 10 db.

The procedure described above determines the number n of observable extrema as a function of five parameters: C, σ/F, F/V, N, and L; the computer program created a three-dimensional table of n as a function of C, σ/F, and F/V for given values of N and L. The left-hand portion of Table 5-1, labeled "Extrema," is a severely abbreviated example of the results. The parameter C is dimensionless; C = 0 denotes no diffusion, and C > 0.3 denotes so much diffusion that successful reduction is not likely. The left-hand column, "Frag.," designates σ/F, where F ranges from 0.5 to 1.2 km; thus we are concerned here with rms fragment distances, from the fragment mean, of up to a few tenths of a kilometer. Table 5-1a, F/V = 0.015, is relevant to fast meteors (velocity V = 33 to 80 km sec^{-1}), and the other sections, to slower meteors. Values of n > 100 have been truncated to 100, and those for n < 3 were computed by using a conventional value for T(0) = 0.48. The letter R denotes cases where the E-component exceeds the D-component; this is important in determining winds, but it is not important for the present purpose.

Examination of Table 5-1 shows that n is not always a monotonically decreasing function of σ/F, but sometimes is of the form shown in Figure 5-1. When, as at Q in Figure 5-1, n has a relative minimum n_0, σ/F can be determined from n only if $n < n_0$. When $n \geq n_0$, all that can be said is that $\sigma/F \leq s_0$. The right-hand half of Table 5-1, labeled "Fragment Spread," gives values of σ/F as a function of n, obtained by inverse interpolation of an unabbreviated version of the entries under "Extrema." When n has a relative minimum, as in Figure 5-1, the table uses P Q R S for computing σ/F, but only the section R S will later be used.

5.3 Results on Fragment Spread

We used the procedure just described to compute, as far as possible, a value of the fragment spread σ for each of 17,917 synoptic-year meteors and for each of 9691 meteors observed in 1961–65 that had meaningful diffusion heights. The synoptic-year sample is, of course, less biased by observational limitations, but the 1961–65 sample represents larger meteors and is also more homogeneous in heights.

Table 5-1. Computed numbers of extrema.

a) F/V .015
NOISE 2.0
DYN.LIM. 10DB

EXTREMA

LOEW C / FRAG.	0.0	.05	.1	.2	.3	.5
0.00	9.3	12.9	13.0	13.0R	9.6R	3.7R
.02	9.2	12.7	13.0	13.0R	9.6R	3.6R
.04	8.7	12.0	13.0	13.0R	9.6R	3.5R
.06	8.0	11.2	13.0	13.0R	9.7R	3.4R
.08	7.3	9.6	13.0	13.0R	10.0R	3.2R
.10	6.5	8.0	11.8	13.0R	10.7R	2.9R
.12	5.9	6.6	9.6	13.0	11.9R	2.3R
.14	5.3	5.5	7.3	13.0	13.0R	2.0R
.16	4.8	4.7	5.5	12.1	13.0R	1.8R
.18	4.4	4.0	4.2	9.1	13.0	1.7R
.20	4.0	3.5	3.4	6.2	13.0	1.6R
.22	3.7	3.1	2.7	4.1	9.8	1.6R
.24	3.5	2.5	2.1	2.7	6.8	1.6R
.26	3.2	2.2	1.9	1.9	4.2	1.6R
.28	2.9	2.0	1.7	1.6	2.2	1.7R
.30	2.6	1.9	1.6	1.5	1.6	1.9R

R ECHO PHASE ROTATES 360 DEGREES

FRAGMENT SPREAD

EXTR.	0.0	.05	.1	.2	.3	.5
2	.35	.28	.25	.25	.29	.14
4	.20	.18	.19	.22	.26	0.00*
6	.12	.13	.15	.20	.25	0.00*
8	.06	.10	.13	.19	.23	0.00*
10	0.00*	.08	.12	.17	0.00*	0.00*
12	0.00*	.04	.10	.16	0.00*	0.00*
14	0.00*	0.00*	0.00*	0.00*	0.00*	0.00*
16	0.00*	0.00*	0.00*	0.00*	0.00*	0.00*
18	0.00*	0.00*	0.00*	0.00*	0.00*	0.00*
20	0.00*	0.00*	0.00*	0.00*	0.00*	0.00*
22	0.00*	0.00*	0.00*	0.00*	0.00*	0.00*
24	0.00*	0.00*	0.00*	0.00*	0.00*	0.00*
26	0.00*	0.00*	0.00*	0.00*	0.00*	0.00*
28	0.00*	0.00*	0.00*	0.00*	0.00*	0.00*
30	0.00*	0.00*	0.00*	0.00*	0.00*	0.00*

* COMPUTED SPREAD IS NEGATIVE

b) F/V .030
NOISE 2.0
DYN.LIM. 10DB

EXTREMA

LOEW C / FRAG.	0.0	.05	.1	.2	.3	.5
0.00	21.4	53.0	53.9R	27.5R	12.0R	3.9R
.02	20.1	51.6	54.1R	27.9R	11.9R	3.9R
.04	17.1	45.3	54.4	29.7R	11.8R	3.8R
.06	14.1	29.9	53.4	34.5R	11.8R	3.6R
.08	11.6	18.7	43.6	48.2R	12.1R	3.3R
.10	9.6	12.7	25.1	54.2R	13.2R	3.1R
.12	8.1	9.3	15.0	48.6	17.0R	2.6R
.14	7.0	7.1	9.7	29.6	53.9R	2.1R
.16	6.2	5.7	6.8	17.8	41.6R	1.9R
.18	5.4	4.7	5.0	11.2	26.3	1.7R
.20	4.8	4.1	3.9	7.3	17.0	1.7R
.22	4.5	3.5	3.2	4.8	11.2	1.6R
.24	4.2	3.0	2.4	3.1	7.5	1.6R
.26	3.8	2.5	2.0	2.0	4.9	1.7R
.28	3.5	2.2	1.8	1.7	2.5	1.9R
.30	3.2	2.1	1.7	1.5	1.7	2.0R

R ECHO PHASE ROTATES 360 DEGREES

FRAGMENT SPREAD

EXTR.	0.0	.05	.1	.2	.3	.5
2	.38	.31	.26	.26	.29	.15
4	.25	.20	.20	.23	.27	0.00*
6	.16	.16	.17	.21	.25	0.00*
8	.12	.13	.15	.20	.24	0.00*
10	.10	.12	.14	.19	.23	0.00*
12	.08	.10	.13	.18	0.00*	0.00*
14	.06	.09	.12	.17	0.00*	0.00*
16	.05	.09	.12	.16	0.00*	0.00*
18	.03	.08	.11	.16	0.00*	0.00*
20	.02	.08	.11	.16	0.00*	0.00*
22	0.00*	.07	.11	.15	0.00*	0.00*
24	0.00*	.07	.10	.15	0.00*	0.00*
26	0.00*	.07	.10	.14	0.00*	0.00*
28	0.00*	.06	.10	0.00*	0.00*	0.00*
30	0.00*	.06	.09	0.00*	0.00*	0.00*

* COMPUTED SPREAD IS NEGATIVE

Table 5-1 (Cont.)

e) F/V .045
NOISE 2.0
DYN.LIM. 10DB

EXTREMA

LOEW C FRAG.	0.0	.05	.1	.2	.3	.5
0.00	32.7	100.0	100.0R	31.0R	12.7R	4.0R
.02	29.3	100.0	100.0R	31.5R	12.6R	4.0R
.04	23.0	93.2	100.0R	33.5R	12.4R	3.8R
.06	17.7	42.6	100.0	40.0R	12.3R	3.6R
.08	13.9	23.2	60.9	92.7R	12.6R	3.4R
.10	11.2	14.8	29.7	100.0R	13.8R	3.2R
.12	9.3	10.4	16.8	58.9	18.2R	2.8R
.14	7.9	7.8	10.6	32.2	76.6R	2.2R
.16	6.8	6.2	7.3	18.8	44.7R	1.9R
.18	6.0	5.0	5.4	11.7	27.4	1.8R
.20	5.3	4.3	4.1	7.6	17.5	1.7R
.22	4.8	3.7	3.3	5.0	11.5	1.6R
.24	4.5	3.2	2.5	3.2	7.7	1.7R
.26	4.1	2.6	2.1	2.1	5.1	1.7R
.28	3.8	2.3	1.9	[illegible]	2.7	1.9R
.30	3.5	2.1	1.7	1.5	1.7	2.1R

R ECHO PHASE ROTATES 360 DEGREES

FRAGMENT SPREAD

EXTR.	0.0	.05	.1	.2	.3	.5
2	.40	.31	.27	.26	.29	.15
4	.27	.21	.20	.23	.27	.02
6	.18	.16	.17	.21	.25	0.00*
8	.14	.14	.16	.20	.24	0.00*
10	.11	.12	.14	.19	.23	0.00*
12	.09	.11	.13	.18	.21	0.00*
14	.08	.10	.13	.17	0.00*	0.00*
16	.07	.10	.12	.17	0.00*	0.00*
18	.06	.09	.12	.16	0.00*	0.00*
20	.05	.09	.11	.16	0.00*	0.00*
22	.04	.08	.11	.15	0.00*	0.00*
24	.04	.08	.11	.15	0.00*	0.00*
26	.03	.08	.10	.15	0.00*	0.00*
28	.02	.07	.10	.14	0.00*	0.00*
30	.02	.07	.10	.14	0.00*	0.00*

* COMPUTED SPREAD IS NEGATIVE

d) F/V .060
NOISE 2.0
DYN.LIM. 10DB

EXTREMA

LOEW C FRAG.	0.0	.05	.1	.2	.3	.5
0.00	43.0	100.0	100.0R	32.8R	13.1R	4.1R
.02	37.0	100.0	100.0R	33.3R	13.0R	4.0R
.04	27.5	100.0	100.0R	35.4R	12.7R	3.9R
.06	20.3	50.5	100.0	42.4R	12.6R	3.7R
.08	15.6	25.8	68.2	100.0R	12.8R	3.4R
.10	12.4	16.0	31.9	100.0R	14.1R	3.2R
.12	10.1	11.1	17.8	61.6	18.8R	2.9R
.14	8.5	8.2	11.1	33.2	79.0R	2.3R
.16	7.3	6.4	7.6	19.3	45.6R	2.0R
.18	6.4	5.2	5.5	12.0	27.8	1.8R
.20	5.7	4.4	4.2	7.7	17.7	1.7R
.22	5.0	3.8	3.4	5.1	11.7	1.7R
.24	4.6	3.3	2.6	3.3	7.8	1.7R
.26	4.3	2.7	2.1	2.1	5.2	1.8R
.28	4.0	2.4	1.9	1.7	2.7	1.9R
.30	3.7	2.2	1.8	1.5	1.7	2.1R

R ECHO PHASE ROTATES 360 DEGREES

FRAGMENT SPREAD

EXTR.	0.0	.05	.1	.2	.3	.5
2	.41	.32	.27	.26	.29	.16
4	.28	.21	.20	.23	.27	.03
6	.19	.17	.17	.21	.25	0.00*
8	.15	.14	.16	.20	.24	0.00*
10	.12	.13	.15	.19	.23	0.00*
12	.10	.12	.14	.18	.22	0.00*
14	.09	.11	.13	.17	0.00*	0.00*
16	.08	.10	.12	.17	0.00*	0.00*
18	.07	.10	.12	.16	0.00*	0.00*
20	.06	.09	.12	.16	0.00*	0.00*
22	.05	.09	.11	.16	0.00*	0.00*
24	.05	.08	.11	.15	0.00*	0.00*
26	.04	.08	.11	.15	0.00*	0.00*
28	.04	.08	.10	.15	0.00*	0.00*
30	.03	.08	.10	.14	0.00*	0.00*

* COMPUTED SPREAD IS NEGATIVE

Table 5-1 (Cont.)

e) F/V .075
NOISE 2.0
DYN.LIM. 10DB

EXTREMA

LOEW C FRAG.	0.0	.05	.1	.2	.3	.5
0.00	52.7	100.0	100.0R	34.1R	13.5R	4.1R
.02	43.8	100.0	100.0R	34.5R	13.3R	4.1R
.04	31.0	100.0	100.0R	36.5R	12.9R	3.9R
.06	22.3	55.8	100.0	43.9R	12.8R	3.7R
.08	16.8	27.7	72.3	100.0R	13.0R	3.5R
.10	13.2	16.9	33.3	100.0R	14.3R	3.2R
.12	10.7	11.6	18.4	62.9	19.1R	3.0R
.14	8.9	8.5	11.5	33.8	80.1R	2.3R
.16	7.7	6.6	7.8	19.7	46.0R	2.0R
.18	6.7	5.4	5.6	12.2	28.1	1.8R
.20	5.9	4.5	4.3	7.8	17.9	1.7R
.22	5.2	3.9	3.4	5.2	11.8	1.7R
.24	4.8	3.3	2.6	3.3	7.9	1.7R
.26	4.5	2.8	2.1	2.1	5.2	1.8R
.28	4.2	2.4	1.9	1.7	2.8	1.9R
.30	3.9	2.2	1.8	1.6	1.7	2.1R

R ECHO PHASE ROTATES 360 DEGREES

FRAGMENT SPREAD

EXTR.	0.0	.05	.1	.2	.3	.5
2	.42	.32	.27	.27	.29	.16
4	.29	.22	.21	.23	.27	.03
6	.20	.17	.18	.21	.25	0.00*
8	.15	.15	.16	.20	.24	0.00*
10	.13	.13	.15	.19	.23	0.00*
12	.11	.12	.14	.18	.22	0.00*
14	.10	.11	.13	.17	0.00*	0.00*
16	.08	.10	.13	.17	0.00*	0.00*
18	.08	.10	.12	.16	0.00*	0.00*
20	.07	.09	.12	.16	0.00*	0.00*
22	.06	.09	.11	.16	0.00*	0.00*
24	.06	.09	.11	.15	0.00*	0.00*
26	.05	.08	.11	.15	0.00*	0.00*
28	.05	.08	.11	.15	0.00*	0.00*
30	.04	.08	.10	.14	0.00*	0.00*

* COMPUTED SPREAD IS NEGATIVE

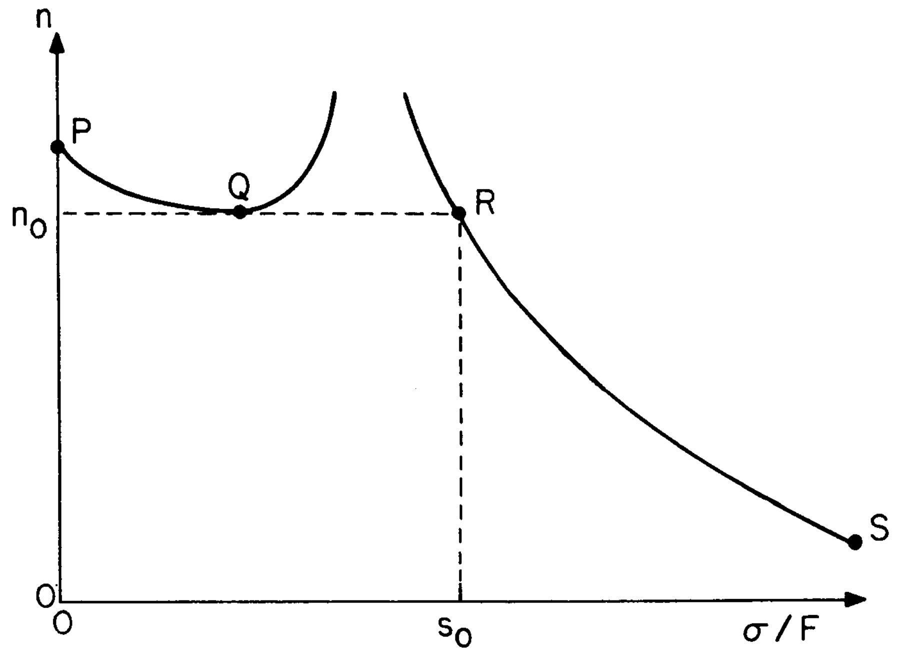

Figure 5-1. An example of the computed observable number n of extrema as a function of fragment spread σ in units of the effective length F of the principal Fresnel zone. See text for discussion.

For each meteor, we used the mean number of extrema measured among all Fresnel patterns accepted by the reduction programs; thus we obtain only a mean measure of the fragment spread. Unfortunately, it was not possible to use the numbers of extrema at individual stations and, therefore, not possible to determine changes in the spread. Moreover, no Fresnel pattern with less than five extrema was ever reduced, so there is a bias against our finding large values of σ.

In view of the significant proportion of meteors for which σ could not be computed, we carried out analyses in two forms. First, where σ was determined, we attempted to find its functional dependence, if any, on other variables. Second, dividing the meteors into three classes – 1) those with σ greater than some given value, 2) those with σ smaller than the given value, and 3) those where σ could not be determined – we attempted to see if other properties showed any meaningful difference among the classes. All in all, a very extensive set of statistics was compiled, but almost all of them revealed nothing, at least to us. In particular, no important relationships seem to exist between σ and perihelion distance, aphelion distance, or inclination. However, the data should be reexamined when we understand better the results that <u>have</u> been found.

Table 5-2 contains the coefficients found by least-squares fits of $\log_{10} \sigma$ to functions of velocity, radar magnitude, radiant zenith distance, and mean height above sea level. We do not interpret them, and they constitute data for a future theory of fragmentation. Values of $\sigma < 0.01$ were omitted from the analysis because they are much too sensitive to observational errors. Undetermined and negative values were, of course, also omitted. Other values of noise give qualitatively similar results. The relatively larger errors of a single observation ("s. e. 1") for the synoptic year probably reflect inhomogeneities in the height data used, leading to errors in the value of C inferred from the heights and thence in the values of σ inferred from C.

Table 5-2. Least-squares fits for $\log_{10} \sigma$ (km).

Data	Number of meteors	Meteors usable	Coefficient of 1	$\log_{10}(V/30)$	M - 11	$\log_{10}(\cos Z/0.707)$	h - 90	s.e. 1
1961-65 noise = 2	9690	8062	-1.08 ±0.03	-0.20 ±0.02	-0.01 ±0.00	+0.05 ±0.01	+0.007 ±0.000	0.17
1961-65 noise = 4	9690	6260	-1.20 ±0.05	-0.36 ±0.02	-0.02 ±0.00	+0.02 ±0.02	+0.010 ±0.001	0.21
Synoptic year noise = 1	17576	10909	-0.94 ±0.04	-0.31 ±0.02	-0.02 ±0.00	-0.00 ±0.02	+0.005 ±0.000	0.30
Synoptic year noise = 2	17576	10017	-1.05 ±0.02	-0.37 ±0.02	-0.02 ±0.00	-0.00 ±0.02	+0.010 ±0.000	0.29

Table 5-3 contains coefficients of least-squares fits of mean height to the other variables used in Table 5-2. It was prepared for another purpose, but is presented here as further data for a future theory.

Table 5-3. Least-squares fits for $\frac{1}{2}(h_{beg} + h_{end})$ (km).

Data	Number of meteors	Coefficient of 1	$\log_{10}(V/30)$	M - 11	$\log_{10}(\cos Z/0.707)$	s.e. 1
1961-65	9691	+87.04 ±0.19	+22.18 ±0.46	-1.94 ±0.08	-3.43 ±0.47	6.02
Synoptic year	17917	+90.84 ±0.06	+19.96 ±0.37	-0.38 ±0.06	-5.08 ±0.41	7.16

Table 5-4 presents an example of the second form of the statistics described above; moreover, it contains a most puzzling result. On any simple model, we should expect a smooth inverse relation between velocity and spread, but here we observe that spread is largest for $16 \leq V < 25$, next largest for $40 \leq V$, next for $25 \leq V < 40$, and smallest for $V < 16$. This unexpected relationship provides not only more data for a future theory, but also an obstacle to further analysis until it is elucidated. Thus far, we have drawn only two minor conclusions from Table 5-4: first, that the confusing appearance of many of the statistics we computed and then did not present here may be explained by the unexpected relation between V and σ; second, that our previous estimates of $N = 2$ for 1961–65 and $N = 1$ for the synoptic year are better than $N = 4$ and $N = 2$, respectively, as evidenced by the large proportion of undetermined σ's at the large values of N.

Table 5-4. Relative numbers of meteors having $\sigma \gtrless 0.1$ km.

		1961–65		Synoptic year	
		Noise = 2	Noise = 4	Noise = 1	Noise = 2
$V < 16$	$\sigma < 0.1$	0.81	0.84	0.85	0.90
	$\sigma > 0.1$	0.19	0.11	0.15	0.09
	undetermined	0.00	0.05	0.00	0.01
	n	151		951	
$16 \leq V < 25$	$\sigma < 0.1$	0.56	0.58	0.40	0.49
	$\sigma > 0.1$	0.43	0.31	0.58	0.47
	undetermined	0.01	0.11	0.02	0.04
	n	1506		4467	
$25 \leq V < 40$	$\sigma < 0.1$	0.64	0.53	0.77	0.60
	$\sigma > 0.1$	0.28	0.11	0.19	0.12
	undetermined	0.08	0.36	0.04	0.28
	n	5817		8963	
$40 \leq V$	$\sigma < 0.1$	0.48	0.45	0.58	0.61
	$\sigma > 0.1$	0.36	0.14	0.33	0.12
	undetermined	0.16	0.41	0.09	0.27
	n	2216		3195	

Table 5-5 contains data comparable to Table 5-4, except that the dividing value for σ is 0.03 km. It does not contain a surprise as Table 5-4 did, but shows that very small values of σ are relatively uncommon.

Table 5-5. Relative numbers of meteors having $\sigma \gtrless 0.03$ km.

		1961–65 noise = 2	Synoptic year noise = 1
$V < 16$	$\sigma < 0.03$	0.00	0.00
	$\sigma > 0.03$	1.00	1.00
	undetermined	0.00	0.00
	n	151	951
$16 \leq V < 25$	$\sigma < 0.03$	0.02	0.02
	$\sigma > 0.03$	0.97	0.94
	undetermined	0.01	0.04
	n	1506	4467
$25 \leq V < 40$	$\sigma < 0.03$	0.05	0.03
	$\sigma > 0.03$	0.82	0.38
	undetermined	0.13	0.59
	n	5817	8963
$40 \leq V$	$\sigma < 0.03$	0.07	0.05
	$\sigma > 0.03$	0.83	0.78
	undetermined	0.10	0.17
	n	2216	3195

5.4 Conclusions

We badly need a physical theory of fragmentation to interpret the observations presented in Section 5.3 and thus to understand other observations. The amplitudes of the Fresnel patterns from the synoptic year should be analyzed. The approximate magnitude of the fragment spread along the trajectory found in our previous report (Southworth and Sekanina, 1974, Table 2) is well confirmed. [Note the differing definitions of w (1974) and σ (this report).]

The conclusion in our 1974 report that we have no evidence for observational selection by fragmentation is shakily confirmed. That conclusion rested on the bunching of the data to low values of the spread and, in particular, on the absence of higher spreads at low velocity. The analysis reported here shows a broader distribution of the spread than was envisaged before. Moreover, while few large spreads occur at the lowest velocities, many do in the interval $16 \leq V < 25$.

6. OBSERVATIONAL BIASES

6.1 Radiant Zenith Distance

Southworth and Sekanina (1974, p. 12) included a note added in proof stating that we had just realized a systematic bias due to the fact that the radar system was not oriented to observe long trails from meteors with small cos Z_R. The orientation was, of course, in the original design of the system, to enable it to observe all of some long trails with a minimum number of stations.

In order to determine the necessary correction, we computed, for each meteor in the synoptic year, the projected extent of the station array on the meteor trajectory. When a perpendicular is dropped onto the trajectory from each station, the projected extent is the distance between the most widely separated perpendiculars. The specular reflection point for any station is approximately halfway between the perpendicular from that station and the perpendicular from the transmitter station; accordingly, the maximum distance between specular reflection points is approximately half the projected extent of the station array. To find the ionization curve, the computer program fitted a quadratic in distance along the trajectory to the logarithm of the line density determined at each specular reflection point. If this quadratic was concave downward, and if it intersected the minimum detectable line density no more than 4 km before the first specular reflection point and again no more than 2 km after the last observed Fresnel extremum, the ionization curve was classified as well-determined. A quadratic intersecting the minimum detectable line density outside either limit was truncated at that limit, and the curve was classified as not well-determined. A quadratic concave upward was replaced by a rectangle bounded at those limits and classified as not well-determined.

The trail length is the distance between the intersections of the quadratic with the minimum detectable line density or the ends of the curve as limited above. Allowing roughly 2 km for the distance between the last specular reflection point and the last observed Fresnel extremum, a not-well-determined trail length is therefore limited to, at most,

$$L_{length} \approx 0.5\, E_p + 8 \text{ km} \quad , \tag{6-1}$$

where E_p is the projected extent of the station array. Well-determined lengths are systematically shorter than those that are not.

Some exceptions arise to the limit expressed in equation (6-1). In an attempt to correct for minor observational deficiencies, those ionization curves that had been truncated at either the beginning or the end (not both) by less than half the distance between the maximum and the intersection with the minimum detectable line density had that truncation restored for this purpose, and the curve was reclassified as well-determined.

We divided the meteors into groups: $E_p \leq 10$ km, $10 < E_p \leq 20$, $20 < E_p \leq 30$, and $30 < E_p$; we also divided them by magnitudes $\lesseqgtr 11$ and by well-determined and not-well-determined ionization curves. In each group, we then fitted coefficients A and B by least-squares of the form

$$\ell n\,(h_{beg} - h_{end}) = A + B\,\ell n \left(\frac{\cos Z_R}{0.7071}\right) \quad , \tag{6-2}$$

where h_{beg} and h_{end} are the heights above sea level of the beginning and end of the trail. Table 6-1 gives the values found for A and B and various other data. Table 6-1a gives well-determined ionization curves, and Table 6-1b presents those that are not well-determined. The logarithmic (geometric) mean is denoted by L MN, and the antilogarithm of the rms deviation of the logarithm from the mean of the logarithms, by L SD. MAX and MIN are the largest and smallest values in the group; PR. 1 is the error that will be exceeded in 10% of trails, using Student's criterion; and PROJ is the mean projected station extent. The numbers of meteors with ionization curves extended for the purpose of this study, and therefore not strictly subject to the limit in equation (6-1), are designated (BEG) and (END).

Figure 6-1 shows the regression lines for well-determined ionization curves fainter than magnitude 11. They have been terminated at the 1/e points in the distribution of $\ell n\,(\cos Z_R/0.7071)$ to illustrate the range of $\cos Z_R$ occurring in each group.

Table 6-1. Statistics of vertical trail length and cos Z_R.

a) Well-determined ionization curves

	GOOD ION C PROJ GT 30		GOOD ION C PROJ 20-30		GOOD ION C PROJ 10-20		GOOD ION C PROJ LE 10	
MAGN	GT 11	LE 11	GT 11	LE 11	GT 11	LE 11	GT 11	LE 11
NOBS	273	163	3641	2036	1382	851	86	60
(BEG)	43	16	574	206	204	91	4	0
(END)	10	10	248	176	103	70	6	0
HB-HE								
L MN	7.81	8.65	8.29	8.93	6.43	6.98	7.17	6.66
L SD	3.00	3.21	3.10	3.25	2.70	2.89	1.70	1.19
MAX	19.4	18.8	23.0	25.6	19.6	20.2	14.2	10.0
MIN	3.0	3.1	1.2	2.2	0.9	0.9	4.1	4.7
COSZR								
L MN	0.655	0.670	0.715	0.721	0.587	0.632	0.796	0.818
L SD	0.103	0.091	0.142	0.135	0.230	0.238	0.101	0.091
MAX	0.75	0.75	0.90	0.90	0.94	0.94	0.93	0.93
MIN	0.29	0.31	0.12	0.18	0.09	0.10	0.54	0.58
A	2.1120	2.2002	2.1072	2.1799	2.0044	2.0298	1.8909	1.8694
PR. 1	0.0407	0.0496	0.0095	0.0129	0.0143	0.0173	0.0546	0.0639
B	0.7408	0.7889	0.6919	0.4748	0.7721	0.7725	0.6730	0.1874
PR. 1	0.2343	0.3407	0.0478	0.0686	0.0330	0.0440	0.3154	0.3507
PROJ	31.45	31.37	25.06	24.91	15.78	15.80	8.17	8.21

b) Not well-determined ionization curves

	LOWBND I C PROJ GT 30		LOWBND I C PROJ 20-30		LOWBND I C PROJ 10-20		LOWBND I C PROJ LE 10	
MAGN	GT 11	LE 11	GT 11	LE 11	GT 11	LE 11	GT 11	LE 11
NOBS	352	97	3674	1361	2701	983	134	68
(BEG)	0	0	0	0	0	0	0	0
(END)	0	0	0	0	0	0	0	0
HB-HE								
L MN	8.36	9.21	9.07	9.87	6.75	7.26	8.51	9.06
L SD	2.46	3.31	2.55	2.71	2.55	2.90	1.30	1.87
MAX	19.2	19.1	20.9	19.2	23.0	20.6	16.7	17.8
MIN	1.7	3.5	1.2	1.7	1.2	1.4	6.1	5.8
COSZR								
L MN	0.656	0.637	0.698	0.716	0.548	0.563	0.794	0.812
L SD	0.112	0.117	0.155	0.141	0.215	0.227	0.100	0.100
MAX	0.75	0.75	0.90	0.90	0.94	0.94	0.94	0.94
MIN	0.20	0.33	0.12	0.11	0.09	0.10	0.53	0.53
A	2.1897	2.3056	2.2149	2.2808	2.1259	2.1820	2.0875	2.0866
PR. 1	0.0242	0.0637	0.0061	0.0105	0.0067	0.0112	0.0278	0.0544
B	0.8899	0.8195	0.7635	0.7149	0.8507	0.8758	0.4610	0.8499
PR. 1	0.1300	0.3035	0.0275	0.0536	0.0142	0.0242	0.1627	0.2952
PROJ	31.53	31.55	24.65	24.51	15.41	15.74	8.57	8.03

Lines for brighter meteors, or for not-well-determined ionization curves, are similar, but they are systematically displaced upward and are rather less regular. It is evident that a regression line fitted to all the data would show a steeper slope and that it would not properly represent the physical relationship. Moreover, there is still reason to fear that some of the separate regression lines are also subject to selection effects. Dotted lines in Figure 6-1 show the upper bound L_{hb-he} within the figure for a meteor of each group that has the average projected station extent for that group and that did not have its ionization curve arbitrarily extended, which is

$$L_{hb-he} = (0.5\ E_p + 8) \cos Z_R \quad . \tag{6-3}$$

It seems likely that the regression line for the group $10 \leq E_p < 20$ has been biased.

In order to correct our statistics, we must decide on a relation between trail length and $\cos Z_R$. Taking an approximate weighted average of the values of B in Table 6-1 with $E_p > 20$, we adopt

$$B = 0.7 \pm 0.1 \quad . \tag{6-4}$$

6.2 Projected Station Extent

We need further to correct for the tendency of the limitation in projected station extent to cause us to underestimate the trail length and thus the mass of a meteor. (It is not, however, necessary to include any new correction for the size or shape of the atmospheric volume observed by the radar system.) Figure 6-2 is a plot of the A-coefficients in Table 6-1, and empirical straight lines have been drawn through points for well-determined and not-well-determined curves. In principle, both curves should have horizontal asymptotes at the right, but we accept them as practical approximations. The convergence of the lines definitely suggests that not-well-determined curves would be well-determined if only the station array were large enough. To correct our statistics, we adopt the average slope 0.18 of the two lines and estimate that the trail length is independent of E_p above $E_p = 40$. The corresponding correction factor for the system sensitivity that must be inserted into existing computer programs is

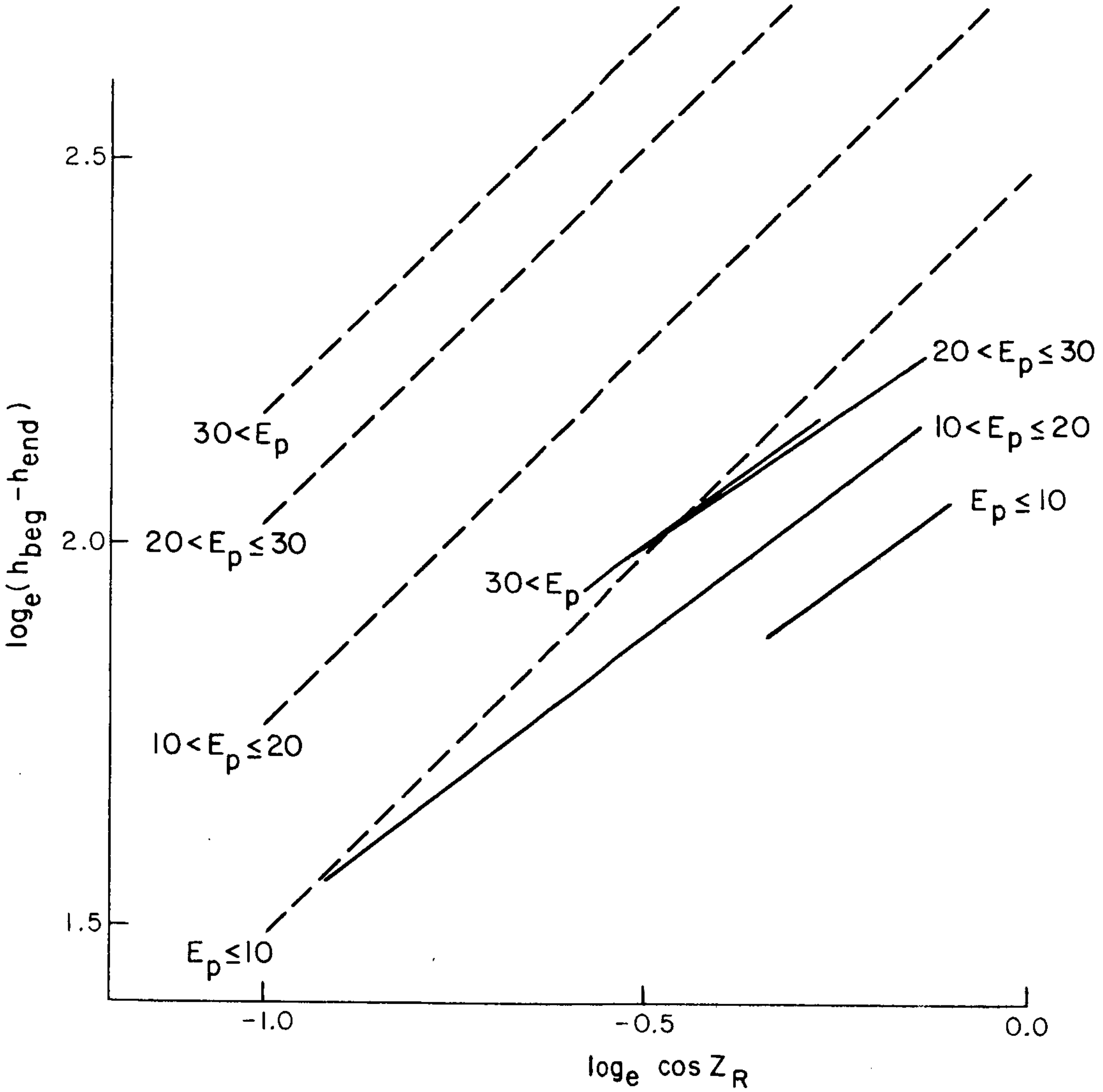

Figure 6-1. Least-squares fits (solid lines) and mean upper bounds (dotted lines) of vertical trail length to cos Z_R, for groups of projected station extent for synoptic-year meteors, with well-determined ionization curves, fainter than magnitude 11.

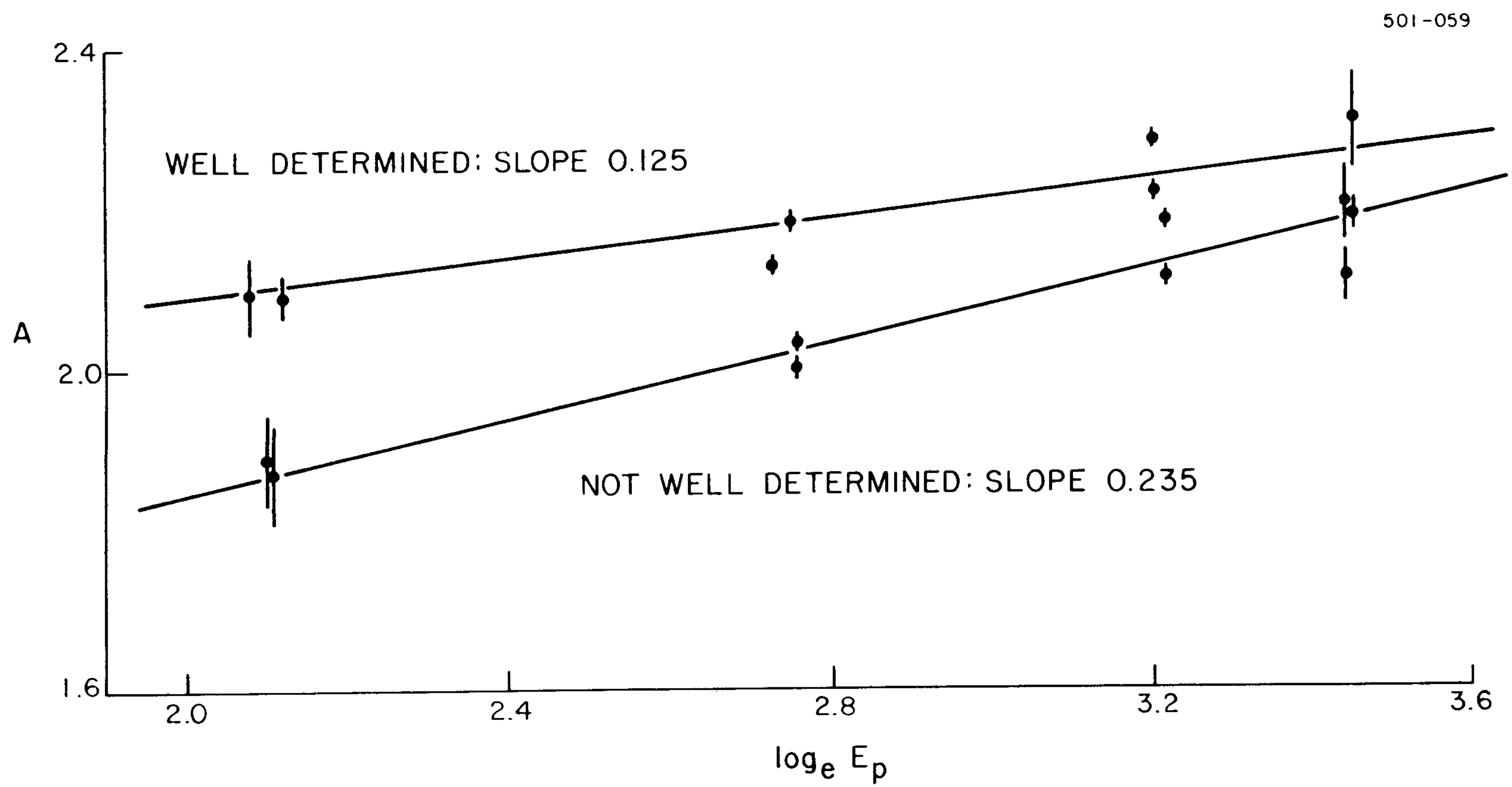

Figure 6-2. Coefficients A [see eq. (6-2) and Table 6-1] as functions of mean projected station extent E_p.

$$F = \left(\frac{E_p}{40}\right)^{0.18} , \qquad (6\text{-}5)$$

and the revised mean vertical trail length is

$$h_{beg} - h_{end} = 12.3\ (\cos Z_R)^{0.7} . \qquad (6\text{-}6)$$

Equation (6-6) replaces equation (16) from Southworth and Sekanina (1974), which we recognized as suspect while reading the proofs of the report, and which read

$$h_{beg} - h_{end} = 10.7\ (\cos Z_R)^{0.89} .$$

The differences, though real, are much too small to invalidate any of the conclusions we drew from it.

6.3 Antenna Sensitivity

In Southworth and Sekanina (1973), we described a revision of the previously adopted radiant sensitivity pattern, based on measurements of antenna sensitivity. There is, however, a companion factor to the radiant sensitivity, which takes into account, as a function of declination, the interval of right ascension within which the radiant sensitivity is large enough to be applied, since radiants outside that interval are assigned zero weight. We find that this companion factor was not changed at that time; consequently, we have now changed it. The effect is not large.

7. ORBITAL DISTRIBUTIONS

7.1 Data Samples

This section presents tables of the distributions of velocity, radiant, and orbital elements of meteors observed in the synoptic year and in 1961–65. Most of the tables represent the data in three forms: 1) unweighted, 2) reduced to equal masses in the atmosphere, and 3) reduced to equal masses in space at the earth's distance from the sun. We use three forms to facilitate comparison with the great variety of other published forms. Observations from earth satellites should be compared with the second form, and observations not restricted to the ecliptic (e.g., comets), with the third form.

The weights are computed as described in Southworth and Sekanina (1973), except for the changes discussed in Section 6. There is no correction for fragmentation. The correction for diffusion, empirically developed for the synoptic-year meteors, can be only approximate for the 1961–65 meteors. No correction could be intelligently made for the known bias against low velocities in 1961–65 caused by recombination (Southworth, 1973).

Table 7-1 contains the number of observations used for the different samples presented. Meteors with slant ranges over 400 km were omitted from all samples because they are especially subject to errors caused by wind shears. Those with slant ranges under 70 km were not included, because such ranges are likely to be recording errors. Meteors outside the main lobe of the antenna pattern were left out because they have less accurate reductions and are likely to be unrepresentatively larger than meteors in the main lobe. A few 1961–65 meteors with seemingly erroneous masses were also omitted. Finally, we did not include any meteors from the space samples with radiants south of the ecliptic, because we cannot get a complete sample of southern radiants.

Table 7-1. Number of meteors used.

	Synoptic year	1961–65
Total reduced	19698	19180
Observed sample	14076	14520
Atmospheric sample	14076	14520
Space sample	12321	11920

Table 7-2 contains the unweighted distribution of mass in the synoptic-year and 1961–65 observed samples. The mean difference in equipment sensitivity between the two periods was approximately 22 db, corresponding to a factor of 12.6 in mass. This factor, however, is far from being completely reflected in the mass distributions, because of the relative lack of low-velocity meteors in the earlier sample.

Table 7-2. Distribution of mass.

Mass (g)	Synoptic year	1961–65
10^{-1}		
	0.006	0.048
10^{-2}		
	0.096	0.326
10^{-3}		
	0.384	0.457
10^{-4}		
	0.397	0.152
10^{-5}		
	0.109	0.019
10^{-6}		
	0.009	0.000
10^{-7}		

For the synoptic year, the tables in this section supersede the corresponding tables and figures in Southworth and Sekanina (1973) (the 1961–65 meteors have not been previously published in this form). Moreover, the space densities in the 1973 report also require revision, which we hope to publish separately.

7.2 Velocities

Table 7-3 contains the distribution of no-atmosphere velocities for the six samples. Each entry is the fraction of one sample having velocities in a 5-km sec^{-1} interval, except that the last interval includes all velocities over 70 km sec^{-1}. Entries smaller than 0.010 are in a compressed form of scientific notation; for example, 39-4 means $39. \times 10^{-4}$ (note the position of the decimal point).

Table 7-3. Distribution of no-atmosphere velocity.

Velocity (km sec^{-1})	Synoptic year			1961–65		
	Observed	Atmospheric	Space	Observed	Atmospheric	Space
10	0.029	0.701	0.256	81-4	0.593	0.150
15	0.084	0.214	0.398	0.037	0.232	0.323
20	0.160	0.062	0.221	0.101	0.111	0.281
25	0.195	0.017	0.083	0.182	0.043	0.148
30	0.201	48-4	0.031	0.225	0.015	0.068
35	0.144	12-4	85-4	0.185	42-4	0.024
40	0.068	22-5	18-4	0.099	92-5	54-4
45	0.031	47-6	32-5	0.046	19-5	11-4
50	0.033	23-6	13-5	0.040	79-6	25-5
55	0.031	13-6	50-6	0.042	49-6	12-5
60	0.017	43-7	12-6	0.026	20-6	42-6
65	50-4	87-8	20-7	79-4	40-7	38-7
70	50-5	79-9	14-8	12-4	35-8	36-8

The synoptic-year distribution is little changed from our 1973 report, with a then-unprecedented preponderance of low velocities; 1961–65 is closer to other observers' distribution.

7.3 Radiants

Tables 7-4 through 7-9 show the radiant distribution in the six samples as a function of celestial longitude measured from the sun LAMBDA and celestial latitude BETA. Each entry is the mean radiant density, per unit area, in a 5° interval of latitude and longitude. The unit of density is one-tenth the mean radiant density in the north celestial hemisphere; thus, "10" represents mean density. The entries have been smoothed with a triangular weighting function in longitude and latitude. The latitudinal

Table 7-4. Radiant distribution from the synoptic-year observed sample.

BETA LAMBDA		10		20		30		40		50		60		70		80		90		100		110		120		130		140		150		160		170		180
90	21	21	21	21	21	21	21	21	21	21	21	21	21	21	22	22	21	21	21	21	21	21	21	21	21	21	21	21	21	22	22	22	22	23	23	23
85	16	17	16	16	16	16	17	17	17	17	17	17	16	16	16	15	15	14	14	14	15	15	15	16	17	17	18	19	19	20	20	20	20	21	22	23
80	18	16	15	15	14	15	15	14	13	12	11	10	9	9	10	10	10	10	10	10	10	11	12	13	13	13	12	12	13	14	15	17	19	21	21	21
75	17	15	13	13	12	12	11	10	9	7	5	4	4	4	4	5	6	6	6	5	6	7	8	8	8	7	7	8	9	10	10	12	14	17	19	18
70	15	13	11	9	8	7	7	6	5	4	4	4	4	3	3	3	3	3	3	3	3	4	5	5	4	3	4	5	6	7	7	7	9	11	13	14
65	13	11	8	6	5	5	5	4	3	3	3	4	3	3	2	3	2	2	2	2	2	3	3	3	2	2	2	3	4	4	5	6	8	9	11	13
60	13	10	6	6	5	5	4	4	3	3	2	2	2	1	2	2	2	1	1	2	2	2	2	2	2	2	2	2	3	3	4	5	7	8	11	12
55	11	9	7	5	5	4	4	4	3	2	1	1	1	1	1	1	1	1	1	2	2	2	2	2	2	2	1	1	2	2	2	4	6	7	8	10
50	8	7	6	5	4	4	3	3	2	2	1	1	1	1	1	1	1		1	1	1	1	1	1	1	1	1	1	1	2	3	3	5	6	6	8
45	6	5	5	4	3	3	2	2	1	1	1	1	1	1	1							1	1	1	1			1	1	2	3	3	4	4	5	7
40	5	4	4	3	3	3	2	1	1	1	1	1		1	1	1						1						1	1	2	2	3	3	4	4	6
35	4	4	3	3	3	3	2	1	1	1	1	1		1	1	1		1	1	1								1	1	1	1	2	3	4	5	5
30	4	4	3	2	3	2	2	1	1	1	1	1			1				1	1	1								1	1	1	1	2	4	5	6
25	4	3	3	3	3	2	1	1		1	1	1																	1	1	2	2	2	3	5	7
20	5	3	2	2	2	2	1	1			1	1																	1	1	2	2	2	3	5	7
15	5	4	2	2	1	1																							1	1	1	2	2	3	5	7
10	6	4	2	1	1	1	1																						1	1	1	2	3	3	5	7
5	6	5	3	2	1	1	1			1																			1	1	1	2	2	3	5	9
0	4	4	3	2	1					1																			1	1	1	2	3	3	5	8
-5	4	3	3	2	1					1																			1	1	1	2	3	3	4	5
-10	2	2	2	1	1	1			1																			1	1		1	1	2	2	2	4
-15	2	2	2	1	1	1																											1	1	1	3
-20	1	1	1	1																												1	1	1	1	1
-25	1	1	1																													1	1	1	1	1
-30	1		1																																1	1
-35																																				1
-40																																				1
-45																																				
-50																																				
-55																																				
-60																																				
-65																																				

Table 7-4 (Cont.)

BETA / LAMBDA		190		200		210		220		230		240		250		260		270		280		290		300		310		320		330		340		350		360
90	24	25	25	26	26	27	28	28	29	29	30	30	31	31	31	31	31	30	30	29	29	26	27	27	26	26	25	24	23	23	22	22	22	21	21	21
85	24	26	27	28	29	29	29	30	31	33	35	36	41	44	45	46	45	43	42	40	38	37	36	35	33	32	31	29	27	25	23	22	22	21	20	19
80	21	22	23	24	25	26	26	28	30	33	37	42	46	49	49	48	46	49	50	51	50	47	45	41	39	38	36	33	31	26	24	22	22	22	21	20
75	17	18	19	21	24	25	26	28	31	35	41	47	51	53	52	51	57	56	59	58	56	53	48	44	39	37	36	34	31	28	26	24	23	22	20	19
70	15	16	18	21	24	27	29	31	33	35	39	44	49	52	54	57	64	68	69	65	60	56	52	48	45	42	38	35	32	31	29	27	24	22	19	16
65	15	16	17	19	22	25	27	28	28	29	32	37	43	47	54	63	76	85	87	79	70	63	59	56	52	48	42	38	34	32	31	29	26	23	19	16
60	14	14	15	16	18	21	22	22	22	23	26	29	34	39	47	59	76	90	94	85	74	64	58	54	50	46	41	36	32	30	29	27	25	22	18	15
55	11	12	13	14	15	16	16	17	19	20	22	25	26	30	36	42	56	76	82	69	58	49	43	42	41	38	34	31	28	27	26	23	20	17	14	12
50	10	11	11	12	13	12	12	14	16	17	19	19	19	22	25	27	35	45	48	43	37	32	27	26	27	26	26	26	24	23	23	21	18	14	11	10
45	9	9	9	9	12	12	12	13	14	14	15	14	14	16	16	17	21	26	28	25	22	20	17	16	17	17	18	19	17	17	17	17	16	13	9	8
40	8	9	9	9	12	13	12	11	11	11	11	11	11	12	12	12	16	19	21	18	15	13	12	12	12	12	12	12	14	15	13	12	11	10	9	7
35	7	9	10	11	13	13	11	10	10	9	9	9	9	10	10	12	15	18	18	17	14	11	9	9	9	8	8	10	12	12	11	9	8	7	7	6
30	7	9	9	11	13	13	12	10	8	8	8	8	8	10	11	13	17	18	17	16	14	11	9	8	7	6	8	10	9	9	9	8	7	7	6	5
25	8	9	10	10	12	14	13	10	8	8	7	7	9	10	11	14	17	19	19	15	13	11	10	8	6	5	7	9	9	8	8	7	8	8	6	5
20	8	9	12	13	15	18	17	11	9	8	7	8	10	10	11	13	15	19	20	16	13	11	9	6	5	6	7	8	10	10	9	9	9	9	7	6
15	8	11	15	17	21	26	22	13	9	7	7	9	9	6	10	11	13	15	15	13	12	10	7	5	4	5	6	7	10	11	10	10	11	11	9	7
10	10	15	19	21	25	28	21	11	7	6	6	7	7	6	8	8	8	9	8	7	7	6	5	4	3	4	4	6	9	11	11	11	11	12	11	9
5	13	20	23	23	23	22	15	8	5	4	5	5	4	4	4	4	4	5	4	3	3	3	3	3	3	3	3	4	7	11	13	11	11	13	12	8
0	12	19	22	20	19	18	13	6	4	3	4	4	3	3	3	2	2	3	3	2	2	2	3	3	2	2	3	4	7	10	11	11	11	12	10	6
-5	9	14	15	15	16	15	11	8	4	2	3	3	3	4	3	2	3	4	4	4	3	3	3	4	2	2	3	4	6	7	9	10	10	9	7	5
-10	6	8	9	10	12	11	8	6	4	2	2	3	3	3	3	3	4	4	5	5	4	3	3	3	2	2	3	4	5	6	7	8	7	5	4	3
-15	4	5	5	6	7	7	5	4	3	2	1	2	2	3	2	2	4	4	4	4	3	2	3	3	2	2	3	3	4	4	5	5	4	3	3	2
-20	2	2	3	3	5	5	4	4	2	1	1	1	2	2	2	2	3	4	4	3	1	1	2	2	2	2	2	2	3	2	2	2	2	1	1	1
-25	1	1	1	2	3	3	3	3	2	1	1	2	2	1	1	1	2	3	3	2	1	1	1	1	1	1	1	1	1	1	1	1	1	1	1	1
-30	1	1	1	1	2	2	2	2	1	1	1	1	1	1	1	1	1	2	2	1	1	1	1			1	1	1	1	1	1	1	1	1	1	1
-35	1	1	1	1	1	1	1	1	1	1	1	1	1	1	1	1	1	1	1	1	1	1				1	1	1	1	1	1	1	1	1	1	1
-40	1	1	1	1	1	1	1	1		1	1	1	1	1				1	1	1	1								1	1	1	1	1			
-45						1	1	1											1	1	1										1					
-50																			1	1	1															
-55																		1	1	1	1															
-60																		1	1	1																
-65																																				

Table 7-5. Radiant distribution from the 1961–65 observed sample.

BETA LAMBDA		10		20		30		40		50		60		70		80		90		100		110		120		130		140		150		160		170		180
90	18	18	18	18	18	18	18	18	18	18	18	17	17	17	17	16	16	16	16	15	15	15	15	15	15	15	15	16	16	16	17	17	18	18	19	19
85	15	15	14	14	13	13	13	13	13	13	13	13	12	12	12	11	11	10	10	10	10	10	10	10	11	11	11	12	12	13	13	14	15	16	18	20
80	14	12	10	9	9	9	10	9	9	8	7	7	6	6	6	7	7	7	6	6	5	5	5	6	7	8	8	9	9	11	12	13	13	13	14	15
75	13	12	9	7	6	7	8	8	7	5	5	5	4	4	3	4	4	4	4	3	3	3	3	4	4	5	6	6	7	7	8	8	9	10	10	12
70	11	10	8	6	5	5	5	5	5	4	4	3	3	3	3	2	2	2	2	2	2	2	2	2	3	3	4	4	4	4	4	4	5	7	8	10
65	8	7	5	4	3	3	3	3	2	2	2	2	2	2	1	1	1	1	1	1	2	2	2	2	2	2	2	2	2	2	2	3	3	5	6	8
60	6	5	4	3	2	2	1	1	1	1	1	1	1	1	1	1	1	1	1	1	1	1	1	1	1	1	1	1	1	1	2	3	4	5	6	7
55	5	4	2	2	2	1	1	1	1	1	1	1			1	1	1								1	1	1	1		1	1	2	4	5	6	7
50	4	2	2	2	2	2	2	1	1	1						1			1						1	1	1	1	1	1	1	1	2	4	5	6
45	4	2	2	1	2	2	2	1	1	1															1	1	1	1	1	1	1	1	2	2	3	5
40	4	2	2	2	2	1	1	1																						1	1	1	1	2	3	5
35	3	2	2	2	1	1																									1	1	1	2	3	5
30	3	2	2	1	1			1	1	1																					1	1	1	2	3	5
25	3	3	2	1	1				1	1																						1	1	2	3	5
20	4	3	2	1	1	1			1	1																				1		1	1	2	3	5
15	6	4	2	1	1	1																										1	1	2	4	8
10	6	4	2	1	1	1																										1	1	3	6	11
5	5	3	2	1	1																										1	1	2	3	5	9
0	5	3	2	1																											1	1	2	3	4	7
-5	4	3	1																												1	1	2	3	4	7
-10	3	2	1																												1	1	1	2	3	5
-15	2	1	1																														1	1	2	3
-20	1	1	1																															1	1	2
-25	1	1																																	1	2
-30	1																																	1	1	2
-35																																			1	1
-40																																				
-45					1																															
-50																																				
-55																																				
-60																																				

Table 7-5 (Cont.)

BETA \ LAMBDA		190		200		210		220		230		240		250		260		270		280		290		300		310		320		330		340		350		360
90	20	21	21	21	21	22	22	22	22	22	22	23	22	22	22	22	22	22	22	22	21	21	20	20	20	19	19	19	18	18	18	18	18	18	18	18
85	22	23	25	25	25	24	24	25	25	26	28	30	32	33	34	35	36	36	35	34	33	32	30	28	27	26	24	23	21	20	19	18	18	17	16	16
80	17	20	22	25	26	25	27	28	30	33	37	40	42	47	42	45	45	47	46	43	41	38	36	35	34	32	30	27	25	23	20	19	18	17	16	15
75	14	18	20	23	25	29	32	34	35	36	37	40	44	46	50	54	57	60	60	58	52	45	38	34	33	34	33	32	28	25	21	19	16	14	13	13
70	12	15	18	22	24	27	30	33	34	35	36	40	47	52	58	63	70	76	79	75	65	53	43	38	37	35	34	31	29	25	23	19	16	13	11	11
65	10	13	17	20	22	23	24	26	28	31	34	39	45	49	55	64	77	88	91	84	71	57	47	42	39	36	32	28	26	22	19	16	15	13	12	10
60	10	13	17	18	20	21	22	24	25	26	29	32	35	39	45	57	73	67	90	79	63	50	43	39	35	31	28	24	22	19	16	14	12	11	10	8
55	9	13	16	16	18	21	23	24	22	21	23	25	26	26	33	41	55	76	79	57	40	36	33	29	27	24	20	19	18	16	14	13	10	8	7	6
50	8	11	15	17	18	21	23	22	18	17	18	19	20	22	24	27	34	45	45	33	26	27	25	20	18	18	16	15	15	14	13	11	9	7	5	4
45	7	9	13	16	17	20	22	19	16	14	14	14	14	14	15	18	22	26	24	20	19	19	19	15	11	13	15	14	13	13	12	11	8	6	4	4
40	7	9	11	13	15	17	18	17	15	13	10	11	11	10	12	14	19	22	20	17	16	14	13	10	7	9	12	12	13	13	12	10	8	6	4	4
35	7	9	11	13	15	16	16	16	15	12	9	9	10	10	12	15	19	22	21	18	15	11	9	8	6	7	8	10	12	12	11	10	9	7	5	4
30	8	9	11	13	15	16	16	15	14	12	9	9	10	11	13	16	21	25	24	19	14	10	8	8	7	7	7	10	12	12	11	10	10	8	6	4
25	8	10	12	14	17	18	17	15	14	11	8	10	11	12	14	17	23	26	26	20	16	11	9	8	7	7	8	10	13	14	12	11	11	9	6	5
20	8	12	17	21	26	30	27	19	14	10	8	8	10	13	15	17	21	26	24	19	16	12	9	7	7	7	8	9	13	16	14	13	13	10	8	6
15	11	15	22	29	39	49	40	23	13	9	8	8	9	12	15	14	16	21	19	14	12	11	9	8	8	7	7	9	14	19	18	17	16	12	11	8
10	16	22	28	35	47	54	40	20	10	7	7	7	8	10	11	10	11	13	12	8	7	8	7	7	7	7	7	9	14	19	20	21	20	17	13	10
5	17	26	33	37	43	44	32	17	8	5	5	6	7	8	7	6	6	6	5	5	5	4	4	4	4	5	6	9	13	17	21	24	23	19	14	9
0	14	24	32	36	37	35	26	15	8	5	4	5	6	8	7	5	5	4	4	4	4	4	4	4	4	5	7	11	14	17	21	24	22	17	11	7
-5	12	19	24	28	30	29	22	13	8	5	5	5	6	9	8	6	6	6	5	5	4	5	5	5	4	5	6	10	14	16	19	20	16	12	8	5
-10	8	11	15	17	19	13	15	10	6	4	4	5	5	8	8	6	6	8	7	6	5	5	5	5	4	4	4	6	10	12	14	13	9	7	5	3
-15	4	6	8	9	9	9	8	6	4	3	3	3	3	5	6	5	5	7	7	5	4	4	4	4	4	3	3	5	7	9	8	6	5	4	3	2
-20	3	4	4	4	5	5	6	5	3	3	3	3	2	3	4	4	4	6	6	4	4	3	2	3	3	2	3	4	6	5	4	3	2	2	2	1
-25	2	2	2	3	3	4	4	3	3	3	3	3	2	2	3	3	4	4	4	3	3	2	2	2	1	1	2	2	3	2	2	2	1	1	1	1
-30	2	1	1	2	3	3	3	3	3	3	3	3	2	1	2	2	3	3	2	1	2	2	2	1	1	1	1	2	2	2	1	1	1		1	1
-35	1	1	1	1	2	2	2	2	2	3	3	2	1	1	1	2	2	2	1	1	1	1	1	1	1	1	1	1	2	1	1	1			1	1
-40	1	1	1	1	1	1	1	1	1	2	2	2	1	1	1	1	1	1	1	1	1	1			1	1			1	1	1				1	
-45				1	1	1	1	1	1	1	1	1	1	1	1	1	1	1	1	1	1															
-50							1	1	1	1	1	1	1		1																					
-55									1	1																										
-60																																				

Table 7-6. Radiant distribution from the synoptic-year atmospheric sample.

BETA \ LAMBDA		10		20		30		40		50		60		70		80		90		100		110		120		130		140		150		160		170		180
90	32	31	31	31	31	31	31	31	31	31	31	31	32	32	33	33	33	34	34	34	34	34	34	34	34	34	34	34	33	33	32	32	32	31	31	31
85	34	31	29	28	28	24	28	27	26	26	25	25	24	24	24	24	23	23	23	25	28	32	36	41	45	47	47	46	42	38	34	32	30	29	29	30
80	35	26	26	26	26	30	30	27	24	21	19	19	19	20	20	20	19	17	16	16	18	23	31	39	45	47	46	41	35	31	29	29	34	39	44	47
75	28	21	19	24	29	33	33	28	22	16	14	14	16	16	16	16	18	19	18	15	13	17	23	31	33	32	27	24	21	19	19	23	29	41	52	59
70	24	18	16	18	24	29	30	25	18	13	12	14	14	13	12	14	17	21	21	20	17	18	20	22	21	19	16	15	13	13	13	16	20	28	35	41
65	23	20	16	15	19	25	28	24	18	14	13	14	12	11	10	12	14	16	18	19	20	20	20	18	16	13	12	11	10	10	11	12	13	16	19	21
60	26	22	18	15	18	23	26	24	19	14	11	10	8	6	9	10	10	10	10	13	16	18	19	17	14	11	10	9	9	10	10	10	11	12	12	12
55	25	20	13	11	14	22	26	25	20	13	8	4	3	5	7	9	6	5	5	7	9	13	15	13	13	12	9	8	8	9	10	12	13	11	9	9
50	15	13	10	6	10	16	20	21	18	13	7	5	4	3	5	6	5	3	3	5	7	8	9	10	11	9	7	6	6	10	14	15	13	9	7	8
45	8	10	10	8	7	11	15	15	12	9	7	6	5	5	6	6	3	2	3	5	7	8	7	6	5	4	5	6	6	11	16	14	10	7	6	10
40	7	9	10	10	11	13	13	11	9	8	6	5	5	13	21	14	4	5	8	7	6	6	4	3	2	2	4	6	7	9	11	9	8	7	7	10
35	9	10	10	13	17	17	14	11	10	9	8	5	5	20	32	20	6	9	13	9	4	3	2	1	1	1	3	5	7	9	7	6	8	9	8	8
30	12	14	12	14	21	21	15	9	7	9	10	7	5	13	20	14	6	8	10	8	6	4	1	1	1	1	1	4	10	14	11	7	10	14	14	9
25	11	15	14	15	20	20	12	6	4	7	10	6	5	7	7	6	6	6	5	7	8	6	2	1	1	1	1	5	14	20	17	12	13	19	21	15
20	9	12	14	14	14	11	6	4	3	4	7	7	7	7	6	5	7	7	6	8	10	7	2				1	5	14	20	19	16	14	18	20	15
15	8	10	12	12	11	7	3	3	3	4	5	7	8	9	5	4	5	7	8	10	11	7	2				1	4	10	15	18	18	15	14	14	11
10	8	10	11	12	12	8	3	3	6	7	8	8	8	7	4	2	4	8	11	13	13	8	2		1	2	4	7	9	11	16	20	18	14	12	11
5	9	11	12	12	9	6	4	5	11	15	13	6	5	5	4	3	4	9	14	15	12	7	2	2	4	5	8	10	9	10	18	25	23	17	16	20
0	8	9	12	11	7	4	4	7	15	21	16	8	4	5	5	4	4	8	12	11	8	4	2	3	6	7	7	8	9	11	21	31	29	19	19	24
-5	6	6	6	10	8	5	4	6	15	22	16	7	6	7	6	4	3	5	7	5	2	1	1	3	4	5	5	7	7	8	16	25	24	15	12	14
-10	4	4	5	6	8	6	4	6	15	21	14	7	10	14	11	6	4	5	5	3	1		1	1	1	1	5	8	7	5	7	11	11	8	5	5
-15	3	3	3	4	5	4	3	5	11	14	9	5	12	19	15	8	6	7	6	3	1						2	5	4	3	3	3	3	3	2	2
-20	2	2	2	1	2	2	3	4	6	7	4	3	6	12	10	6	6	9	8	4	1	1	1	1			1	1	1	2	2	2	2	1	1	2
-25	1	1	1	1	1	1	3	4	4	3	2	1	2	3	3	2	3	7	8	4	1	1	2	1			1	1	1	1	2	2	1	1	1	3
-30	1	1	1	2	2	1	2	2	2	1							1	3	4	3	1	1	1	1			1	2	1	1	1	1	1		1	5
-35			1	2	3	2	2	2	1									1	1	1							1	1	1	1	1	1	1	1	2	5
-40			1	3	5	4	5	6	4	1	1	1	1	1												1	2	2	1				1	1	1	4
-45			1	3	5	5	7	10	8	3	2	2	2	1											1	5	8	5	1						1	3
-50			1	2	3	3	5	7	6	4	2	1	1	1											2	7	11	8	2							2
-55			1	1	1	1	2	2	2	2	1	1												1	2	4	5	4	3	1	1			1	1	4
-60																									1	1	1	2	2	1	1	1		1	2	5
-65																												1	1	2	1	1			1	3
-70	1																											1	1	1	2	2	2	2	2	2
-75	2	1																										1	1	2	3	4	5	6	5	4
-80	2	1	1																								1	1	2	3	4	5	5	5	5	5
-85																									1	1	1	1	1	1	1	1	1	1	1	1
-90																																				

Table 7-6 (Cont.)

BETA \ LAMBDA		190		200		210		220		230		240		250		260		270		280		290		300		310		320		330		340		350		360
90	31	32	32	33	33	34	35	35	36	37	38	38	39	40	40	40	41	41	41	41	40	40	40	39	39	38	38	37	36	36	35	34	34	33	33	32
85	31	31	33	34	35	35	36	37	38	38	40	41	42	43	44	44	44	44	43	43	42	43	43	43	44	45	45	46	46	47	47	46	45	43	40	37
80	44	39	34	28	29	31	34	37	37	36	36	36	36	35	33	30	29	31	34	38	40	38	35	34	35	39	43	44	45	45	48	52	56	57	52	44
75	54	43	31	23	20	24	30	37	35	35	36	39	34	26	19	16	16	18	24	30	32	29	24	21	24	29	37	39	39	35	36	43	53	58	52	41
70	40	35	27	21	18	19	23	27	28	29	30	30	25	19	14	12	13	15	18	20	20	18	16	15	18	23	29	33	34	30	29	32	37	39	36	30
65	22	20	18	16	15	15	16	17	17	17	17	16	15	12	11	10	11	13	15	17	17	14	12	11	13	16	21	25	27	25	23	23	25	25	25	24
60	12	12	12	12	13	13	12	10	9	10	9	9	9	10	10	9	9	11	15	17	16	13	9	8	8	10	14	17	19	19	19	21	26	27	28	27
55	10	12	12	10	10	12	8	4	5	8	7	5	5	9	11	8	4	7	17	25	20	10	4	4	4	6	9	15	20	17	13	18	30	35	30	26
50	12	14	13	6	6	6	4	2	4	8	10	6	4	6	8	6	2	5	15	23	18	9	3	2	4	6	7	14	23	23	18	20	27	29	23	16
45	15	15	10	5	3	2	2	2	3	8	11	8	3	3	3	2	1	3	9	14	12	7	3	3	7	11	10	12	26	36	32	27	27	21	12	8
40	14	12	6	3	2	2	3	4	4	6	7	5	2	1	1	1	1	2	7	11	9	5	2	3	10	15	12	12	28	40	34	27	26	18	9	7
35	8	7	4	2	2	3	5	6	4	3	3	3	2	1				2	8	12	9	4	2	3	7	10	8	11	22	27	20	16	16	13	9	7
30	6	5	4	3	3	5	6	5	3	2	3	3	2	1				2	5	8	6	3	3	3	3	3	3	5	9	9	5	4	6	7	7	8
25	9	8	6	4	6	9	7	4	2	2	3	3	2	1				1	2	3	2	2	3	4	2	1	1	1	2	1	1	1	2	4	5	7
20	11	11	8	5	6	13	12	6	2	3	3	4	3	1	1			1	1	2	1	1	2	2	2	2	2	1	1	1	1	1	2	3	4	6
15	9	9	7	6	7	12	13	8	4	3	4	5	4	2	1	1	1	1	2	2	2	1		1	1	2	2	2	2	1	1	1	2	3	5	6
10	10	9	7	6	5	7	8	6	4	3	3	4	3	1	1			1	1	1	1					1	2	2	3	3	2	1	2	4	6	7
5	18	12	8	6	4	5	6	5	3	2	1	1	1	1						1							1	2	4	4	3	2	2	4	6	8
0	21	13	8	5	4	6	7	5	2	1																	1.	2	4	5	3	2	2	4	6	8
-5	14	10	7	4	3	5	5	4	2	1							1	1	1	1	1		1					1	4	6	5	2	2	3	4	6
-10	7	6	7	4	2	2	2	2	2	1							1	2	1	1								1	5	7	5	2	2	2	3	4
-15	4	5	5	3	2	1	1	1	1	1							1	1	1									1	3	5	4	2	2	2	2	2
-20	3	3	3	2	3	4	3	2	1																				1	1	1	1	1	1	1	1
-25	4	4	2	2	4	5	4	1																									1	1	1	1
-30	7	5	2	1	2	3	2	1																								1	2	3	2	1
-35	8	6	2	1	1	1	1																									1	3	4	3	1
-40	8	9	5	1																												1	2	3	2	1
-45	8	9	6	2																												1	2	3	2	1
-50	5	7	6	2																											1	1	2	3	2	1
-55	6	7	6	4	2																											1	1	1	1	1
-60	7	9	7	5	2																															
-65	5	6	5	3	1																										1	2	2	2	1	
-70	2	2	1	1																									1	2	4	6	7	6	4	2
-75	3	2	1																									1	2	4	6	7	8	7	6	4
-80	4	3	2	1	1																						1	1	2	3	3	4	4	4	3	3
-85	1	1	1	1	1	1	1																													
-90																																				

Table 7-7. Radiant distribution from the 1961–65 atmospheric sample.

Beta \ Lambda		10		20		30		40		50		60		70		80		90		100		110		120		130		140		150		160		170		180
90	52	53	54	55	56	56	57	57	57	57	56	55	54	52	50	48	45	43	41	39	37	35	34	33	32	31	31	32	32	33	35	37	38	40	42	44
85	46	45	46	47	49	52	55	57	59	60	60	57	53	48	43	38	32	28	25	23	22	22	23	24	26	26	26	26	27	28	28	29	30	32	34	36
80	40	36	34	34	37	42	45	45	43	40	36	34	33	31	30	28	26	23	19	17	16	18	23	30	35	35	34	31	30	31	32	33	32	30	28	26
75	34	30	24	23	28	36	42	41	36	29	24	22	23	25	28	28	28	26	22	19	16	17	21	28	36	38	35	30	26	27	29	30	28	25	22	23
70	20	18	16	17	22	29	35	37	36	31	26	21	19	19	19	19	18	18	18	18	18	18	19	21	25	28	28	24	19	16	16	17	17	16	16	21
65	11	10	10	12	17	23	29	31	31	27	21	15	11	10	9	9	8	9	11	13	15	14	14	14	16	19	19	15	11	8	8	8	9	11	12	15
60	8	8	9	11	14	18	21	22	20	17	14	10	7	6	6	7	7	7	7	8	8	8	8	9	11	12	11	9	6	5	5	7	8	9	10	10
55	6	5	8	16	21	19	15	13	10	8	7	6	5	4	6	7	8	9	11	7	4	5	6	7	8	10	11	8	5	3	4	5	8	9	10	8
50	4	3	8	20	28	22	11	6	3	3	3	5	5	5	5	6	6	10	14	8	3	5	7	9	12	15	17	15	9	5	3	3	5	9	11	10
45	3	3	7	19	27	20	9	3	2	2	2	3	4	4	6	9	7	7	8	5	2	3	5	12	23	27	24	20	12	6	4	3	3	7	10	9
40	4	4	6	16	23	16	6	3	3	4	4	4	2	3	8	12	11	8	5	2		1	2	9	23	31	26	15	8	4	4	2	2	5	6	6
35	6	4	5	11	15	11	6	5	7	12	13	8	2	2	5	11	18	20	13	3				3	14	24	23	12	4	3	4	4	3	3	4	4
30	7	4	4	5	7	7	5	6	13	22	22	12	4	2	2	7	20	29	19	5				1	6	15	19	13	5	3	5	5	4	3	4	4
25	7	7	5	5	6	5	4	5	13	21	18	9	3	2	1	4	13	19	13	3					2	8	13	11	8	7	6	5	5	5	5	6
20	13	17	15	12	9	6	3	2	6	9	7	3	2	2	1	1	3	5	3	1				1	2	7	12	11	9	9	7	4	4	4	6	8
15	31	39	33	22	15	9	4	1	1	2	1	1											1	2	6	20	29	21	9	6	5	5	4	5	8	13
10	64	63	45	29	19	12	5	1			1							1	1	1		1	2	3	9	29	43	29	8	3	4	5	5	7	11	17
5	79	67	39	25	18	12	5	1									1	4	6	4	1	2	3	3	7	20	29	19	6	4	6	7	7	8	11	14
0	51	40	20	12	11	8	3	1									1	6	9	6	3	5	8	6	3	5	8	6	3	5	8	8	8	9	10	9
-5	16	12	6	3	3	2	1										2	4	6	4	3	8	11	8	3	1	1	2	3	5	7	7	8	11	13	11
-10	4	4	3	3	3	2	1									2	3	3	2	1	1	5	8	7	4	2	1	1	2	3	5	6	7	13	20	17
-15	3	4	4	5	5	4	3	1							1	3	4	3	1			1	2	4	4	2	1		1	1	3	4	6	13	22	18
-20	2	3	6	9	7	5	4	2				1	3	5	4	3	3	2						2	2	2					2	2	4	9	13	11
-25	1	3	7	11	8	3	2	1				3	13	19	13	4	1								1						1	1	2	4	5	4
-30	2	3	5	7	5	2	1	1	1			5	19	29	20	5															1	3	5	4	3	2
-35	2	2	2	2	1	1	2	4	3	1		4	16	24	17	5	1														3	9	13	9	3	1
-40	1	1		1	1	2	4	6	4	1		4	15	23	16	5	1														3	13	19	13	4	
-45				1	2	2	3	4	2	1		5	18	27	18	6	1														2	8	13	9	2	
-50				1	1	1	1	1	1	1	2	4	12	18	13	4	1														1	2	3	2	1	
-55									1	1	2	3	4	4	3	2	1								1	1	1	1	1							
-60									1	1	1	1	1	1	1	1									1	1	2	1	1							
-65																									1	1	1	1	1							
-70																																				

Table 7-7 (Cont.)

Beta \ Lambda		190		200		210		220		230		240		250		260		270		280		290		300		310		320		330		340		350		360
90	46	48	50	52	53	54	54	54	54	54	53	53	52	51	50	49	48	48	47	46	45	45	45	45	45	45	45	45	45	46	46	47	48	49	50	51
85	42	48	54	60	64	67	63	59	53	48	42	38	37	36	36	36	37	38	38	42	47	53	59	66	73	74	74	73	69	65	60	59	55	52	50	48
80	27	30	37	44	50	52	46	38	32	28	29	32	32	33	33	34	36	38	37	37	34	37	43	50	61	65	68	67	65	63	60	58	52	48	45	42
75	25	27	28	30	31	29	24	18	16	20	27	34	36	35	34	34	34	36	37	37	31	25	20	18	21	27	36	43	45	43	38	33	28	27	29	33
70	26	29	30	31	32	29	22	16	15	20	26	32	32	30	26	26	28	31	33	32	26	20	13	10	9	10	15	20	23	22	19	15	13	13	15	19
65	18	21	22	24	25	23	20	15	14	16	19	21	20	17	14	16	19	23	23	22	17	14	10	8	7	6	7	9	10	11	11	10	9	9	10	11
60	10	10	12	12	13	14	13	12	11	10	10	9	8	7	6	8	11	14	16	15	12	9	7	5	4	4	4	5	6	8	9	10	10	11	11	10
55	8	9	9	8	8	9	9	8	7	7	6	4	3	3	4	4	5	7	13	16	11	6	3	3	2	3	3	5	6	8	11	13	19	24	19	9
50	9	10	9	8	7	6	5	4	3	4	4	3	2	3	4	5	5	5	8	10	7	4	5	6	4	2	3	6	9	8	8	11	24	36	22	6
45	8	8	8	7	6	4	3	2	2	2	2	2	2	3	4	9	11	8	4	3	2	5	13	19	13	4	3	8	11	8	5	5	14	21	13	4
40	6	7	6	5	6	8	9	6	3	2	2	2	2	2	4	11	15	10	3			5	19	29	19	6	3	6	8	6	3	3	5	6	5	5
35	5	6	5	5	10	23	29	18	6	2	1	1	2	2	3	7	10	7	2			4	13	19	13	4	2	3	3	3	2	2	4	8	11	9
30	5	6	5	5	13	33	42	27	8	2	1	1	1	1	1	2	3	2	1			1	4	5	4	2	1	1	1	2	3	3	6	13	17	12
25	7	7	5	4	9	22	29	19	6	2	1	1	1	1	1	1	1	2	1				1	1	1	1	1	1	1	2	4	5	7	11	13	10
20	9	8	6	4	5	8	10	7	3	2	1	1	1	1	1	1	2	2	1			1	1	1	1	1	1	1	1	2	4	7	9	8	8	9
15	15	12	9	8	6	6	5	4	3	1	1	1	1	1	1	1	1	2	1			1	1	1	1	1	1	1	1	2	3	6	8	8	10	18
10	20	19	17	13	10	7	6	4	2	1	1	1	1	1	1	1	1	1					1	1	1	1		1	1	1	2	4	7	9	17	41
5	17	23	24	18	10	7	4	3	2	1	1	1	1	1	1	1	1	1							1	1	1	1	1	1	2	4	7	11	22	53
0	12	21	25	18	9	5	3	2	1	1				1	1	1	1	1	1							1	1	2	3	2	2	3	6	9	16	36
-5	11	17	22	17	8	3	2	2	1	1						1	1	1	1	1						1	2	4	5	3	2	2	3	5	7	12
-10	11	12	16	13	7	3	1	1	1	1								1	1							1	3	5	5	3	1	1	2	2	3	4
-15	9	6	7	7	4	2	1	1	1	1																1	3	5	4	2	1	1	1	2	2	2
-20	6	4	3	2	2	1	1	1	1																	1	2	3	2	1		1	1	1	1	1
-25	3	3	2	1	1	1	1																				1	1	1					1	1	1
-30	2	2	1	1	1	1	1				1																								1	2
-35	1	1	1	1					1	1	1																								1	2
-40								1	3	5	3	1																								1
-45								1	5	7	5	1																								
-50								1	3	5	3	1																								
-55								1	1	1	1																									
-60																																				
-65																																				
-70																																				

Table 7-8. Radiant distribution from the synoptic-year space sample.

BETA LAMBDA		10		20		30		40		50		60		70		80		90		100		110		120		130		140		150		160		170		180
90	7	7	7	7	7	7	7	7	7	6	6	6	6	6	6	6	6	6	6	6	6	7	7	7	7	7	7	8	8	8	8	8	8	8	8	8
85	14	13	12	11	11	11	11	10	9	9	8	7	6	5	5	4	4	3	4	5	6	8	10	13	15	15	16	16	15	15	15	14	14	14	14	14
80	21	19	19	19	19	19	17	15	14	11	9	8	6	5	4	3	3	2	3	3	5	8	12	16	19	21	20	19	19	19	20	22	23	24	23	22
75	27	25	23	25	24	23	21	19	16	12	8	6	6	5	4	3	3	2	2	2	4	7	11	16	17	18	19	20	20	20	21	24	27	28	26	24
70	32	28	24	22	21	22	21	17	13	11	9	9	8	6	4	3	2	2	2	2	4	7	10	13	13	14	16	19	19	19	20	23	26	26	27	28
65	35	30	24	19	19	20	21	17	13	12	12	12	9	7	4	4	3	2	2	3	5	7	10	10	9	10	11	14	15	17	20	23	27	29	32	34
60	38	33	26	22	22	24	26	23	19	14	12	9	7	5	4	4	3	2	2	3	5	8	9	9	8	8	8	10	13	16	19	22	28	31	35	33
55	38	30	25	24	25	30	35	31	22	14	8	5	3	3	3	4	3	1	1	2	3	6	8	9	10	9	6	8	13	16	18	23	31	34	31	27
50	26	25	24	21	22	28	30	25	17	10	7	4	3	2	2	2	1	1	1	1	2	4	6	9	11	8	5	7	11	19	25	27	29	29	25	24
45	19	21	21	16	16	19	20	15	9	6	6	5	3	2	2	1	1			1	2	3	4	5	5	4	4	6	10	20	30	27	22	19	18	24
40	16	16	21	18	16	15	14	10	7	5	5	4	2	3	4	3	1			1	2	2	2	2	1	1	4	6	9	16	22	19	17	16	17	22
35	16	18	19	17	18	17	13	9	7	6	5	4	2	4	6	4	1			1	1	1	1	1	1	1	3	5	8	11	11	11	14	18	19	20
30	18	21	17	17	21	21	14	9	6	6	7	5	2	2	4	2	1				1	1		1	1	1	1	3	6	8	8	9	13	19	22	21
25	17	18	17	18	22	19	11	6	4	5	7	5	2	1	1	1					1	1		1	1	1	1	3	6	9	11	12	12	17	24	24
20	13	13	14	15	15	10	6	4	3	3	4	3	2	2	1												1	3	7	10	12	13	11	13	19	22
15	9	9	9	8	6	3	2	2	2	1	2	2	2	1	1													2	5	8	9	10	9	10	13	14
10	6	6	5	4	3	2	1	1	1	1	1	1	1	1														1	3	4	5	7	8	8	8	8
5	5	5	4	2	2	1	1																				1	1	1	2	3	4	5	5	5	6
0																																				

BETA LAMBDA		190		200		210		220		230		240		250		260		270		280		290		300		310		320		330		340		350		360
90	9	9	9	9	9	9	9	9	8	8	8	8	8	8	8	7	7	7	7	7	7	7	7	7	7	7	7	7	7	7	7	7	7	8	8	8
85	14	14	15	15	16	17	17	17	17	15	14	13	12	11	10	9	6	8	8	8	8	9	10	11	12	13	14	14	14	15	15	16	16	16	15	14
80	20	19	19	19	21	24	26	28	25	22	19	17	16	14	12	9	8	7	8	9	11	12	14	16	20	23	26	27	25	23	23	24	26	27	26	24
75	24	25	26	25	25	29	34	37	32	26	22	23	20	16	11	8	6	5	6	9	12	13	14	17	22	28	35	39	39	35	33	32	35	36	34	31
70	31	32	32	29	29	31	34	35	32	26	22	21	19	15	11	8	6	5	5	7	9	11	13	17	22	27	35	41	44	42	40	39	40	38	36	34
65	37	35	33	29	31	31	30	27	23	19	16	15	14	12	10	8	6	4	5	6	8	10	12	16	20	25	31	36	38	37	36	37	39	38	37	36
60	35	32	33	32	33	32	27	21	17	15	13	11	10	10	9	6	5	4	5	7	9	10	11	14	18	23	27	31	33	33	34	37	40	41	40	40
55	27	31	34	30	32	34	21	12	14	16	13	9	8	9	8	5	3	2	5	8	10	9	9	11	15	19	25	32	33	30	31	40	47	44	40	40
50	28	30	28	25	24	21	13	7	9	13	13	10	8	8	7	4	2	2	4	7	9	8	7	8	11	15	20	25	27	29	32	41	47	42	35	30
45	31	29	20	16	15	13	10	8	8	9	10	8	7	6	4	3	2	1	2	4	5	6	5	5	9	13	15	16	21	29	32	36	39	35	28	22
40	28	24	16	12	12	12	12	13	11	8	7	6	5	4	3	2	1	1	1	2	3	3	3	5	7	11	12	13	21	27	25	24	25	26	25	21
35	21	22	19	14	12	12	15	18	12	8	8	6	4	3	2	1	1		1	1	2	2	3	4	5	7	8	12	19	19	16	14	17	21	22	19
30	19	21	19	14	12	13	15	15	10	9	10	7	4	3	2	1				1	2	3	4	4	4	4	5	8	11	10	8	8	12	18	18	16
25	21	19	16	12	13	13	12	10	8	8	7	5	4	3	1	1				1	1	2	4	5	4	3	4	5	6	5	5	6	9	12	13	14
20	19	16	14	13	13	14	12	6	7	7	4	3	3	2	1	1				1	1	2	2	3	3	4	6	5	5	5	4	5	7	9	10	11
15	13	12	13	13	12	13	12	9	6	5	4	3	2	2	1					1	1	1	1	1	2	4	6	5	5	5	4	4	6	8	8	9
10	8	9	10	10	8	8	7	5	4	3	2	2	1	1	1										1	2	3	3	3	4	3	3	4	5	7	7
5	6	6	7	6	5	4	2	2	2	1	1	1	1	1												1	1	2	2	3	2	2	2	3	4	4
0																																				

Table 7-9. Radiant distribution from the 1961−65 space sample.

BETA \ LAMBDA			10		20		30		40		50		60		70		80		90		100		110		120		130		140		150		160		170	180
90	13	13	12	12	12	11	11	10	10	9	9	8	8	7	7	7	6	6	6	6	6	7	7	7	7	8	8	9	9	9	10	10	10	11	11	11
85	25	23	21	20	18	17	16	14	13	11	10	9	8	7	6	5	4	4	4	4	4	5	7	8	10	12	13	15	16	17	18	19	19	19	19	18
80	33	30	26	23	23	23	23	21	19	15	13	11	9	7	6	5	4	4	3	3	3	4	7	11	15	18	20	21	23	25	26	27	27	26	24	24
75	35	31	26	22	24	27	30	29	25	20	16	13	11	8	7	5	4	4	4	4	4	4	7	11	17	21	22	22	21	23	23	25	24	26	26	31
70	28	26	23	21	23	26	30	30	26	23	18	13	9	7	6	4	3	3	3	4	4	5	7	10	14	18	19	18	16	15	14	17	18	23	26	34
65	24	22	21	20	20	21	23	24	23	20	16	11	7	5	4	3	2	2	2	3	4	5	7	9	11	13	14	12	10	10	11	14	17	22	26	31
60	25	21	20	20	18	17	16	15	15	14	12	9	6	3	2	2	2	1	1	2	2	3	5	7	9	11	10	8	7	9	12	16	20	24	26	27
55	21	17	17	19	19	17	14	10	7	8	8	5	2	2	2	2	2	1	1	1	1	2	3	4	7	11	11	9	6	7	9	15	22	28	29	26
50	16	13	13	15	19	20	16	8	4	4	4	3	2	1	1	1	1	1	1	1	1	1	2	5	9	12	15	14	11	8	8	10	16	25	30	29
45	16	14	13	18	23	21	15	8	3	3	2	2	1	1	1	1	1	1	1			1	2	6	13	15	16	17	13	10	9	7	10	19	25	26
40	19	15	14	22	26	18	11	6	3	2	2	2	1		1	1	1						1	5	11	14	12	10	7	8	9	7	8	14	17	19
35	22	15	13	16	17	10	6	4	4	4	4	2	1		1	1	1							2	5	8	6	3	3	5	9	9	8	10	13	16
30	21	14	9	8	7	5	3	4	8	10	7	3	1												2	3	3	2	2	5	9	12	11	11	13	16
25	17	14	9	6	5	4	2	3	9	12	8	2	1	1												1	2	3	5	7	8	10	11	13	15	19
20	19	18	12	7	7	5	2	2	5	7	4	1														1	2	3	6	9	7	6	8	10	14	20
15	20	22	14	7	7	6	3	1	1	1	1																1	2	4	5	5	4	5	7	12	19
10	14	15	9	5	5	4	2																			1	1	1	1	1	2	3	4	6	11	16
5	6	5	4	3	3	3	2																				1			1	1	2	3	5	7	10
0																																				

BETA \ LAMBDA			190		200		210		220		230		240		250		260		270		280		290		300		310		320		330		340		350	360
90	11	11	11	11	11	11	10	10	10	9	9	9	8	8	8	8	8	8	8	8	8	8	9	9	10	10	11	11	11	12	12	12	13	13	13	13
85	18	18	18	18	17	16	15	14	13	12	12	12	11	10	9	8	7	7	6	7	8	10	12	13	15	16	18	20	21	23	25	27	28	28	28	26
80	24	25	25	25	23	21	19	16	16	17	18	19	17	15	12	10	8	7	6	7	8	10	11	13	16	17	20	23	27	31	34	37	37	38	37	35
75	32	35	31	30	28	28	26	22	20	20	21	23	21	18	15	12	10	8	7	8	10	11	11	11	12	14	19	24	27	30	31	32	30	30	31	34
70	38	42	37	36	35	35	32	28	24	23	23	23	21	19	15	12	9	8	8	10	11	12	12	12	12	14	17	21	24	26	27	26	25	24	25	27
65	35	38	38	37	36	35	34	31	27	25	23	21	19	16	12	9	8	7	7	8	10	12	13	13	14	14	16	18	21	23	23	23	24	26	27	26
60	29	31	33	32	31	30	31	30	29	26	22	18	15	12	9	7	6	5	4	6	8	10	11	12	13	14	15	17	20	24	24	25	26	30	32	29
55	26	30	33	31	28	27	26	24	23	25	22	15	10	9	8	7	5	3	2	3	6	8	9	9	10	11	11	15	20	23	27	29	35	48	45	29
50	28	30	32	33	30	25	21	17	14	17	16	12	9	8	7	6	4	2	1	2	4	6	7	7	7	8	10	14	19	22	22	25	46	66	45	20
45	27	28	28	29	26	24	20	14	12	14	13	10	9	7	6	5	3	2	1	1	2	5	8	9	7	7	12	16	20	21	18	19	35	45	29	16
40	26	28	24	23	23	22	19	14	12	12	10	9	9	7	5	4	2	1	1	1	1	4	8	10	8	7	12	16	18	17	15	16	19	20	18	19
35	23	27	25	23	22	22	19	15	13	11	8	7	7	6	4	3	2	1		1	1	3	6	8	7	6	9	11	12	12	13	13	16	23	31	30
30	21	25	26	23	23	25	21	16	14	12	8	5	5	4	3	2	1	1			1	2	3	4	5	5	6	7	10	13	14	13	17	32	43	34
25	23	25	24	20	18	20	19	15	13	12	7	4	4	3	2	2	1	1		1	1	2	2	3	3	5	5	5	8	13	13	14	18	26	31	25
20	25	24	22	20	17	17	18	16	13	9	6	4	3	2	2	2	1	1			1	2	2	2	3	4	4	4	6	9	11	15	21	20	18	19
15	22	21	20	21	19	19	19	16	12	7	4	4	3	2	1	1	1				1	2	2	2	3	3	4	4	5	7	8	13	18	18	17	17
10	17	16	17	17	17	17	14	10	6	4	3	2	2	1	1	1						1	1	1	2	2	2	3	4	5	5	8	11	12	12	12
5	11	11	12	11	11	10	7	4	3	2	2	1	1	1									1	1	1	1	1	1	2	3	3	5	6	7	7	6
0																																				

smoothing was continuous over the north celestial pole, and the longitudinal smoothing involved nearly equal great-circle intervals of longitude at all latitudes. In smoothing the "space" samples, which are truncated at the ecliptic, we assumed a mirror-image distribution in the southern hemisphere.

Comparison of these tables with our 1973 report shows no large changes. (Note that the table entries in 1973 were differently defined, and harder to interpret.) The 1961–65 data are remarkably similar to those from the synoptic year. The strong concentration of relative velocities into two clusters (four, including the southern hemisphere) toward and away from the sun in longitude, but at high angles to the ecliptic, needs further discussion.

7.4 Orbital Elements

Tables 7-10 through 7-15 present distributions of $1/a$, e, q, q', i, and ω, respectively, for the six samples. The first five show little difference from our 1973 report for the synoptic year. Differences between 1961–65 and the synoptic year are evidently associated with the relative lack of slow meteors in the former period, but they have not been otherwise analyzed.

Table 7-15 is new and is introduced to help understand Tables 7-6 and 7-9 (the space-sample radiant distributions). The space samples in Table 7-15 show a marked dip in the frequency of ω near 0° and 180°; in other words, it shows a tendency for the nodes to avoid the neighborhood of perihelion and aphelion. This is equivalent to avoiding $\lambda - \lambda_{\odot} = 90°$ or 270° for the radiants. Qualitative explanations can be framed in terms of either Jupiter perturbations of parent comets or collisions near the ecliptic plane (for example, the asteroid belt), but they have not been worked out in any detail.

Tables 7-16 through 7-21 give two-dimensional distributions of $1/a$ and e, $1/a$ and i, and e and i, for both space samples. They are independently scaled to a largest entry of 1000, but the row and column sums make it easy to change scales. In Tables 7-16 and 7-17, the areas above the triangular array correspond to orbits with perihelion outside the earth's orbit, and the areas below, to orbits with aphelion inside the earth's orbit. The apparently hyperbolic orbits ($e > 1$) were probably displaced from the top right corner of the triangular array by observational error.

Table 7-10. Distribution of inverse semimajor axis.

1/a	Synoptic year			1961–65		
	Observed	Atmospheric	Space	Observed	Atmospheric	Space
0.0	0.010	52-5	13-4	0.021	94-5	28-4
0.1	0.015	25-4	24-4	0.021	13-4	31-4
0.2	0.028	31-4	71-4	0.043	77-4	0.015
0.3	0.056	0.011	0.022	0.064	0.015	0.033
0.4	0.085	0.042	0.060	0.087	0.027	0.049
0.5	0.102	0.051	0.083	0.102	0.073	0.104
0.6	0.092	0.060	0.088	0.092	0.098	0.107
0.7	0.085	0.102	0.098	0.084	0.076	0.101
0.8	0.078	0.122	0.113	0.081	0.136	0.112
0.9	0.080	0.153	0.127	0.079	0.171	0.127
1.0	0.088	0.187	0.133	0.080	0.174	0.124
1.1	0.088	0.140	0.111	0.070	0.090	0.072
1.2	0.061	0.066	0.060	0.051	0.062	0.054
1.3	0.045	0.040	0.041	0.040	0.042	0.035
1.4	0.031	68-4	0.020	0.027	0.011	0.022
1.5	0.023	60-4	0.017	0.021	48-4	0.015
1.6	0.014	44-4	62-4	0.014	28-4	89-4
1.7	0.012	21-4	67-4	0.012	35-4	79-4
1.8	65-4	84-5	18-4	70-4	39-4	50-4
1.9	21-4	28-5	39-5	36-4	63-5	83-5
2.0	14-5	20-6	13-6	62-5	66-6	11-5

The small but significant correlations between 1/a and i and between e and i need study, just as the strong interrelation between 1/a and e needs further examination, to help understand the nature of meteors.

Table 7-11. Distribution of eccentricity.

e	Synoptic year			1961–65		
	Observed	Atmospheric	Space	Observed	Atmospheric	Space
0.0	0.051	0.169	0.050	0.042	0.144	0.021
0.1	0.074	0.269	0.142	0.052	0.208	0.097
0.2	0.082	0.166	0.162	0.059	0.220	0.126
0.3	0.090	0.143	0.158	0.067	0.088	0.118
0.4	0.102	0.082	0.142	0.079	0.110	0.161
0.5	0.123	0.078	0.135	0.099	0.101	0.172
0.6	0.136	0.060	0.120	0.122	0.059	0.127
0.7	0.139	0.023	0.060	0.144	0.040	0.102
0.8	0.118	71–4	0.024	0.178	0.023	0.057
0.9	0.076	33–4	71–4	0.137	50–4	0.017
1.0	0.010	52–5	13–4	0.021	94–5	28–4

Table 7-12. Distribution of perihelion distance.

q	Synoptic year			1961–65		
	Observed	Atmospheric	Space	Observed	Atmospheric	Space
0.0	0.040	11–4	47–4	0.070	43–4	0.014
0.1	0.073	41–4	0.017	0.113	0.011	0.035
0.2	0.067	77–4	0.026	0.087	0.013	0.038
0.3	0.070	0.012	0.035	0.079	0.015	0.045
0.4	0.070	0.015	0.045	0.080	0.024	0.064
0.5	0.071	0.025	0.055	0.070	0.028	0.079
0.6	0.086	0.069	0.102	0.071	0.084	0.114
0.7	0.092	0.096	0.137	0.071	0.107	0.139
0.8	0.129	0.187	0.214	0.094	0.128	0.169
0.9	0.245	0.464	0.333	0.228	0.496	0.289
1.0	0.057	0.119	0.032	0.037	0.090	0.015

Table 7-13. Distribution of aphelion distance.

q′	Synoptic year			1961–65		
	Observed	Atmospheric	Space	Observed	Atmospheric	Space
1.0	0.015	0.020	47-4	0.016	0.024	54-4
1.5	0.326	0.557	0.434	0.263	0.501	0.355
2.0	0.141	0.176	0.189	0.135	0.190	0.200
2.5	0.104	0.083	0.106	0.105	0.071	0.114
3.0	0.079	0.048	0.073	0.088	0.076	0.089
3.5	0.066	0.033	0.054	0.071	0.054	0.083
4.0	0.053	0.023	0.039	0.053	0.026	0.037
4.5	0.042	0.020	0.030	0.043	0.017	0.031
5.0	0.030	0.016	0.024	0.030	73-4	0.013
6.0	0.038	97-4	0.017	0.045	0.011	0.023
7.0	0.024	61-4	0.011	0.028	54-4	0.012
8.0	0.016	14-4	48-4	0.020	55-4	0.013
9.0	99-4	10-4	41-4	0.012	22-4	37-4
10.0	81-4	56-5	18-4	0.011	25-4	29-4
	0.047	57-4	93-4	0.078	75-4	0.019

Table 7-14. Distribution of inclination.

i (degrees)	Synoptic year Observed	Synoptic year Atmospheric	Synoptic year Space	1961–65 Observed	1961–65 Atmospheric	1961–65 Space
0						
	0.026	0.163	78-4	0.024	0.165	77-4
2						
	0.025	0.136	0.026	0.027	0.091	0.021
4						
	0.024	0.138	0.054	0.027	0.124	0.040
6						
	0.022	0.118	0.068	0.023	0.121	0.062
8						
	0.020	0.068	0.057	0.021	0.066	0.037
10						
	0.048	0.163	0.188	0.045	0.149	0.159
15						
	0.048	0.087	0.180	0.046	0.093	0.150
20						
	0.052	0.053	0.141	0.048	0.066	0.133
25						
	0.066	0.031	0.102	0.047	0.044	0.116
30						
	0.060	0.018	0.065	0.048	0.030	0.088
35						
	0.061	99-4	0.040	0.056	0.020	0.064
40						
	0.123	91-4	0.041	0.111	0.017	0.066
50						
	0.124	37-4	0.019	0.118	81-4	0.035
60						
	0.110	15-4	78-4	0.108	35-4	0.015
70						
	0.064	42-5	23-4	0.073	12-4	53-4
80						
	0.018	71-6	37-5	0.024	24-5	10-4
90						
	0.011	30-6	16-5	91-4	58-6	33-5
100						
	0.011	19-6	12-5	0.014	63-6	31-5
110						
	0.015	20-6	12-5	0.018	60-6	27-5
120						
	0.017	15-6	84-6	0.019	53-6	16-5
130						
	0.016	11-6	64-6	0.021	51-6	15-5
140						
	0.019	16-6	51-6	0.024	43-6	76-6
150						
	0.016	90-7	20-6	0.022	34-6	56-6
160						
	0.011	54-7	96-7	0.015	23-6	23-6
170						
	58-4	29-8	13-7	99-4	19-6	95-7
180						

Table 7-15. Distribution of argument of perihelion.

ω (degrees)	Synoptic year Observed	Synoptic year Atmospheric	Synoptic year Space	1961–65 Observed	1961–65 Atmospheric	1961–65 Space
0	0.047	0.053	0.022	0.038	0.042	0.020
20	0.052	0.052	0.044	0.050	0.016	0.033
40	0.048	0.061	0.060	0.046	0.042	0.041
60	0.047	0.038	0.054	0.044	0.049	0.061
80	0.051	0.057	0.065	0.045	0.092	0.071
100	0.056	0.044	0.064	0.049	0.067	0.060
120	0.073	0.072	0.095	0.061	0.072	0.078
140	0.071	0.075	0.084	0.072	0.076	0.075
160	0.067	0.087	0.032	0.065	0.062	0.035
180	0.070	0.078	0.037	0.072	0.093	0.039
200	0.062	0.068	0.072	0.069	0.102	0.066
220	0.056	0.051	0.083	0.058	0.039	0.073
240	0.046	0.048	0.071	0.049	0.028	0.071
260	0.047	0.032	0.063	0.050	0.031	0.069
280	0.048	0.032	0.053	0.054	0.037	0.066
300	0.050	0.026	0.036	0.061	0.030	0.055
320	0.061	0.070	0.045	0.073	0.051	0.062
340	0.048	0.055	0.021	0.045	0.071	0.026
360						

Table 7-16. Joint distribution of 1/a and e from the synoptic-year space sample.

1/a \ e	0.1	0.2	0.3	0.4	0.5	0.6	0.7	0.8	0.9	1.0		Sum
-1.0											0	0
-0.9											0	0
-0.8											0	0
-0.7											0	0
-0.6											2	2
-0.5											0	0
-0.4											1	1
-0.3											1	1
-0.2											7	7
-0.1											16	16
0.0										52		52
0.1									127	26		153
0.2							0	361	111	6		478
0.3						23	948	302	30	4		1306
0.4					2	1000	638	125	27	4		1795
0.5				21	835	733	240	62	17	4		1912
0.6			3	847	822	245	120	56	16	5		2113
0.7		2	838	974	338	152	74	49	18	4		2450
0.8	3	856	820	568	260	117	72	22	19	6		2742
0.9	548	964	635	329	183	101	67	33	9	5		2873
1.0	520	908	473	142	120	101	84	34	19	4		2405
1.1	5	288	523	221	95	62	52	31	15	3		1295
1.2		44	201	240	197	75	71	41	15	4		889
1.3			0	73	159	95	41	34	18	6		425
1.4				0	56	164	70	61	22	5		378
1.5						41	65	16	12	1		135
1.6						0	59	62	17	6		144
1.7								12	21	6		39
1.8									5	3		8
1.9										0		0
2.0												
Sum	1076	3061	3493	3414	3066	2909	2601	1301	518	153	29	21621

Table 7-17. Joint distribution of 1/a and e from the 1961–65 space sample.

1/a \ e	0.1	0.2	0.3	0.4	0.5	0.6	0.7	0.8	0.9	1.0		Sum
-1.0											2	2
-0.9											2	2
-0.8											1	1
-0.7											4	4
-0.6											1	1
-0.5											2	2
-0.4											2	2
-0.3											2	2
-0.2											6	6
-0.1											30	30
0.0									0	55		55
0.1								0	225	44		269
0.2								434	142	20		596
0.3						0	440	350	81	12		882
0.4						1000	590	208	56	15		1868
0.5				0	663	719	340	124	48	18		1912
0.6			9	521	643	307	170	93	44	16		1804
0.7		1	474	613	377	287	131	66	49	13		2010
0.8		519	723	330	229	204	142	69	45	10		2272
0.9	211	652	396	297	359	113	92	62	35	11		2227
1.0	157	294	207	96	275	66	85	66	35	12		1292
1.1	0	268	269	102	126	79	34	46	29	9		960
1.2		6	168	106	77	84	81	77	22	11		631
1.3			1	40	70	143	46	54	33	8		396
1.4				0	67	42	40	67	39	12		266
1.5					0	42	48	26	37	5		159
1.6							26	53	53	9		141
1.7							1	28	44	17		90
1.8									6	9		15
1.9										2		2
2.0												
Sum	368	1739	2247	2105	2886	3086	2266	1822	1024	306	50	17900

Table 7-18. Joint distribution of 1/a and i from the synoptic-year space sample.

1/a \ i	0	10	20	30	40	50	60	70	80	90	100	110	120	130	140	150	160	170	180	Sum
-1.0							0	0			0		0							0
-0.9							0													0
-0.8		0			0															0
-0.7			0																	0
-0.6	2				0				0				0		0					2
-0.5	0			0	0			0		0										0
-0.4		1			0	0		0							0					1
-0.3	0	0	1	1			0	0						0			0			1
-0.2	0	1	5	0		0	0		0	0				0	0	0				6
-0.1	1	5	4	0	2	1	1	0	0	0		0	0		0		0	0		14
0.0	2	11	12	7	7	4	1	0	0	0	0	0			0	0	0	0		45
0.1	6	30	50	22	16	5	2	1	0	0	0	0	0	0	0	0	0	0		131
0.2	72	100	134	64	23	11	4	1	0	0	0	0	0	0	0	0	0	0		410
0.3	264	404	268	123	42	14	5	2	0	0	0	0	0	0	0	0	0	0		1122
0.4	304	662	337	160	50	20	6	2	0	0	0	0	0	0	0	0	0	0		1542
0.5	313	620	460	182	46	14	5	1	0	0	0	0	0	0	0	0	0	0		1642
0.6	460	791	337	140	56	23	7	1	0	0	0	0	0	0	0	0	0	0		1815
0.7	597	668	584	176	49	20	8	2	0	0	0	0	0	0	0	0	0	0		2104
0.8	625	852	600	187	53	25	9	3	0	0	0	0	0	0	0	0	0	0		2355
0.9	526	1000	587	234	77	27	13	3	0	0	0	0	0	0	0	0	0	0		2468
1.0	364	749	597	217	84	33	18	4	0	0	0	0	0	0	0	0	0	0		2066
1.1	236	370	229	138	74	38	19	6	0	0	0	0	0	0	0	0	0	0		1112
1.2	79	330	104	125	68	38	13	4	1	0	0	0	0	0	0	0	0	0		763
1.3	52	78	56	86	44	30	14	3	1	0	0	0	0	0	0	0	0	0		365
1.4	14	108	78	60	25	26	9	2	1	0	0	0	0	0	0	0	0	0		325
1.5	33	19	11	24	8	11	5	2	0	0	0	0	0	0	0	0		0		116
1.6	6	17	41	12	25	14	4	3	0	0	0	0	0	0	0	0		0		124
1.7	0	3	6	8	8	2	2	2	0	0	0	0	0		0	0	0			33
1.8	0	1	1	1	1	3	0		0	0		0	0							7
1.9	0													0						0
2.0																				
Sum	3957	6820	4503	1967	760	357	145	43	7	3	2	2	2	1	1	0	0	0		18569

Table 7-19. Joint distribution of 1/a and i from the 1961−65 space sample.

1/a \ i	0–10	10–20	20–30	30–40	40–50	50–60	60–70	70–80	80–90	90–100	100–110	110–120	120–130	130–140	140–150	150–160	160–170	170–180	Sum
-1.0–-0.9	0	2	0	0	0		0	0											2
-0.9–-0.8	1		1																2
-0.8–-0.7			1						0		0					0			1
-0.7–-0.6			3	0	0				0										4
-0.6–-0.5			1			0	0												1
-0.5–-0.4		1		0		0	0			0					0	0			2
-0.4–-0.3			0	2	0	0			0			0			0				2
-0.3–-0.2	0				1	0	1	0		0		0				0	0		2
-0.2–-0.1	1	0		1	2	1	0	1	0		0					0	0	0	7
-0.1–0.0	2	11	4	7	5	3	1	0	0	0		0	0	0		0	0	0	33
0.0–0.1	6	7	15	4	12	9	5	1	0	0	0	0	0		0	0	0	0	60
0.1–0.2	37	111	43	43	41	15	5	3	0	0	0	0	0	0	0	0	0	0	298
0.2–0.3	62	264	121	125	52	22	8	4	1	0	0	0	0	0	0	0	0	0	660
0.3–0.4	170	272	227	164	93	35	11	3	1	0	0	0	0	0	0	0	0	0	976
0.4–0.5	512	553	637	222	85	40	12	3	1	0	0	0	0	0	0	0	0	0	2066
0.5–0.6	406	808	471	280	94	39	11	5	1	0	0	0	0	0	0	0	0	0	2115
0.6–0.7	388	656	485	290	116	44	10	5	1	0	0	0	0	0	0	0	0	0	1995
0.7–0.8	302	766	666	309	111	40	22	6	1	0	0	0	0	0	0	0	0	0	2223
0.8–0.9	554	912	556	270	138	49	26	6	1	0	0	0	0	0	0	0	0	0	2513
0.9–1.0	281	1000	677	285	124	58	26	8	1	0	1	0	0	0	0	0	0	0	2463
1.0–1.1	219	287	353	353	111	69	25	9	1	0	0	0	0	1	0	0	0	0	1429
1.1–1.2	180	250	259	188	92	52	28	9	3	1	0	0	0	0	0	0	0	0	1062
1.2–1.3	124	115	115	166	84	56	23	11	1	1	1	0	0	0	0	0	0	0	698
1.3–1.4	51	49	77	133	48	46	21	8	2	0	1	0	0	0	0	0	0	0	438
1.4–1.5	6	10	85	81	43	41	16	9	1	1	1	0	0	0	0	0	0	0	295
1.5–1.6	3	2	70	16	35	27	14	4	2	1	1	1	0	0	0	0	0	0	176
1.6–1.7	9	18	27	44	4	36	11	4	1	0	0	0	0	0	0	0	0	0	156
1.7–1.8	7	19	16	22	11	11	7	3	1	0	1	0	0	0	0	0	0	0	99
1.8–1.9	0		2	2	2	3	3	2	1			0	0		0	0		0	16
1.9–2.0				0		1	1	0				0							2
Sum	3320	6114	4912	3008	1305	695	289	105	21	7	6	5	3	3	2	1	0	0	19798

Table 7-20. Joint distribution of e and i from the synoptic-year space sample.

e \ i	0 10	20	30	40	50	60	70	80	90	100	110	120	130	140	150	160	170	180	Sum
0.1	192	393	164	46	13	4	2	1	0	0	0	0	0	0	0	0	0	0	816
0.2	714	910	468	162	45	13	8	2	0	0	0	0	0	0	0	0	0	0	2322
0.3	597	1000	696	240	68	31	14	4	1	0	0	0	0	0	0	0	0	0	2650
0.4	543	938	656	285	97	45	18	6	0	0	0	0	0	0	0	0	0	0	2590
0.5	364	884	593	283	120	55	20	5	1	0	0	0	0	0	0	0	0	0	2325
0.6	450	742	581	261	101	47	17	5	1	0	0	0	0	0	0	0	0	0	2206
0.7	399	765	416	233	83	47	22	5	1	0	0	0	0	0	0	0	0	0	1972
0.8	186	292	247	128	73	37	17	5	1	0	1	0	0	0	0	0	0	0	987
0.9	40	73	113	78	53	22	7	4	1	1	0	1	0	0	0	0	0	0	393
1.0	6	19	35	20	16	14	3	2	1	0	0	0	0	0	0	0	0	0	116
1.1	2	6	9	1	2	1	1	0	0	0	0	0	0	0	0	0	0	0	22
Sum	3494	6023	3977	1737	671	315	128	38	6	3	2	2	1	1	1	0	0	0	16399

Table 7-21. Joint distribution of e and i from the 1961–65 space sample.

e \ i	0–10	10–20	20–30	30–40	40–50	50–60	60–70	70–80	80–90	90–100	100–110	110–120	120–130	130–140	140–150	150–160	160–170	170–180	Sum
0.1	59	153	52	41	18	7	4	1	0	0	0	0	0	0	0	0	0	0	335
0.2	286	604	439	174	40	24	12	4	0	0	0	0	0	0	0	0	0	0	1584
0.3	402	661	535	284	93	43	19	8	1	0	0	0	0	0	0	0	0	0	2046
0.4	354	387	587	318	158	67	35	8	2	0	0	0	0	0	0	0	0	0	1917
0.5	285	1000	603	498	126	70	31	11	2	0	0	0	0	0	0	0	0	0	2628
0.6	556	876	690	393	159	91	27	13	2	1	1	0	0	0	0	0	0	0	2809
0.7	347	555	572	285	170	84	36	10	2	0	0	0	0	0	0	0	0	0	2063
0.8	286	510	304	262	147	102	32	11	2	1	1	1	0	1	0	0	0	0	1659
0.9	137	232	191	159	110	59	23	11	3	2	2	1	1	0	0	0	0	0	932
1.0	18	44	62	52	46	22	19	9	2	1	1	1	0	1	0	0	0	0	278
1.1	4	12	8	9	7	3	2	1	0	0	0	0	0	0	0	0	0	0	46
Sum	2734	5033	4044	2476	1075	572	238	87	17	5	5	4	3	2	1	1	0	0	16299

8. CONCLUSIONS

8.1 Stream Distributions

We have developed a computer technique for determining the two parameters Λ and σ of the D-distribution of meteor orbits in a stream, and we have applied this to the 256 streams found earlier (Southworth and Sekanina, 1973) in the synoptic-year data. Moreover, we have relaxed the screening restrictions for high-inclination and retrograde streams, discovering an additional 20 streams. We have found that about 16% of all meteors in the sample belong to the detected streams.

8.2 Associations of Streams with Adonis

Four synoptic-year streams match the orbit of the minor planet Adonis rather closely. We undertook to see whether these streams could be understood as meteors ejected from Adonis at some time within the last 12000 years, taking into account reasonable circumstances of ejection, secular perturbations on the meteors and Adonis, and radiation pressure. However, we do not find persuasive evidence for such a relationship.

8.3 Meteor Heights

We have improved on our earlier investigation (1973) of meteor heights, revising the punched reduction output to a more homogeneous basis of diffusion heights. Nonetheless, we still do not find Ceplecha's "discrete levels" of meteor height, nor any important relationships between height and orbital characteristics other than velocity.

8.4 Fragmentation

The spread of fragments of a meteoroid along the trajectory has been computed for meteors observed in 1961–65 and in the synoptic year, by using the measured number of Fresnel extrema and taking into account diffusion and the limited dynamic range of the radar receivers. These spreads will, we hope, constitute some of the data for a badly needed physical theory of fragmentation.

Our previous conclusion (Southworth and Sekanina, 1973) that fragmentation does not constitute a significant selection effect is insecurely confirmed.

No important relationship was found between fragment spread and orbital elements, but a puzzling relationship with velocity has appeared.

8.5 Selection Effects

The statistics of the length of the ionized column have been revised, taking into account the projected extent of the station network on individual trajectories. This has yielded new parameters for the relation between column length and radiant zenith distance, important both for a physical theory of fragmentation and for a revision of our corrections for selection effects.

8.6 Orbital Statistics

We used the revised corrections for selection effects to update our 1973 orbital statistics from the synoptic year and to compute parallel statistics for meteors observed in 1961–65.

9. REFERENCES

CEPLECHA, Z.

1967. Classification of meteor orbits. Smithsonian Contr. Astrophys., vol. 11, pp. 35-60.

1968. Discrete levels of meteor beginning height. Smithsonian Astrophys. Obs. Spec. Rep. No. 279, 54 pp.

GREENHOW, J. S., and NEUFELD, E. L.

1955. The diffusion of ionized meteor trails in the upper atmosphere. Journ. Atmos. Terr. Phys., vol. 6, pp. 133-140.

LOEWENTHAL, M.

1956. On meteor echoes from underdense trails at very high frequencies. Tech. Rep. 132, Lincoln Laboratory, Massachusetts Institute of Technology, 69 pp.

McKINLEY, D. W. R.

1961. <u>Meteor Science and Engineering</u>. McGraw-Hill Book Co., New York, 309 pp.

PROBSTEIN, R. F.

1968. The dusty gasdynamics of comet heads. In <u>Problems of Hydrodynamics and Continuum Mechanics</u>, Society of Industrial and Applied Mathematics, Philadelphia, p. 568.

SEKANINA, Z.

1970a. Statistical model of meteor streams. I. Analysis of the model. Icarus, vol. 13, pp. 459-474.

1970b. Statistical model of meteor streams. II. Major showers. Icarus, vol. 13, pp. 475-493.

1971. On the age of a radio meteor stream associated with minor planet Adonis (abstract). Bull. Amer. Astron. Soc., vol. 3, p. 271.

1973. Statistical model of meteor streams. III. Stream search among 19303 radio meteors. Icarus, vol. 18, pp. 253-284.

SOUTHWORTH, R. B.

1962a. Theoretical Fresnel patterns of radio meteors. Harvard Coll. Obs. Radio Meteor Proj. Res. Rep. 14, 60 pp.

SOUTHWORTH, R. B.

1962b. Theoretical Fresnel patterns. Presented at the Fall International Scientific Radio Union Meeting, Ottawa, Canada, October.

1973. Recombination in radar meteors. In Evolutionary and Physical Properties of Meteoroids, Proc. IAU Colloq. No. 13, ed. by C. L. Hemenway, P. M. Millman, and A. F. Cook, NASA SP-319, pp. 13-21.

SOUTHWORTH, R. B., and HAWKINS, G. S.

1963. Statistics of meteor streams. Smithsonian Contr. Astrophys., vol. 7, pp. 261-285.

SOUTHWORTH, R. B., and SEKANINA, Z.

1973. Physical and dynamical studies of meteors. NASA CR-2316, 106 pp.

1974. Physical and dynamical studies of meteors. NASA CR-132535, 35 pp.

WHIPPLE, F. L.

1950. A comet model. I. The acceleration of Comet Encke. Astrophys. Journ., vol. 111, pp. 375-394.

1954. Photographic meteor orbits and their distribution in space. Astron. Journ., vol. 59, pp. 201-217.

NASA-Langley, 1975 CR-2615